Vol. 8, no. 3, 2024 eISSN 2587-8999
PEER-REVIEWED SCIENTIFIC AND THEORETICAL JOURNAL

Computational Mathematics and Information Technologies

Computational Mathematics

Mathematical Modelling

Information Technologies

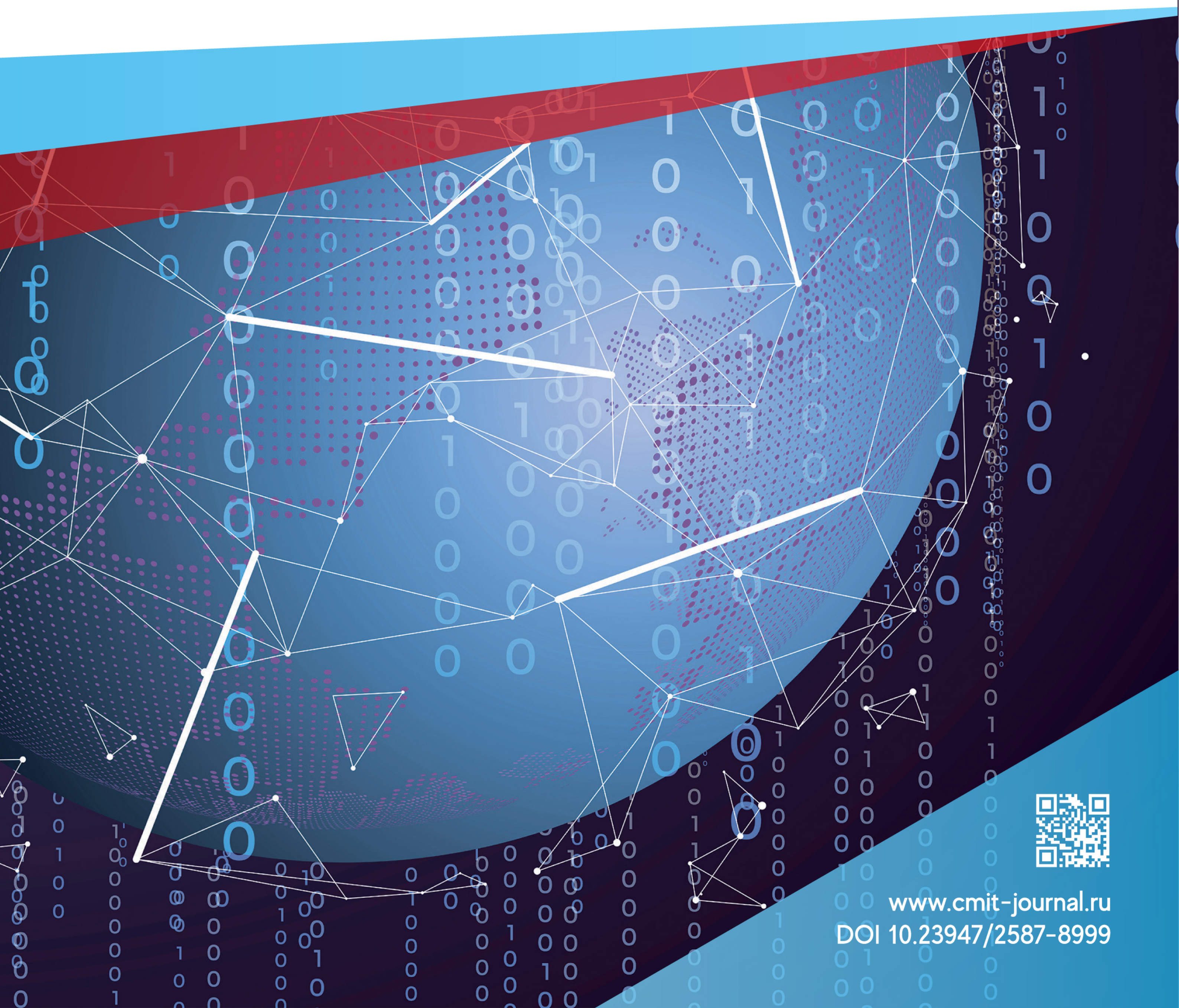

www.cmit-journal.ru
DOI 10.23947/2587-8999

Computational Mathematics and Information Technologies

Peer-reviewed scientific and theoretical journal (published since 2017)

eISSN 2587-8999
DOI: 10.23947/2587-8999

Vol. 8, no. 3, 2024

The scope of "Computational Mathematics and Information Technologies" is focused on fundamental and applied research according to the following scientific sections:

1. Computational Mathematics
2. Mathematical Modelling
3. Information Technologies

Indexing	RSCI, Crossref, Cyberleninka
Name of the body that registered the publication	Mass media registration certificate ЭЛ № ФС 77-66529 dated July 21, 2016 issued by the Federal Service for Supervision of Communications, Information Technology and Mass Media
Founder and publisher	Federal State Budgetary Educational Institution of Higher Education Don State Technical University (DSTU)
Periodicity	4 issues per year
Address of the founder and publisher	1, Gagarin sq., Rostov-on-Don, 344003, Russian Federation
E-mail	CMIT-EJ@yandex.ru
Telephone	+7(863) 273–85–14
Website	https://cmit-journal.ru
Date of publication	30.09.2024

Computational Mathematics and Information Technologies

Рецензируемый научно-теоретический журнал (издаётся с 2017 года)

eISSN 2587-8999
DOI: 10.23947/2587-8999

Том 8, № 3, 2024

Журнал «Computational Mathematics and Information Technologies» ориентирован на фундаментальные и прикладные исследования по следующим научным разделам:

1. Вычислительная математика
2. Математическое моделирование
3. Информационные технологии

Индексация	РИНЦ, CrossRef, CyberLeninka
Наименование органа, зарегистрировавшего издание	Свидетельство о регистрации средства массовой информации ЭЛ № ФС 77 – 66529 от 21 июля 2016 г., выдано Федеральной службой по надзору в сфере связи, информационных технологий и массовых коммуникаций
Учредитель и издатель	Федеральное государственное бюджетное образовательное учреждение высшего образования «Донской государственный технический университет» (ДГТУ)
Периодичность	4 выпуска в год
Адрес учредителя и издателя	344003, Российская Федерация, г. Ростов-на-Дону, пл. Гагарина, 1
E-mail	CMIT-EJ@yandex.ru
Телефон	+7(863) 273–85–14
Сайт	https://cmit-journal.ru
Дата выхода в свет	30.09.2024

Contents

Содержание

ANNIVERSARY OF THE SCIENTIST
ЮБИЛЕЙ УЧЕНОГО

In Commemoration of the Anniversary of Corresponding Member of the Russian Academy of Sciences, Doctor of Physical and Mathematical Sciences, Professor Alexander Ivanovich Sukhinov

Alexander Ivanovich Sukhinov is the head of the Department of Mathematics and Informatics at Don State Technical University, Director of the Research Institute of Mathematical Modeling and Forecasting of Complex Systems, Doctor of Physical and Mathematical Sciences, Professor, Corresponding Member of the Russian Academy of Sciences (RAS), and Honored Scientist of the Russian Federation.

A.I. Sukhinov has developed and studied scalable parallel methods for solving grid equations of diffusion-convection-reaction, including the minimal correction method and the adaptive alternating-triangular method for problems with a non-self-adjoint operator, which demonstrate the best convergence rate under constraints imposed by the grid Peclet number. He has also constructed and investigated efficient parallel algorithms for solving diffusion-convection-reaction and hydrophysics problems based on splitting schemes and scalable methods for grid equations, which take into account the architecture of advanced high-performance computing systems with massive parallelism.

A.I. Sukhinov created, studied, and implemented on distributed-memory supercomputers a complex of interconnected 3D precision models of hydrodynamics, heat, salt, suspension transport, and biogeochemical cycles for coastal systems. These models accurately reproduce vertical mass exchange and are stable for depth variations of up to 40–50 times. Based on these models, vortex structures were discovered in the Sea of Azov and the Mediterranean Sea, along with hypoxic zones and anaerobic contamination, as well as highly accurate predictions of extreme storm surges.

A.I. Sukhinov constructed a correct linearization of the initial-boundary problem for a quasilinear parabolic equation describing sediment transport in coastal systems and proved the convergence of the solutions of the linearized problems to the solution of the original nonlinear problem. He also studied the "closeness" of solutions to the initial-boundary problems for models of the dynamics of biogeochemical cycles, described by ten diffusion-convection equations with nonlinear and linearized source functions.

A.I. Sukhinov implemented a monotonic difference scheme approximating the initial-boundary problem for the biogeochemical cycle dynamics model, described by ten unsteady three-dimensional diffusion-convection equations with nonlinear source functions. The resulting discrete model of biogeochemical cycles was applied to a real coastal ecosystem — the Sea of Azov; simulation results using real data demonstrated the ability to make valid predictions of the geographic dynamics of phytoplankton population distribution under changing weather and climate conditions, such as increasing salinity and decreasing freshwater inflow.

For the parallel numerical solution of hydrophysics problems in marine and coastal systems, A.I. Sukhinov developed explicit parallel algorithms based on the introduction (following B.N. Chetverushkin's regularization method) of second-order difference derivatives into discrete models with the correct determination of permissible regularization multiplier values, which allowed the reduction of the parallel solution time for hydrophysics problems by 50–70 times compared to other known discrete models, including for storm surge prediction and the consequences of natural and man-made disasters.

A.I. Sukhinov participated in 17 expeditions to the Sea of Azov, the Mediterranean Sea, and other locations. In 2001, he contributed to the discovery of a vast hydrogen sulfide contamination zone in the Sea of Azov. Based on the developed models, the mechanism of this catastrophe was explained, and the existence of large-scale closed circulations in the eastern part of the Sea of Azov was uncovered, acting as giant natural traps for pollutants and plankton populations — the so-called S-structures.

On the initiative of A.I. Sukhinov and under his leadership, major projects were carried out from 2015 to 2023 under the Federal Target Program "Research and Development in the Interests of Developing Russia's Scientific and Technological Complex for 2014–2020", the Russian Science Foundation, the Russian Foundation for Basic Research, and others, with a total budget exceeding 280 million rubles.

A.I. Sukhinov engages in significant scientific and organizational work. In 2019, he was elected a Corresponding Member of RAS in the Department of Mathematical Sciences. He is an expert for the Russian Foundation for Basic Research, the Russian Science Foundation, RAS, and the Directorate of Scientific and Technological Programs of the Ministry of Education and Science of Russia. He chairs the Dissertation Council 24.2.297.10 at Don State Technical University in the specialty "Mathematical Modeling, Numerical Methods, and Software Systems", and is also a member of the dissertation councils at Southern Federal University and North-Caucasian Federal University. He serves on the editorial boards of three peer-reviewed journals and one journal indexed in Scopus, and he is a member of the program committees of three prestigious international and national conferences.

The results of A.I. Sukhinov's scientific research and experimental development have been implemented in enterprises in Russia and the Rostov region (Donenergomash, Don Technologies, etc.). His work has been published in over 430 papers, including five monographs, 10 textbooks, and 14 patents and certificates of authorship. From 2019 to 2023, he published more than 100 scientific works, including over 60 indexed in the Scopus and Web of Science databases.

A.I. Sukhinov makes a significant contribution to the development and improvement of the educational process and the training of engineering and scientific-pedagogical personnel. The precision mathematical models and supercomputer software systems developed under his guidance have been implemented in the educational process. He has supervised the preparation of four Doctors of Science and 33 Candidates of Science. His students have won seven grants from the Russian Science Foundation and the Russian Foundation for Basic Research, as well as a Presidential Grant for Young Scientists from 2015 to 2022.

The editorial team of the journal Computational Mathematics and Information Technologies, along with Alexander Ivanovich's colleagues, congratulates the esteemed celebrant, wishing him good health, new scientific discoveries, and the joy of seeing the results of his work! May there be many more successful projects and grateful students ahead!

INFORMATION TECHNOLOGIES
ИНФОРМАЦИОННЫЕ ТЕХНОЛОГИИ

Check for updates

Original Empirical Research

UDC 51–76, 519.6
https://doi.org/10.23947/2587-8999-2024-8-3-9-22

Mathematical Modelling of Spatially Inhomogeneous Non-Stationary Interaction of Pests with Transgenic and Non-Modified Crops Considering Taxis

Alexander I. Sukhinov[1] ✉, **Irina A. Bugaeva**[2]
[1] Don State Technical University, Rostov-on-Don, Russian Federation
[2] Southern Federal University, Rostov-on-Don, Russian Federation
✉ sukhinov@gmail.com

Abstract

Introduction. This paper addresses a unified spatially inhomogeneous, non-stationary model of interaction between genetically modified crop resources (corn) and the corn borer pest, which is also present on a relatively small section of non-modified corn. The model assumes that insect pests influence both types of crops and are capable of independent movement (taxis) towards the gradient of plant resources. It also considers diffusion processes in the dynamics of all components of the unified model, biomass growth, genetic characteristics of both types of plant resources, processes of crop consumption, phenomena of growth and degradation, diffusion, and mutation of pests. The model allows for predictive calculations aimed at reducing crop losses and increasing the resistance of transgenic crops to pests by slowing down the natural mutation rate of pest.

Materials and Methods. The mathematical model is an extension of Kostitsin's model and is formulated as an initial-boundary value problem for a nonlinear system of convection-diffusion equations. These equations describe the spatiotemporal dynamics of biomass density changes in two types of crops — transgenic and non-modified — as well as the specific populations (densities) of three genotypes of pests (the corn borer) resulting from mutations. The authors linearized the convection-diffusion equations by applying a time-lag method on the time grid, with nonlinear terms from each equation taken from the previous time layer. The terms describing taxis are presented in a symmetric form, ensuring the skew-symmetry of the corresponding continuous operator and, in the case of spatial grid approximation, the finite-difference operator.

Results. A stable monotonic finite-difference scheme is developed, approximating the original problem with second-order accuracy on a uniform 2D spatial grid. Numerical solutions of model problems are provided, qualitatively corresponding to observed processes. Solutions are obtained for various ratios of modified and non-modified sections of the field.

Discussion and Conclusion. The obtained results regarding pest behavior, depending on the type of taxis, could significantly extend the time for pests to acquire *Bt* resistance. The concentration dynamics of pests moving in the direction of the food gradient differs markedly from the concentration of pests moving towards a mate for reproduction.

Keywords: mathematical modelling, genetically modified corn, crops, fast and slow taxis

For citation. Sukhinov A.I., Bugaeva I.A. Mathematical Modelling of Spatially Inhomogeneous Non-Stationary Interaction of Pests with Transgenic and Non-Modified Crops Considering Taxis. *Computational Mathematics and Information Technologies*. 2024;8(3):9–22. https://doi.org/10.23947/2587-8999-2024-8-3-9-22

Оригинальное эмпирическое исследование

Математическое моделирование пространственно-неоднородного нестационарного взаимодействия вредителей с трансгенной и немодифицированной агрокультурами с учетом таксиса

А.И. Сухинов[1], **И.А. Бугаева**[2]

[1] Донской государственный технический университет, г. Ростов-на-Дону, Российская Федерация

[2] Южный федеральный университет, г. Ростов-на-Дону, Российская Федерация

sukhinov@gmail.com

Аннотация

Введение. Рассматривается объединенная пространственно-неоднородная нестационарная модель взаимодействия генетически модифицированного растительного ресурса (кукурузы) при наличии на поле вредителя — кукурузного мотылька, также локализованного на относительно небольшом участке поля немодифицированной кукурузы. Предполагается, что на обе растительные культуры воздействуют насекомые-вредители, способные к самостоятельному перемещению (таксису) в направлении градиента растительного ресурса. Также рассматриваемая модель учитывает диффузионные процессы в динамике всех компонентов объединенной модели, рост биомассы, генетические особенности обоих видов растительного ресурса и процессов выедания агрокультур, явления роста и деградации, диффузии и мутации вредителей и дает возможность, на основе прогностических расчетов, с одной стороны, уменьшить потери урожая, с другой стороны — повысить стойкость трансгенной агрокультуры к воздействию вредителя за счет снижения скорости его естественной мутации.

Материалы и методы. Математическая модель представляет собой развитие модели Костицына и является начально-краевой задачей для нелинейной системы уравнений конвекции-диффузии, которые описывают пространственно-временную динамику изменения плотности биомассы двух типов агрокультуры — трансгенной и немодифицированной, а также удельные численности (плотности) образовавшихся в результате мутаций трех генотипов вредителей (кукурузного мотылька).

Авторами выполнена линеаризация уравнений диффузии-конвекции по правым частям на временной сетке — нелинейные члены, входящие в каждое из уравнений, берутся с запаздыванием на предыдущем временном слое. Члены, определяющие таксис, представлены в так называемой симметричной форме, гарантирующей кососимметричность соответствующего непрерывного оператора, а при аппроксимации на пространственной сетке — и разностного оператора.

Результаты исследования. Построена устойчивая монотонная разностная схема, аппроксимирующая исходную задачу со вторым порядком на пространственной равномерной 2D сетке. Приведены результаты численного решения модельных задач, качественно согласующиеся с реально наблюдаемыми процессами. Получены решения для различных соотношений модифицированного и немодифицированного участков поля.

Обсуждение и заключения. Полученные результаты учета поведения вредителей в зависимости от типа таксиса могут позволить существенно увеличить время приобретения *Bt*-устойчивости. При этом динамика концентрации вредителей, перемещающихся в направлении градиента поиска пищи, значительно отличается от концентрации вредителей, перемещающихся в направлении партнёра для размножения.

Ключевые слова: математическое моделирование, генетически модифицированная кукуруза, агрокультура, быстрый и медленный таксис

Для цитирования. Сухинов А.И., Бугаева И.А. Математическое моделирование пространственно-неоднородного нестационарного взаимодействия вредителей с трансгенной и немодифицированной агрокультурами с учетом таксиса. *Computational Mathematics and Information Technologies*. 2024;8(3):9–22. https://doi.org/10.23947/2587-8999-2024-8-3-9-22

Introduction. A unified spatially inhomogeneous non-stationary model is considered, describing the interaction of genetically modified crop resources (corn) [1–5] in the presence of pests, specifically the corn borer, which is also localized within a relatively small section of the field growing non-modified corn. It is assumed that insect pests affect both types of crops and are capable of moving independently in the direction of the plant resource gradient, thus accounting for the phenomenon of taxis [6, 7]. Furthermore, the model incorporates diffusion processes in the dynamics of all components of the unified model.

The arrangement of two types of crops of the same species — transgenic and non-modified — on the same plot of land (field), with the non-modified crop occupying a significantly smaller area, allows for the localization of a large proportion of pests in this smaller area [8–13]. By selecting the relative size of this area and considering factors such as soil fertility, biomass growth, diffusion, and genetic characteristics of both types of crop resources, predictive calculations based on the developed model can be used to reduce crop losses. The processes of crop consumption, growth, degradation, taxis, diffusion, and pest mutation are also accounted for additionally, this approach increases the resistance of transgenic crops to pest damage by slowing the natural mutation rate of pests.

Materials and Methods. The mathematical model is formulated as an initial-boundary value problem for nonlinear convection-diffusion equations with nonlinear functions on the right-hand side [14–17]. These equations describe the spatiotemporal dynamics of biomass density changes for two types of crops — transgenic and non-modified — as well as the density of three pest genotypes, which arise due to mutations in the corn borer.

Transgenic corn lines resistant to pests, producing *"Cry 3 Bt"* toxin crystals, are engineered using the bacterium *Bacillus thuringiensis var*. Tenebrionis. It is assumed that the gene responsible for *Bt*-resistance in an individual pest can exist in two states, referred to as alleles: the *Bt*-susceptible allele (*s*-allele) or the *Bt*-resistant allele (*r*-allele) [15–17]. These two alleles form three pest genotypes: *Bt*-susceptible genotypes (*ss* and *rs*, if *Bt*-resistance is recessive) and the *Bt*-resistant genotype (*rr*). The proposed approach is based on a modified demo-genetic model of Kostitsin [1, 15–21], which describes the dynamics of competing pest genotypes using Lotka-Volterra equations [2, 3].

In this work, the convection-diffusion equations were linearized on the time grid, where the nonlinear terms [22, 23] in each equation were taken with a delay from the previous time layer. The terms defining taxis are analogous to advective transport terms and are presented in a symmetric form that ensures the skew-symmetry of the corresponding continuous operator. When approximated on a spatial grid, this also ensures the skew-symmetry of the finite-difference operator. This approach, with relatively mild restrictions on the time step during the approximation on a 2D spatial grid, allows for the construction of a stable monotonic finite-difference scheme.

Formulation of the Initial-Boundary Value Problem. Let $R = R(x, y, t)$ represent the biomass growth of the studied crop, and r_R be the Malthusian growth rate coefficient. The well-known equation for the dynamics of biomass density takes the form:

$$\frac{\partial R}{\partial t} = \delta_R \Delta R + r_R R(1 - \frac{R}{K_R}) - aRN, \tag{1}$$

$$r_R = r_R + g(x, y, t).$$

where $g(x, y, t)$ is a function accounting for the fertility of a specific field section.

It is assumed that two types of plant resources exist — "regular" and transgenic crops:

$$R = R_1 + R_2, \tag{2}$$

where $R_1 = \alpha(x, y)\, R$ is the initial biomass of the regular plant resource, $R_2 = (1 - \alpha\,(x, y))R$ is the initial biomass of the transgenic plant resource, $N = N_{ss} + N_{rs} + N_{rr}$ is the total pest population density, $N_{ij} = N_{ij}(\mathbf{x}, y, t)$ is the density of genotype *ij* at point $(\mathbf{x}, y) \in \Omega$ at time t ($i, j = r$ или s); N_{ss}, N_{rs}, N_{rr} are the pest population densities correspond to the respective genotypes, K_R is the carrying capacity of the environment, δ_R is the diffusion coefficient for the plant resource, $\alpha(x, y)$ is the competition coefficient between the two types of plant resources (which can be neglected if the distance between patches exceeds 5 meters).

For each pest genotype, where necessary, indices are used in the notation: *ss* and *rs* for *Bt*-susceptible genotypes and *rr* for the *Bt*-resistant genotype.

Recall that the goal of using transgenic crops to suppress the pest population in agricultural fields is to reduce the risk of the pest adapting to the *Bt*-toxin [8–13, 15, 16], produced by the transgenic crop, within the given spatial configuration of the system and under the prescribed "high-dose/refuge" strategy scenarios recommended for managing pest resistance to *Bt* plants. The "high-dose" means that the toxicity level of the *Bt*-crops is sufficiently high to kill nearly all pest larvae. The small percentage of surviving (*Bt*-resistant) individuals should be controlled by designating special areas on or near the transgenic fields where non-modified crops (refuges) are planted. These refuges serve as a source of *Bt*-susceptible individuals, which, by mating with *Bt*-resistant individuals, should decrease the proportion of resistant offspring.

The biomass growth for both types of crops, considering diffusion, is modeled by the following equations:

$$\begin{cases} \dfrac{\partial R_1}{\partial t} = \delta_R \Delta R_1 + r_R R_1 (1 - \dfrac{R}{K_R}) - aR_1 N, \\ \dfrac{\partial R_2}{\partial t} = \delta_R \Delta R_2 + r_R R_2 (1 - \dfrac{R}{K_R}) - aR_2 N_{rr}. \end{cases} \tag{3}$$

Let's introduce the functions that describe the offspring distribution f_{ij}, where the indices *i, j* represent the genotypes *ss, rs, ss:*

$$f_{ij}:\begin{cases} f_{ss}\left(N_{ss},N_{sr},N_{rr}\right)=W_{ss}\dfrac{1}{N}\left(N_{ss}+\dfrac{N_{rs}}{2}\right)^2, \\ f_{sr}\left(N_{ss},N_{sr},N_{rr}\right)=W_{rs}\dfrac{2}{N}\left(N_{ss}+\dfrac{N_{rs}}{2}\right)\left(\dfrac{N_{rs}}{2}+N_{rr}\right), \\ f_{rr}\left(N_{ss},N_{rs},N_{rr}\right)=W_{rr}\dfrac{1}{N}\left(\dfrac{N_{rs}}{2}+N_{rr}\right)^2. \end{cases} \tag{4}$$

The primary *Bt*-resistance management strategy, the "high-dose/refuge" approach, is modeled as follows. It is assumed that the pest's habitat Ω may consist of an arbitrary number of areas planted either with *Bt*-corn (Ω_{Bt}), or regular corn (Ω_{ref}). Let $\sigma \in (0,1)$ be the selection coefficient for *Bt*-resistance. Then, the fitness of the pest genotypes is expressed as:

$$\begin{gathered} W_{rr}=1-c, \ \text{на всем } \Omega; \\ W_{rs}\left(\mathbf{x}\right)=\begin{cases} 1-h_c\, c, & \mathbf{x}\in\Omega_{ref}; \\ 1-\sigma+h_\sigma\left(\sigma-c\right), & \mathbf{x}\in\Omega_{Bt}; \end{cases} \\ W_{ss}\left(\mathbf{x}\right)=\begin{cases} 1, & \mathbf{x}\in\Omega_{ref}; \\ 1-\sigma, & \mathbf{x}\in\Omega_{Bt}, \end{cases} \end{gathered} \tag{5}$$

where *c* is the cost that the *Bt*-resistant genotype pays for the advantage it has on *Bt*-fields; h_σ is the dominance level of selection for *Bt*-resistance; h_c is the dominance level of the cost *c*, the parameters σ, *c*, h_σ, $h_c \in [0,1]$ are determined empirically.

Let *a* represent the search activity coefficient of the corn borer, characterizing its sensitivity to the heterogeneity of corn distribution, *b* be the fertility coefficient, μ — the mortality rate of genotypes, α — the competition coefficient between them. $W_{ij} \in [0,1]$ denotes the fitness coefficient of genotype *ij* in the environment, determining its survival depending on its localization in the habitat (on *Bt*-plants or in a refuge). It is worth noting that when the coefficients (i. e., the habitat is homogeneous and serves as a refuge), summing the system of equations leads to a simple logistic growth equation for the entire population.

Results. To solve the task at hand, we modify the Kostytsyn›s demo-genetic model (1) by adding terms accounting for taxis:

$$\begin{cases} \dfrac{\partial N_{ss}}{\partial t}+\nabla(N_{ss}v_{ss})=\delta\Delta N_{ss}+eaRW_{ss}\dfrac{1}{N}(N_{ss}+\dfrac{N_{rs}}{2})^2-\mu N_{ss}, \\ \dfrac{\partial N_{rs}}{\partial t}+\nabla(N_{rs}v_{rs})=\delta\Delta N_{rs}+eaRW_{rs}\dfrac{2}{N}(N_{ss}+\dfrac{N_{rs}}{2})* \\ *(N_{rr}+\dfrac{N_{rs}}{2})-\mu N_{rs}, \\ \dfrac{\partial N_{rr}}{\partial t}+\nabla(N_{rr}v_{rr})=\delta\Delta N_{rr}+eaRW_{rr}\dfrac{1}{N}(N_{rr}+\dfrac{N_{rs}}{2})^2-\mu N_{rr}, \end{cases} \tag{6}$$

where $K_R=\left(b-\mu\right)/\alpha$ is the environmental capacity, δ_R is the diffusion coefficient of the plant resource, W_{ij} are the adaptability coefficients for pests with the *ij*-th genotype, f_{ij} proportions determining the distribution of pest offspring among the three considered genotypes *ij* (*ss*, *sr*, *rr*) (4), $N_{ij}=N_{ij}(\mathbf{x},y,t)$ is the density of the *ij* genotype at point $(\mathbf{x}, y) \in \Omega$ at time *t* (*i*, *j* = *r* or *s*), N_{ss}, N_{rs}, N_{rr} are the densities of the corresponding pest genotypes, $N = N_{ss} + N_{rs} + N_{rr}$ is the total population density, μ is the mortality coefficient for the genotypes, v_{ss}, v_{sr}, v_{rr}, или $v_{ij}(x, y, t)$ are the velocities of pest movement in the spatial variables *x* and *y* for the corresponding types in the direction of the plant resource gradient.

For two types of taxis (fast and slow), the biological significance and the equations governing them will be presented below. Each type is characterized by its ability to locate areas with high prey concentrations. The moth's search behavior is modeled based on the assumption that the acceleration of the pest's movement is proportional to the gradient of plant density or the change in biomass growth:

$$\frac{\mathrm{d}v_{ij}}{\mathrm{d}t}=k\nabla R+\delta_v\Delta v_{ij}, \tag{7}$$

where $R = R(x, y, t)$ represents the biomass growth of the plant resource population at point (x, y) at time *t*; $v_{ij}(x, y, t)$ denotes the velocities of pest movement, Δ is the Laplace operator, ∇ is the gradient operator.

Here and further, the habitat boundaries of the community are assumed to be uninhabited, meaning that both diffusion and advective flows of individuals across the boundaries are absent:

$$\nabla N_{ij} \bullet n = 0,\ v \bullet n = 0,\ (x,y) \in \partial\Omega\ . \tag{8}$$

Here n is an external normal to the border $\partial\Omega$; Ω is the spatially two-dimensional region representing the pest's habitat; $(x, y) \in \Omega$ (x, y) the closure of this region Ω. Such a formulation of boundary conditions allows for a natural ecological interpretation, specifically the spatial isolation of the trophic community.

Let us now consider the pest dynamics equations, where pest activity is determined by the sum of the densities of two species of insect pests:

$$N = N^{(1)} + N^{(2)} \tag{9}$$

where $N^{(1)}$ и $N^{(2)}$ and are the pest densities in the passive and active state, respectively.

Considering equation (9), the system of equations (6) for the passive behavior of pests can be rewritten as equations (10):

$$\begin{cases} \dfrac{\partial N_{ss}^{(1)}}{\partial t} + \nabla(N_{ss}^{(1)} v_{ss}^{(1)}) = \delta^{(1)} \Delta N_{ss}^{(1)} + eaR_1 W_{ss} \dfrac{1}{N^{(1)}} \left(N_{ss}^{(1)} + \dfrac{N_{rs}^{(1)}}{2} \right)^2 - \mu N_{ss}^{(1)} - \beta N N_{ss}^{(1)}, \\ \dfrac{\partial N_{rs}^{(1)}}{\partial t} + \nabla(N_{rs}^{(1)} v_{rs}^{(1)}) = \delta^{(1)} \Delta N_{rs}^{(1)} + eaR_1 W_{rs} \dfrac{2}{N^{(1)}} \left(N_{ss}^{(1)} + \dfrac{N_{rs}^{(1)}}{2} \right) \cdot \left(N_{rr}^{(1)} + \dfrac{N_{rs}^{(1)}}{2} \right) - \mu N_{rs}^{(1)} - \beta N N_{rs}^{(1)}, \\ \dfrac{\partial N_{rr}^{(1)}}{\partial t} + \nabla(N_{rr}^{(1)} v_{rr}^{(1)}) = \delta^{(1)} \Delta N_{rr}^{(1)} + eaRW_{rr} \dfrac{1}{N^{(1)}} \left(N_{rr}^{(1)} + \dfrac{N_{rs}^{(1)}}{2} \right)^2 - \mu N_{rr}^{(1)} - \beta N N_{rr}^{(1)}, \\ (x,y) \in \Omega(x,y),\ 0 < t \le T, \\ N_{ij}^{(1)}(x_0, y_0, 0) = N_{ij}^{*}, R_1(x_0, y_0, 0) = R_1^{*}, \\ \nabla N_{ij}^{(1)} \bullet n = 0,\ \nabla v_{ij}^{(1)} \bullet n = 0, (x,y) \in \partial\Omega. \end{cases} \tag{10}$$

In the active state, considering that the pest, which is susceptible to the pesticide, only consumes the conventional plant resource (and not the transgenic crop), we derive the following system of equations (11):

$$\begin{cases} \dfrac{\partial N_{ss}^{(2)}}{\partial t} + \nabla(N_{ss}^{(2)} v^{(2)}) = \delta^{(2)} \Delta N_{ss}^{(2)} + eaR_1 W_{ss} \dfrac{1}{N^{(2)}} \left(N_{ss}^{(2)} + \dfrac{N_{rs}^{(2)}}{2} \right)^2 - \mu N_{ss}^{(2)} - \beta N N_{ss}^{(2)}, \\ \dfrac{\partial N_{rs}^{(2)}}{\partial t} + \nabla(N_{rs}^{(2)} v^{(2)}) = \delta^{(2)} \Delta N_{rs}^{(2)} + eaR_1 W_{rs} \dfrac{2}{N^{(2)}} \left(N_{ss}^{(2)} + \dfrac{N_{rs}^{(2)}}{2} \right) \cdot \left(N_{rr}^{(2)} + \dfrac{N_{rs}^{(2)}}{2} \right) - \mu N_{rs}^{(2)} - \beta N N_{rs}^{(2)}, \\ \dfrac{\partial N_{rr}^{(2)}}{\partial t} + \nabla(N_{rr}^{(2)} v^{(2)}) = \delta^{(2)} \Delta N_{rr}^{(2)} + eaRW_{rr} \dfrac{1}{N^{(2)}} \left(N_{rr}^{(2)} + \dfrac{N_{rs}^{(2)}}{2} \right)^2 - \mu N_{rr}^{(2)} - \beta N N_{rr}^{(2)}, \\ (x,y) \in \Omega(x,y),\ 0 < t \le T, \\ N_{ij}^{(2)}(x_0, y_0, 0) = N_{ij}^{**}, R_1(x_0, y_0, 0) = R_1^{*}, \\ \nabla N_{ij}^{(2)} \bullet n = 0,\ \nabla v_{ij}^{(2)} \bullet n = 0, (x,y) \in \partial\Omega. \end{cases} \tag{11}$$

By summing the first three equations, we obtain (11*):

$$\begin{cases} \dfrac{\partial N_{ss}^{(2)}}{\partial t} + \nabla(N_{ss}^{(2)} v^{(2)}) = \delta^{(2)} \Delta N_{ss}^{(2)} + eaR_1 N^{(2)} - \mu N_{ss}^{(2)} - \beta N N^{(2)}, \\ (x,y) \in \Omega(x,y),\ 0 < t \le T, \\ N_{ij}^{(2)}(x_0, y_0, 0) = N_{ij}^{**}, R_1(x_0, y_0, 0) = R_1^{*}, \\ \nabla N_{ij}^{(2)} \bullet n = 0,\ \nabla v_{ij}^{(2)} \bullet n = 0, (x,y) \in \partial\Omega. \end{cases} \tag{11*}$$

Slow taxis in the passive state for the three types of insect pests is described by the following equations (12):

$$\begin{cases} v_{ss}^{(1)} + \alpha\left(\dfrac{\partial v_{ss}^{(1)}}{\partial t} + \nabla(N_{ss}^{(1)} v_{ss}^{(1)})\right) = \delta_v^{(1)} \Delta v_{ss}^{(1)} + k^{(1)} \nabla R_1, \\ v_{rs}^{(1)} + \alpha\left(\dfrac{\partial v_{rs}^{(1)}}{\partial t} + \nabla(N_{rs}^{(1)} v_{rs}^{(1)})\right) = \delta_v^{(1)} \Delta v_{rs}^{(1)} + k^{(1)} \nabla R_1, \\ v_{rr}^{(1)} + \alpha\left(\dfrac{\partial v_{rr}^{(1)}}{\partial t} + \nabla(N_{rr}^{(1)} v_{rr}^{(1)})\right) = \delta_v^{(1)} \Delta v_{rr}^{(1)} + k^{(1)} \nabla R, \\ (x,y) \in \Omega(x,y),\ 0 < t \le T, \\ N_{ij}^{(1)}(x_0, y_0, 0) = N_{ij}^{*}, R(x_0, y_0, 0) = R^{*}, \\ \nabla N_{ij}^{(1)} \bullet n = 0,\ \nabla v_{ij}^{(1)} \bullet n = 0, (x,y) \in \partial\Omega. \end{cases} \tag{12}$$

Fast taxis in the active state is described by a single equation for pesticide-resistant insect pests (13), since genotype-specific traits are not significant when searching for a mating partner:

$$v^{(2)} = k^{(2)} \nabla N^{(2)} + \delta_v^{(2)} \Delta v^{(2)}. \tag{13}$$

In equations (12)–(13), all velocities $v_{ij}^{(1)}, v_{ij}^{(2)}, ij \in (ss, sr, rr)$ are spatially two-dimensional vectors.

To linearize the system (3)–(11), considering the initial and boundary conditions, we construct a uniform time grid ω_τ over the time interval $0 < t \le T$, where T is the characteristic period of crop maturation (from early spring to late summer), with a time step τ:

$$\omega_\tau = \left\{ t_k = k\tau, k = 0,1,\dots,N; N\tau = T \right\}. \tag{14}$$

On this constructed time grid, we build a sequence of linearized initial-boundary value problems, which are interconnected at each step by the initial and final values. The idea behind such linearization is that all nonlinear terms in the corresponding partial differential equations are taken from the values at the previous time layer relative to the current one. For the first time layer, the appropriate initial conditions are used.

Let the solutions of the sequence of linearized initial-boundary value problems be denoted the same as the solution to the original nonlinear problem (3)–(13).

Initially, for each t_k, starting from the initial moment t_0 the velocities of slow and fast taxis are determined from equations (15) and (16), respectively. The value of k, $k = 1,\dots,N$ is fixed for all initial-boundary value problems of the linearized system of partial differential equations solved at the given time layer $t_{k-1} < t \le t_k$, $k = 1,\dots,N$:

$$\begin{cases} \dfrac{\partial v_{ij}^{(1),(k)}}{\partial t} + \dfrac{1}{2}(v_{ij}^{(1),(k)} \nabla N_{ij}^{(1)}(t_{k-1}) + \nabla(N_{ij}^{(1)}(t_{k-1}) v_{ij}^{(1),(k)})) + \\ + \dfrac{1}{\alpha} \Delta v_{ij}^{(1),(k)} = \dfrac{1}{\alpha}(\delta_v^{(1)} \Delta v_{ij}^{(1),(k)} + k^{(1)} \nabla R_1^{(k-1)}(t_{k-1})), \\ v_{ij}^{(1),(0)} = V_{ij}^{*}, v_{ij}^{(1),(k)}(t_{k-1}) = v_{ij}^{(1),(k-1)}(t_{k-1}), k = 1,\dots,N, \\ t_{k-1} < t \le t_k, (x,y) \in \Omega(x,y), \\ N_{ij}^{(1)}(x_0, y_0, t_0) = N_{ij}^{(1)}(x_0, y_0, 0) = N_{ij}^{*}(x,y), R_1^{0}(x_0, y_0, 0) = R^{*}(x,y), \\ \nabla(N_{ij}^{(1)} \bullet n) = 0,\ \nabla v_{ij}^{(1),(k-1)} \bullet n = 0,\ ij \in (ss, sr, rr), (x,y) \in \partial\Omega. \end{cases} \tag{15}$$

$$\begin{cases} v^{(2),(k)} = k^{(2)} \nabla N^{(2),(k-1)} + \delta_v^{(2)} \Delta v^{(2),(k)} \\ v_{ij}^{(2),(0)} = V^{**},\ N_{ij}^{(2),(0)}(x_0, y_0, t_0) = N_{ij}^{**}(x,y), \\ v_{ij}^{(2),(k)}(t_{k-1}) = v_{ij}^{(2),(k-1)}(t_{k-1}), \\ t_{k-1} < t \le t_k,\ k = 1,\dots,N,\ (x,y) \in \Omega(x,y). \end{cases} \tag{16}$$

In relations (15) and (16), the initial conditions $V_{ij}^{*}, V^{**}, R^{*}(x,y), N_{ij}^{*}(x,y), N_{ij}^{**}(x,y)$ are represented by known functions. For the sake of brevity, we will not separately specify the initial and boundary conditions for systems (17)–(19).

Here and throughout, for the system (17)–(19), the value of the parameter k is fixed and is the same as in equations (15)–(16). It remains constant across all systems (17)–(19) until the corresponding initial-boundary value problems are solved within the given time interval $t_{k-1} < t \le t_k$.

For system (3), we have the following:

$$\begin{cases} \dfrac{\partial R_1^{(k)}}{\partial t} = \delta_R \Delta R_1^{(k)} + r_R R_1^{(k)}\left(1 - \dfrac{R_1^{(k-1)}(t_{k-1}) + R_2^{(k-1)}(t_{k-1})}{K_R}\right) - aR_1^{(k)}\left(N^{(1),(k-1)}(t_{k-1}) + N^{(2),(k-1)}(t_{k-1})\right), \\ \dfrac{\partial R_2^{(k)}}{\partial t} = \delta_R \Delta R_2^{(k)} + r_R R_2^{(k)}\left(1 - \dfrac{R_1^{(k-1)}(t_{k-1}) + R_2^{(k-1)}(t_{k-1})}{K_R}\right) - aR_2^{(k)} N_{rr}^{(k-1)}(t_{k-1}), \\ R_1^{(k)}(t_{k-1}) = R_1^{(k-1)}(t_{k-1}), R_2^{(k)}(t_{k-1}) = R_2^{(k-1)}(t_{k-1}), \\ t_{k-1} < t \le t_k,\ k = 1,\dots,N,\ (x,y) \in \Omega(x,y). \end{cases} \tag{17}$$

For system (10), we have the following:

$$\begin{cases} \dfrac{\partial N_{ss}^{(1),(k)}}{\partial t} + \dfrac{1}{2}\left(\nabla(N_{ss}^{(1),(k)} v_{ss}^{(1),(k-1)}) + \nabla N_{ss}^{(1),(k)} v_{ss}^{(1),(k-1)}\right) = \delta^{(1)} \Delta N_{ss}^{(1),(k-1)} + \\ + eaR_1^{(k-1)}(t_{k-1}) W_{ss} \dfrac{1}{N^{(1),(k)}} \left(N_{ss}^{(1),(k)} + \dfrac{N_{rs}^{(1),(k-1)}(t_{k-1})}{2} \right)^2 - \mu N_{ss}^{(1),(k)} - \beta N^{(k)} N_{ss}^{(1),(k)}, \\ \dfrac{\partial N_{rs}^{(1),(k)}}{\partial t} + \dfrac{1}{2}\left(\nabla(N_{rs}^{(1),(k)} v_{rs}^{(1),(k-1)}) + \nabla N_{rs}^{(1),(k)} v_{rs}^{(1),(k-1)}\right) = \delta^{(1)} \Delta N_{rs}^{(1),(k-1)} + \\ + eaR_1^{(k-1)}(t_{k-1}) W_{rs} \dfrac{1}{N^{(1),(k)}} \left(N_{ss}^{(1),(k-1)}(t_{k-1}) + \dfrac{N_{rs}^{(1),(k)}}{2} \right) \cdot \\ \cdot \left(N_{rr}^{(1),(k-1)}(t_{k-1}) + \dfrac{N_{rs}^{(1),(k)}}{2} \right) - \mu N_{rs}^{(1),(k)} - \beta N^{(k)} N_{rs}^{(1),(k)}, \\ \dfrac{\partial N_{rr}^{(1),(k)}}{\partial t} + \dfrac{1}{2}\left(\nabla(N_{rr}^{(1),(k)} v_{rr}^{(1),(k-1)}) + \nabla N_{rr}^{(1),(k)} v_{rr}^{(1),(k-1)}\right) = \delta^{(1)} \Delta N_{rr}^{(1)} + \\ + ea(R_1^{(k-1)}(t_{k-1}) + R_2^{(k-1)}(t_{k-1})) W_{rr} \dfrac{1}{N^{(1),(k)}} \left(N_{rr}^{(1),(k)} + \dfrac{N_{rs}^{(1),(k-1)}(t_{k-1})}{2} \right)^2 - \mu N_{rr}^{(1),(k)} - \beta N^{(\mathrm{k})} N_{rr}^{(1),(k)}, \\ R_1^{(k)}(t_{k-1}) = R_1^{(k-1)}(t_{k-1}), R_2^{(k)}(t_{k-1}) = R_2^{(k-1)}(t_{k-1}), \\ N_{ss}^{(1),(k)}(t_{k-1}) = N_{ss}^{(1),(k-1)}(t_{k-1}), N_{rs}^{(1),(k)}(t_{k-1}) = N_{rs}^{(1),(k-1)}(t_{k-1}), \\ N_{rr}^{(1),(k)}(t_{k-1}) = N_{rr}^{(1),(k-1)}(t_{k-1}), t_{k-1} < t \le t_k, k = 1,\dots,N;\ (x,y) \in \partial\Omega. \end{cases} \tag{18}$$

For the system of equations (11*), we have the linearized formulation (19).

Subsequently, all linearized initial-boundary value problems are approximated on an extended uniform two-dimensional grid using implicit schemes with second-order accuracy with respect to spatial grid steps and first-order accuracy with respect to the time step. Considering the limited speed of pest movement and the symmetric form of the terms describing taxis (skew-symmetry of the corresponding grid operator), it is possible (by selecting a sufficiently small time step) to satisfy the conditions for the applicability of the discrete maximum principle and the positive definiteness of the grid operator for each equation in the system (15)–(19) in the Hilbert space of grid functions. Consequently, we obtain a stable difference scheme. Due to the considerable complexity and volume of work, these studies are expected to be carried out in future research planned on this topic.

$$\begin{cases} \dfrac{\partial v^{(2),(k)}}{\partial t} + \dfrac{1}{2}\left(\nabla(N^{(2),(k)}(t_{k-1}) v^{(2),(k-1)}) + \nabla N^{(2),(k)}(t_{k-1}) v^{(2),(k-1)}\right) = \\ = \delta_v^{(2)} \Delta N^{(2),(k)} - \beta N^{(k)} N^{(2),(k)}, \\ \\ R_1^{(k)}(t_{k-1}) = R_1^{(k-1)}(t_{k-1}), R_2^{(k)}(t_{k-1}) = R_2^{(k-1)}(t_{k-1}), \\ N_{ss}^{(1),(k)}(t_{k-1}) = N_{ss}^{(1),(k-1)}(t_{k-1}), N_{rs}^{(1),(k)}(t_{k-1}) = N_{rs}^{(1),(k-1)}(t_{k-1}), \\ N_{rr}^{(1),(k)}(t_{k-1}) = N_{rr}^{(1),(k-1)}(t_{k-1}), t_{k-1} < t \le t_k, k = 1,\dots,N;\ (x,y) \in \partial\Omega. \end{cases} \tag{19}$$

The resulting system of difference equations, which approximates the sequence of initial-boundary value problems (15)–(19) with a sufficiently small time step (hundreds or thousands of seconds), exhibits strict diagonal dominance. It is advisable to solve it using the Seidel method, which converges at a rate of geometric progression.

To model possible scenarios of the behavior of a biological system consisting of predators and prey, a software package was developed [21]. A two-dimensional grid of size 100×100 units is considered, with a spatial step of 1 and a time step of 0.01. The weight for the difference scheme is set to 0.5. At the initial moment of simulation, the prey concentration was set to a constant value of 1, while the initial predator concentration is shown in Figures 9 and 10. The following parameters were used to simulate changes in population concentrations: the mortality coefficients for the plant resource $\beta_1 = \beta_2 = 1$, the predator growth coefficient, which is taken as the product of the pest's efficiency coefficient e and the pest's resource search efficiency coefficient a: $ea = 1$, and the taxis coefficients $k^{(1)} = k^{(2)} = 40$. For equations (1)–(7), it is assumed that the mobility of the different moth genotypes is the same $\delta = 1$ the pest mortality coefficient $\mu = 6.84$, the carrying capacity of the environment $K_r = 5*106$ kg/km^2, and the Malthusian growth coefficient $r_R = 25.3$ year^{-1}. In all numerical experiments, it was assumed that at the initial moment, the pest density was uniformly distributed over space at $N^0 = 2{,}948 \times 10^6$ individuals/km^2.

According to the authors' assumptions, at the beginning of the study period, there are pests with dominant (*ss*) and mixed (*rs*) genes that lack resistance to transgenic crops. Pests with recessive traits (*rr*-genotype) emerge as a result of crossbreeding by the end of the first month after the first generation reproduces. For the first few months, recessive traits manifest only in individuals with slow taxis. The movement of pests is directed inward, towards areas planted with conventional crops (referred to as "refuges"). Here, through crossbreeding, the insects lose their resistance to transgenic crops.

As food sources are depleted, the boundaries of these areas "smooth out", naturally evening out the spatial distribution of pests [18, 20, 21]. Pest behavior changes by the second year. Over the first two years, the dynamics of the pests shift significantly depending on their activity — whether they are feeding or reproducing. Rapid consumption of the conventional plant resource inevitably leads pests towards the biomass gradient of the transgenic crops. However, successful reproduction is only possible in areas with conventional crops, which highlights the significant role of both fast and slow taxis in the model. Consequently, the movement of all pests is directed away from the "refuge" areas. As they deplete the conventional crop zones, the pests move toward regions where its biomass increases, eventually entering the transgenic fields, where they reproduce and gradually acquire resistance to transgenic plant varieties.

It should be noted that the main field cannot border other modified crops. Figures 1 and 2 present recommendations for farmers from the company's official website.

As the total area of "refuges" increases (>20 %), the acquisition of Bt-resistance slows down, which aligns with the widely accepted recommendations for the size of "conventional" plots on genetically modified fields — ranging from 5 % to 20 % (Fig. 1).

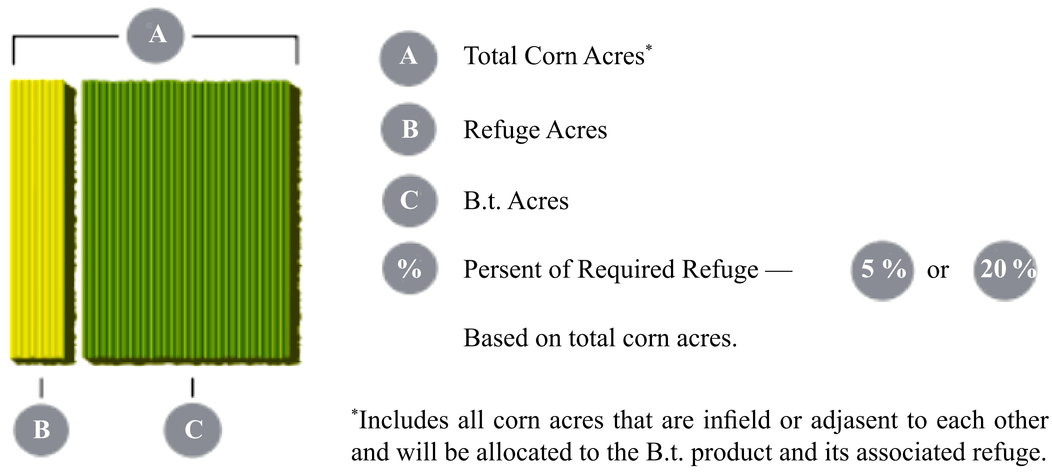

Fig. 1. Recommended sizes of "refuges"

while the transgenic variety is indicated in green (Fig. 1 and 2). Here, the "striping of refuges" may be uneven across the field, and their placement depends on the agro-climatic conditions (Fig. 2).

Now, let us consider the dynamics of pest distribution under various configurations of "refuges" on fields with modified crops. The study period for pest dynamics is set at $t = 10$ conditional years. It is reasonable to assume that the boundaries of the main field should be "surrounded" by corn that does not possess *Bt*-resistance to facilitate easier access to the "refuge" for pests.

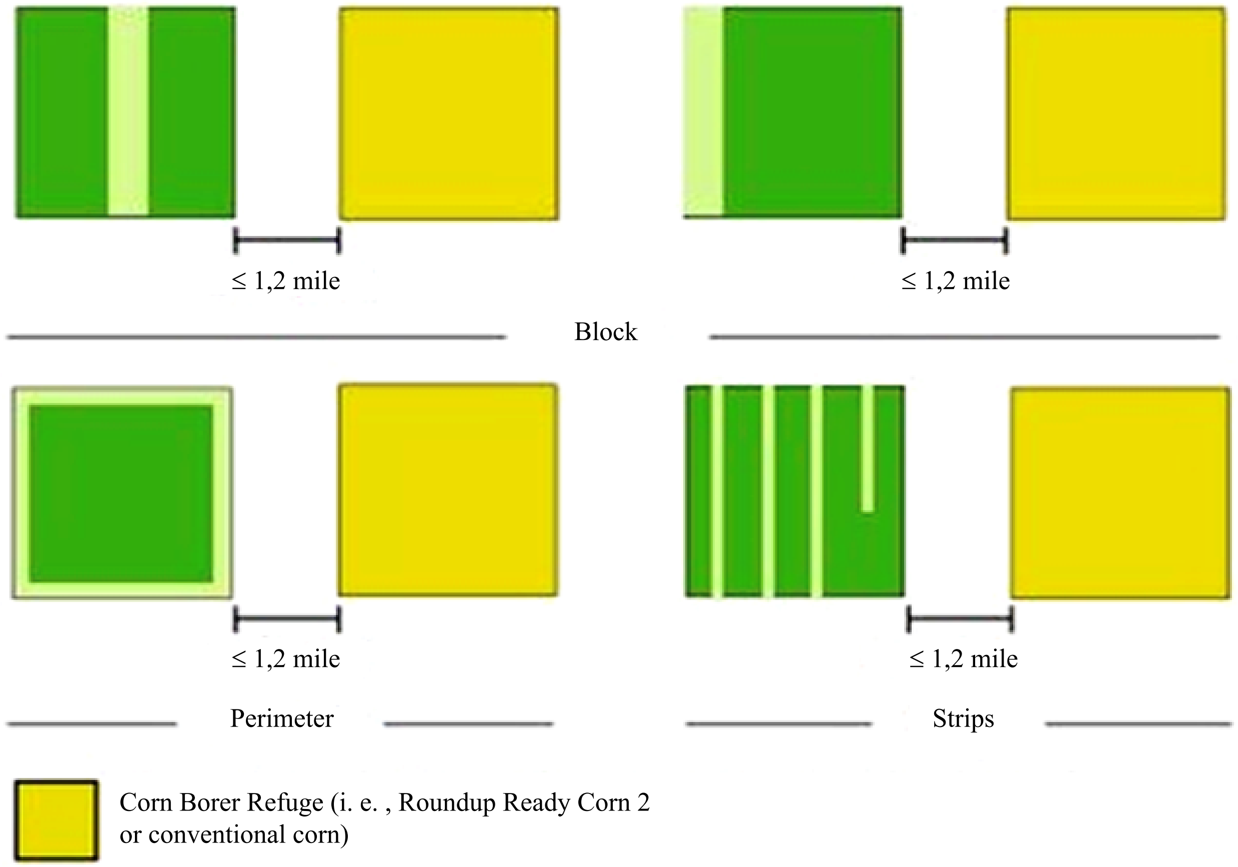

Let us consider the first type of refuge placement, where a single plot of conventional corn is located at the center of the field.

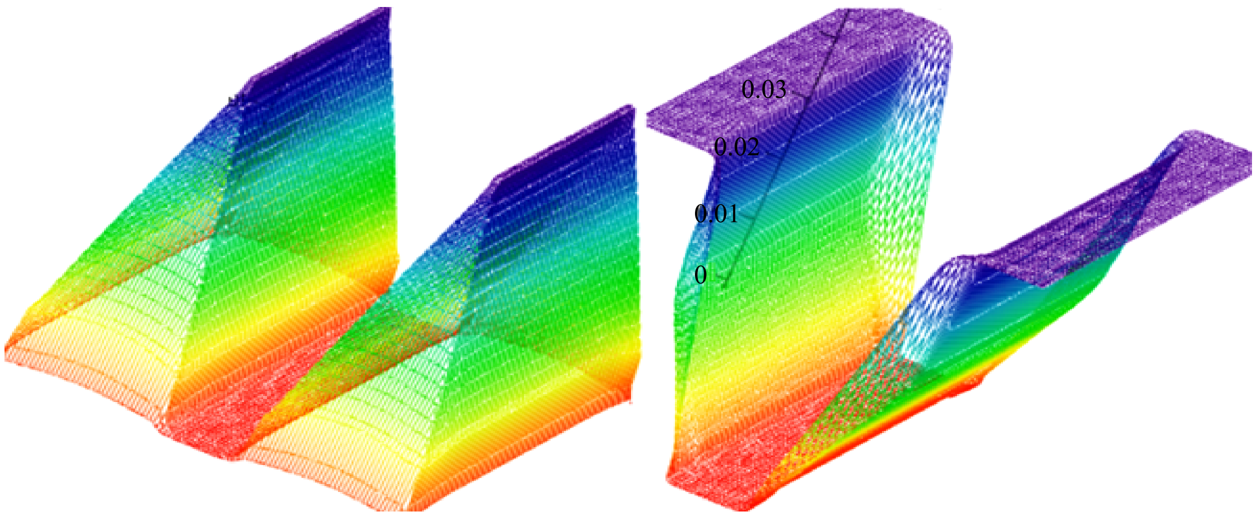

Fig. 3. Depletion of plant resource on transgenic field with a single "refuge" at t = 10

By depleting the safe areas of "conventional" crops, the pest is driven in search of food toward the transgenic region. Let us examine the depletion of plant resources by the pest in more detail. Fig. 3 illustrates two areas of depletion, where the boundary consists of conventional and transgenic crops. The plots of "conventional" crops are depleted more rapidly.

In May 2013, RapidEye began monitoring large agricultural plots from space, allowing for the first comparison between numerical research results and the actual conditions of agricultural lands. An overview of satellite images of the U.S. Corn Belt revealed a predominance of the fourth type of distribution, which is easily explained in terms of cultivation convenience and field management. The color differences between the plots (an example of the adjacency of "conventional" and modified varieties of corn is presented in Fig. 4) are attributed to the quality of the plants, their adaptability to the environment, and their immunity to pests.

Fig. 4. Proximity of conventional and modified corn varieties[1]

The influence of the spatial configuration of refuges on the effectiveness of the "high dose — refuge" strategy was investigated for fixed values of refuge percentage and pest mobility in the simplest case, where the pest's range is represented as a rectangle $\Omega = [0, L_x] \times [0, L_y]$. Numerical experiments with the demo-genetic model demonstrated that for a total moth range of 16 km by 16 km, positioning a single strip of refuge in the center of the field approximately halves the time T_{10}, significantly increasing the level of infestation of the *Bt*-field by moths. Dividing a single strip of "refuge" into several strips enhances refuge effectiveness.

A comparison of the results of numerical simulations in cases where the boundaries were also "refuges" or belonged to the main transgenic part of the field indicated the superiority of the first type of distribution.

The depletion of food with a "striped" arrangement of "refuges" is clearly illustrated in Fig. 5. Depletion occurs more rapidly at the boundaries of the area than in the central "refuges", and the presence of boundary "refuges" facilitates quicker depletion of the "conventional" crop.

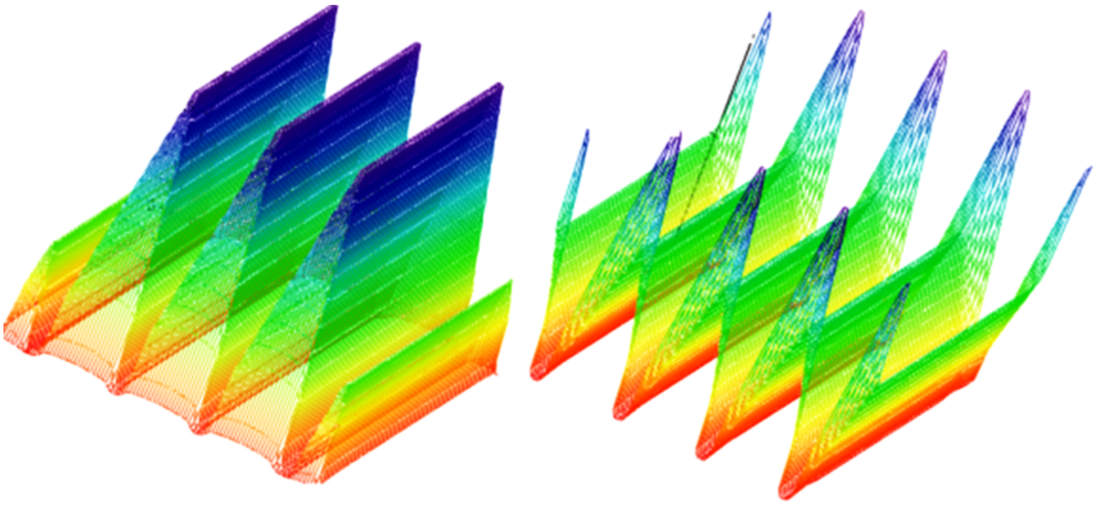

Fig. 5. Depletion of plant resource on transgenic field with four "refuges"

A similar effect is observed for refuges of rectangular or square shapes (Fig. 6 and 7). Let us consider a refuge arrangement where four square plots of "conventional" corn are positioned at the center of the transgenic field. The presence of "refuges" of varying sizes and arrangements is justified only in cases of significant height variation across the field. However, in such cases, a three-dimensional model of pest dynamics would need to be developed. The results obtained confirm our hypothesis that the distribution of "refuges" across the main field area should not touch the boundaries of the region; otherwise, we reduce the likelihood of pests accessing the "refuges".

Forecasting pest dynamics over a period of $t = 100$ reveals that the overall behavioral model of pests during resource depletion remains consistent (Fig. 7). The foliage and fruits of plants are most adversely affected by insect pests, which aligns with natural observations.

It is noteworthy that even with a single "refuge", the depletion pattern can be quite unusual, depending on the selective characteristics of the corn variety and the landscape features (Fig. 8).

[1]Photo from http://www.monsanto.com

The number of pests increases much more slowly relative to the decrease in their mortality coefficients, indicating the need to investigate the influence of other model parameters on population dynamics.

Let us now examine the dynamics of pests based on various mortality coefficients. For the European corn borer, *Ostrinia nubilalis*, this coefficient is $\mu = 6.845$. Other corn pests exhibit significantly greater survivability. In the area under consideration, let the adaptation coefficients of the genotypes to the environment be $w_{ss} = w_{rs} = 0.45$, $w_{rr} = 0.1$ (with *Bt*-resistance at 10 %), he duration of the study is set at 2 years.

Figure 9 illustrates the dynamics of concentration with a linear increase in pest survivability.

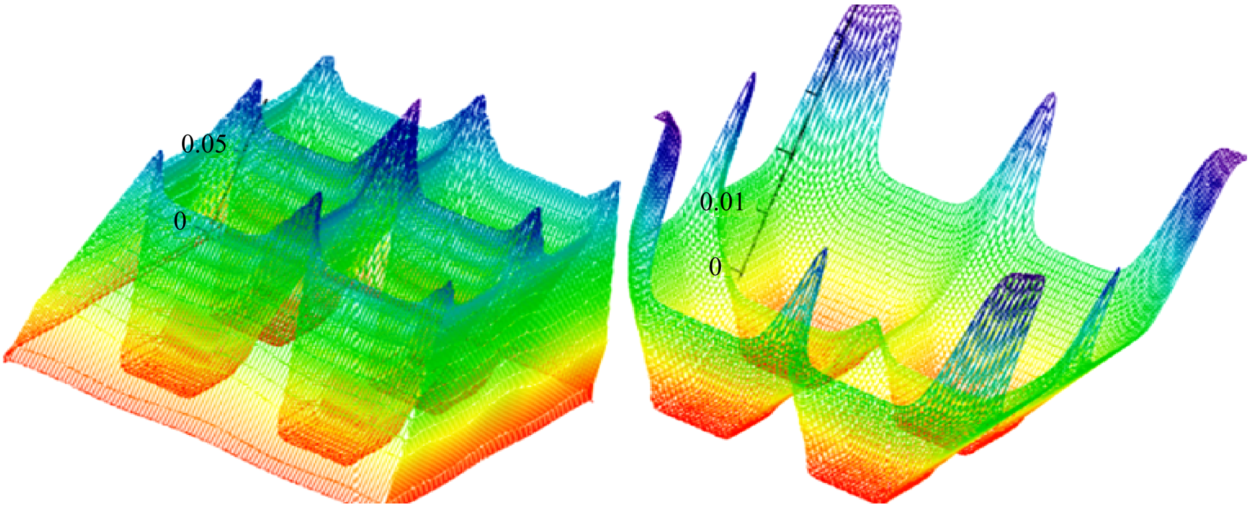

Fig. 6. Depletion of plant resource on transgenic field with four rectangular “refuges”

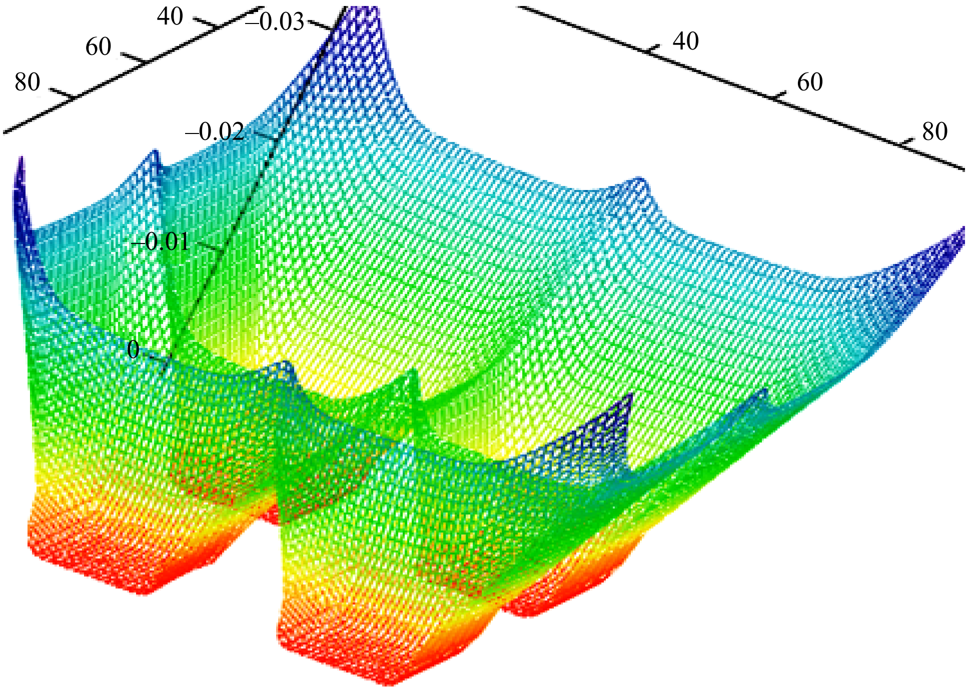

Fig. 7. Depletion of plant resource on transgenic field with four square “refuges”

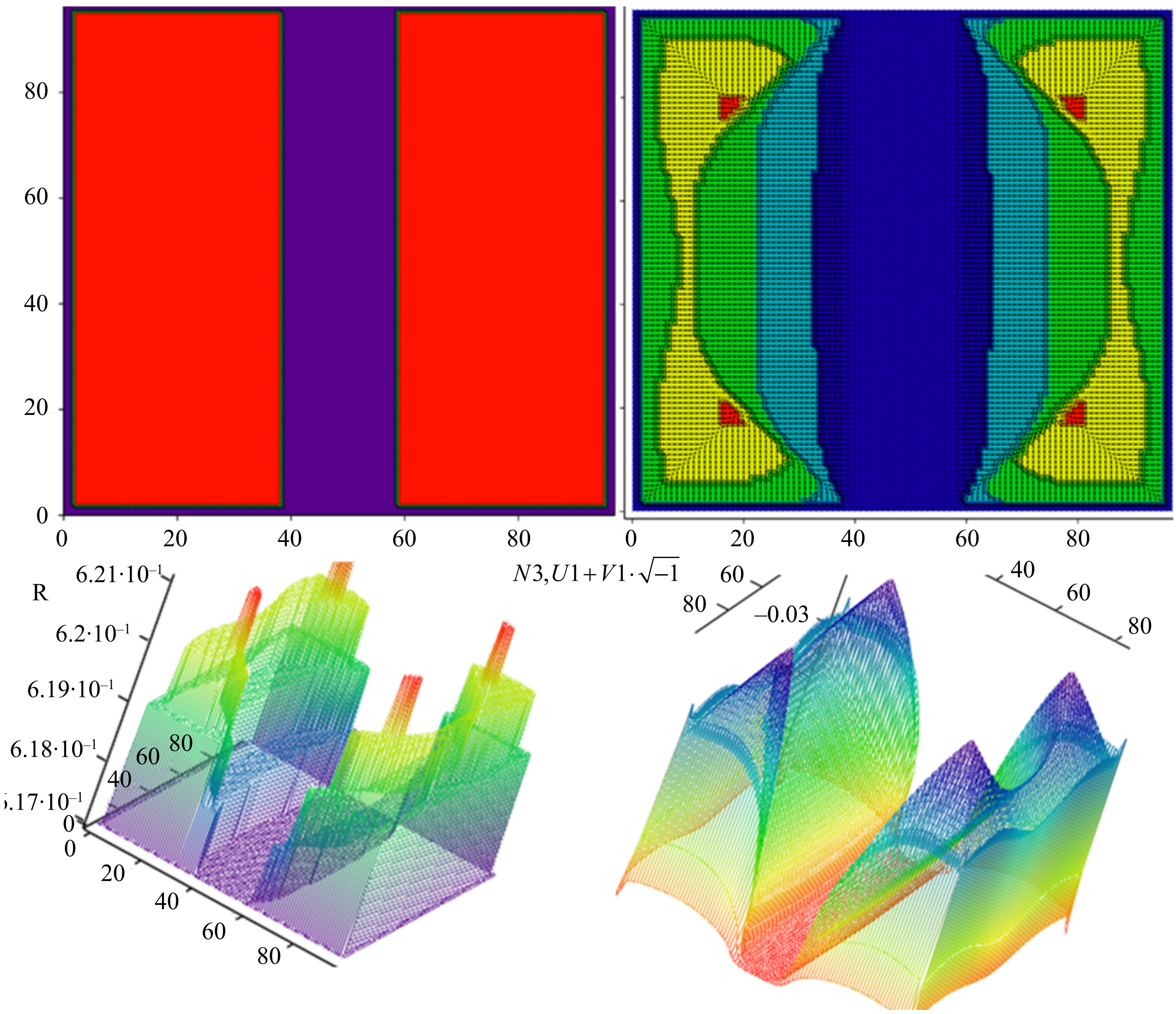

Fig. 8. Forecasting pest dynamics on a field with a single "refuge"

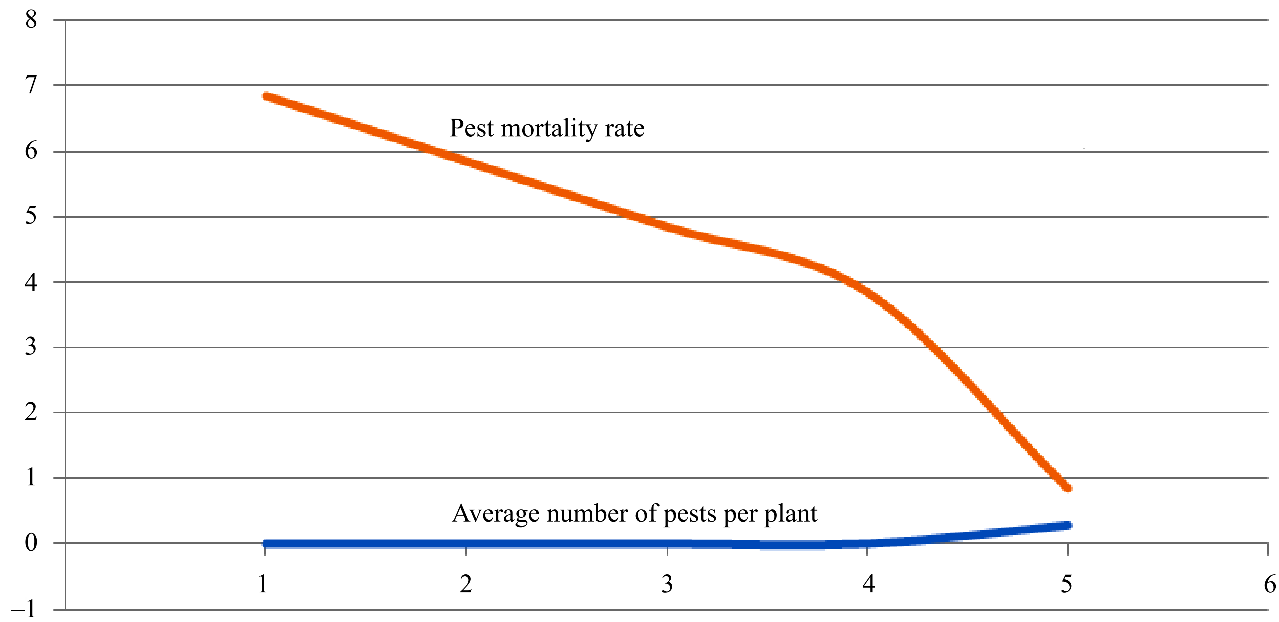

Fig. 9. Pest concentration dynamics at different mortality coefficients

Discussion and Conclusion. Despite the fact that the total area of "refuges" remains unchanged relative to the total field area at 20 %, the depletion of resources occurs faster with a larger number of "refuges" For a given habitat size increasing the number of refuges by reducing their size while maintaining the overall 20 % refuge area can decrease the effectiveness of the "high dose — refuge" strategy. It is reasonable to assume that the easier it is for pests to reach the "refuges", the quicker they lose their resistance to the toxin. To make it easier for pests to access the "refuges", it is necessary to reduce the size of the refuges while preserving the 20 % ratio of the total field area. A key feature of the model presented is the differentiation of pests based on the type of taxis they exhibit, which significantly influences the pest population dynamics.

References:

1. Kostitzin V. A. *Biologie mathèmatique*. Librairie Armand Colin. Paris. 1937. 223 p.
2. Volterra V. *Leçons sur la theorie mathematique de la lutte pour la vie*. Paris. Gauthier Villar. 1931. 222 p.
3. Lotka A. J. *Elements of Mathematical Biology*. New York, NY: Dover Publ. Inc.; 1956. 208 p.
4. Svirizhev Y.M., Logofet D.O. *Stability of Biological Communities*. Moscow: Nauka; 1978. 352 p. (in Russ.)
5. Svirizhev Y.M., Pasekov V.P. *Fundamentals of Mathematical Genetics*. Moscow: Nauka; 1982. 512 p. (in Russ.)
6. Bazykin A.D. *Mathematical Biophysics of Interacting Populations*. Moscow: Nauka; 1985. 165 p. (in Russ.)
7. Riznichenko G.Yu., Rubin A.B. *Mathematical Models of Biological Production Processes*. Moscow: Moscow State University Press; 1993. 301 p. (in Russ.)
8. Bourguet D., Chaufaux J., Segui M. N., Buisson C., Hinton J. L., Stodola T. J., et al. Frequency of alleles conferring resistance to Bt maize in French and US corn belt populations of the European corn borer, Ostrinia nubilalis. *Theoretical and Applied Genetics*. 2003;106(7):1225–1233. https://doi.org/10.1007/s00122-002-1172-1
9. Storer N., Peck S., Gould F., Duyn, J., Kennedy G. Spatial Processes in the Evolution of Resistance in Helicoverpa zea (Lepidoptera: Noctuidae) to Bt Transgenic Corn and Cotton in a Mixed Agroecosystem: A Biology-Rich Stochastic Simulation Model. *Journal of economic entomology*. 2003;96:156–172. https://doi.org/10.1603/0022-0493-96.1.156
10. Vacher C., Bourguet D., Desquilbet M., Lemarié M., Ambec S., Hochberg M.E., Fees or refuges: which is better for the sustainable management of insect resistance to transgenic bt corn? *Biology letters*. 2006;2(2):198–202. https://doi.org/10.1098/rsbl.2005.0418
11. Vacher C., Weis A.E., Hermann D., Kossler T.M., Young C. Hochberg M.E. Impact of ecological factors on the initial invasion of bt transgenes into wild populations. *Theoretical and applied genetics*. 2004;109:806-814. https://doi.org/10.1007/s00122-004-1696-7
12. Icoz I., Saxena D., Andow D. A., Zwahlen C. and Stotzky G. Microbial populations and enzyme activities in soil in situ under transgenic corn expressing Cry proteins from Bacillus thuringiensis. *Journal of Environmental Quality*. 2008;37(2):647–662. https://doi.org/10.2134/jeq2007.0352
13. Olson D. M., Andow D. A. Patch size and edges and insect populations in landscapes. *Oecologia*. 2008;155(3):549–558. https://doi.org/10.1007/s00442-007-0933-6
14. Tyutyunov, Yu.V., Sapukhina, N.Yu., Morgulis, A.B., Govorukhin, V.N. Mathematical Model of Active Migrations as a Feeding Strategy in Trophic Communities. *Journal of General Biology*. 2001;62(3):253–262. (in Russ.)
15. Zhadanovskaya, E.A. *Modeling the Spatiotemporal Dynamics of the European Corn Borer under the Influence of Transgenic Corn*. PhD Dissertation in Physical and Mathematical Sciences. Rostov-on-Don; 2006. 171 p. (in Russ.)
16. Zhadanovskaya, E.A., Tyutyunov, Yu.V., Arditi, R. A Spatial Model of Corn Borer Resistance Development to Transgenic Corn Using the "High Dose-Refuge" Strategy. In: *Proceedings of the XXXII School-Seminar on Mathematical Modeling in Issues of Rational Nature Management. Ecology. Economics. Informatics*. Rostov-on-Don: SKNC VSH; 2004. P. 22–23. (in Russ.)
17. Tyutyunov Yu., Zhadanovskaya E., Bourguet D., Arditi R. Landscape refuges delay resistance of the European Corn Borer to Bt-maize: a demo-genetic dynamic model. *Theoretical population biology*. 2008;74(1):138–146. https://doi.org/10.1016/j.tpb.2008.05.005
18. Sukhinov, A.I., Kazharova, I.A. The Structure of the Spatial Distribution of Corn as a Consequence of Dynamic Self-Organization Processes. In: *Proceedings of the International Russian-Azerbaijan Symposium "Mixed-Type Equations and Related Problems of Analysis and Informatics"*. Nalchik: Elbrus Journal Editorial; 2008. P. 157–158. (in Russ.)
19. Pasekov, V.P. Population Variability and Biometric Models of Trait Coordination in Organisms. *Journal of General Biology*. 2010;71(1):7–18. (in Russ.)
20. Ilyichev, V.G. Evolutionary Stability of Biological Communities. *Journal of General Biology*. 2010;71(1):63–74. (in Russ.)
21. Lyapunova, I.A. On a Demo-Genetic Model of Insect Adaptation to Changes in the Food Base. *Izvestiya SFedU. Technical Sciences*. 2013;4(141):235–239. (in Russ.)
22. Sukhinov, A.I., Chistyakov, A.E., Protsenko, E.A., Protsenko, S.V. *Modeling Complex Systems*. Rostov-on-Don: Don State Technical University; 2019. 241 p. (in Russ.)

23. Sukhinov, A.I., Chistyakov, A.E., Sidoryakina, V.V., Protsenko, S.V. A Difference Scheme with Optimal Weight for the Diffusion-Convection Equation. *Computational Methods and Programming*. 2019;20(3):283–292. (in Russ.) https://doi.org/10.26089/NumMet.v20r325

About the Authors:

Alexander I. Sukhinov, Corresponding member of RAS, Dr.Sci. (Phys.-Math), Professor, Director of the Research Institute "Mathematical Modelling and Forecasting of Complex Systems", Don State Technical University (1, Gagarin Sq., Rostov-on-Don, 344003, Russian Federation), ORCID, MathSciNet, SPIN-code, ResearcherID, ScopusID,, sukhinov@gmail.com

Irina A. Bugayeva, PhD in Technology, Associate Professor at the Institute of Computer Technologies and Information Security, Southern Federal University (105/42, B. Sadovaya St., Rostov-on-Don, 344006, Russian Federation), ORCID, MathSciNet, SPIN-code, ResearcherID, ScopusID, ialyapunova@sfedu.ru

Claimed Contributorship: **all authors have made an equivalent contribution to the preparation of the publication.**

Conflict of Interest Statement: **the authors declare no conflict of interest.**

All authors have read and approved the final manuscript.

Об авторах:

Александр Иванович Сухинов, член-корреспондент РАН, доктор физико-математических наук, профессор, директор НИИ Математического моделирования и прогнозирования сложных систем, Донской государственный технический университет (344003, Российская Федерация, г. Ростов-на-Дону, пл. Гагарина, 1), ORCID, MathSciNet, SPIN-код, ResearcherID, ScopusID, sukhinov@gmail.com

Ирина Артуровна Бугаева, кандидат технических наук, доцент института компьютерных технологий и информационной безопасности, Южный федеральный университет (344006, Российская Федерация г. Ростов-на-Дону, ул. Б. Садовая, 105/42), ORCID, MathSciNet, SPIN-код, ResearcherID, ScopusID, ialyapunova@sfedu.ru

Заявленный вклад авторов: **все авторы сделали эквивалентный вклад в подготовку публикации.**

Конфликт интересов: **авторы заявляют об отсутствии конфликта интересов.**

Все авторы прочитали и одобрили окончательный вариант рукописи.

Received / Поступила в редакцию 26.08.2024
Revised / Поступила после рецензирования 09.09.2024
Accepted / Принята к публикации 12.09.2024

MATHEMATICAL MODELLING
МАТЕМАТИЧЕСКОЕ МОДЕЛИРОВАНИЕ

Original Theoretical Research

UDC 519.6
https://doi.org/10.23947/2587-8999-2024-8-3-23-33

A Modified Bubnov-Galerkin Method for Solving Boundary Value Problems with Linear Ordinary Differential Equations

Natalya K. Volosova[1], **Konstantin A. Volosov**[2], **Aleksandra K. Volosova**[2], **Dmitriy F. Pastukhov**[3] ✉, **Yuriy F. Pastukhov**[3]
[1] Bauman Moscow State Technical University, Moscow, Russian Federation
[2] Russian University of Transport, Moscow, Russian Federation
[3] Polotsk State University named after Euphrosyne of Polotsk, Novopolotsk, Republic of Belarus

Abstract
Introduction. The paper considers the solution of boundary value problems on an interval for linear ordinary differential equations, in which the coefficients and the right-hand side are continuous functions. The conditions for the orthogonality of the residual equation to the coordinate functions are supplemented by a system of linearly independent boundary conditions. The number of coordinate functions m must exceed the order n of the differential equation.
Materials and Methods. To numerically solve the boundary value problem, a system of linearly independent coordinate functions is proposed on a symmetric interval $[-1,1]$, where each function has a unit Chebyshev's norm. A modified Petrov-Galerkin method is applied, incorporating linearly independent boundary conditions from the original problem into the system of linear algebraic equations. An integral quadrature formula with twelfth-order error is used to compute the scalar product of two functions.
Results. A criterion for the existence and uniqueness of a solution to the boundary value problem is obtained, provided that n linearly independent solutions of the homogeneous differential equation are known. Formulas are derived for the matrix coefficients and the coefficients of the right-hand side in the system of linear algebraic equations for the vector expansion of the solution in terms of the coordinate function system. These formulas are obtained for second- and third-order linear differential equations. The modified Bubnov-Galerkin method is formulated for differential equations of arbitrary order.
Discussion and Conclusions. he derived formulas for the generalized Bubnov-Galerkin method may be useful for solving boundary value problems involving linear ordinary differential equations. Three boundary value problems with second- and third-order differential equations are numerically solved, with the uniform norm of the residual not exceeding 10^{-11}.

Keywords: numerical methods, ordinary differential equations, boundary value problems, Galerkin method, hydrodynamics

For citation. Volosova N.K., Volosov K.A., Volosova A.K., Pastukhov D.F., Pastukhov Yu.F. A Modified Bubnov-Galerkin Method for Solving Boundary Value Problems with Linear Ordinary Differential Equations. *Computational Mathematics and Information Technologies*. 2024;8(3):23–33. https://doi.org/10.23947/2587-8999-2024-8-3-23-33

Оригинальное теоретическое исследование

Модифицированный метод Бубнова-Галеркина для решения краевых задач с линейным обыкновенным дифференциальным уравнением

Н.К. Волосова[1], **К.А. Волосов**[2], **А.К. Волосова**[2], **Д.Ф. Пастухов**[3]✉, **Ю.Ф. Пастухов**[3]
[1] Московский государственный технический университет им. Н.Э. Баумана, г. Москва, Российская Федерация
[2] Российский университет транспорта, г. Москва, Российская Федерация
[3] Полоцкий государственный университет им. Евфросинии Полоцкой, г. Новополоцк, Республика Беларусь
✉dmitrij.pastuhov@mail.ru

Аннотация
Введение. Рассматривается решение краевых задач на отрезке с линейными обыкновенными дифференциальными уравнениями, в которых коэффициенты и правая часть являются непрерывными функциями. Условия ортогональности невязки уравнения координатным функциям дополняются системой линейно независимых краевых условий задачи. Число координатных функций m должно быть больше порядка n дифференциального уравнения.
Материалы и методы. Для численного решения краевой задачи предложена система линейно независимых координатных функций на симметричном отрезке $[-1,1]$ с единичной нормой Чебышева каждой функции системы. Применен модифицированный метод Петрова-Галеркина с включением линейно независимых краевых условий исходной задачи в систему линейных алгебраических уравнений. Применена интегральная квадратурная формула с двенадцатым порядком погрешности для вычисления скалярного произведения двух функций.
Результаты исследования. Получен критерий существования и единственности решения краевой задачи, при условии, что известны n линейно независимых решений однородного дифференциального уравнения. Получены формулы для матричных коэффициентов и коэффициентов правой части системы линейных алгебраических уравнений для вектора разложения решения по системе координатных функций. Формулы получены для линейных дифференциальных уравнений второго и третьего порядков. Модифицированный метод Бубнова-Галеркина сформулирован для уравнения произвольного порядка.
Обсуждение и заключение. Полученные формулы обобщенного метода Бубнова-Галеркина могут быть полезными для решения краевых задач с линейными обыкновенными дифференциальными уравнениями. Численно решены три краевых задачи с уравнениями второго и третьего порядков, равномерная норма невязки не превышает 10^{-11}.

Ключевые слова: численные методы, обыкновенные дифференциальные уравнения, краевые задачи, метод Галеркина, гидродинамика

Для цитирования. Волосова Н.К., Волосов К.А., Волосова А.К., Пастухов Д.Ф., Пастухов Ю.Ф. Модифицированный метод Бубнова-Галеркина для решения краевых задач с линейным обыкновенным дифференциальным уравнением. *Computational Mathematics and Information Technologies*. 2024;8(3):23–33. https://doi.org/10.23947/2587-8999-2024-8-3-23-33

Introduction. Boundary value problems involving ordinary differential equations can be classified by the order of the equation. For instance, in hydrodynamics problems, these equations may be of the first [1], second [2], or third order [3–4].

The most well-known methods for solving boundary value problems on an interval with ordinary differential equations are the sweep method and the shooting method [5]. In these methods, the unknown function is sought on a given grid (the so-called grid function). In this study, the solution is found in a functional form using a system of linearly independent coordinate functions that are smooth and bounded in absolute value on the symmetric interval $[-1, 1]$. The unknown solution function is expanded in a basis of linearly independent coordinate functions. Using the Bubnov-Galerkin method [6], where the residual of the differential or integral equation is orthogonal to the coordinate functions, the expansion coefficients of the solution are determined from the orthogonality conditions.

In [7], it was shown that in the simplest classical variational problem (a boundary value problem), the solution must be sought in the class of admissible functions defined by the boundary conditions. This idea was used by the authors in the modified Bubnov-Galerkin method, incorporating $n-1$ (where n is the order of the equation) linearly independent boundary conditions into a system of m linear algebraic equations. The number of orthogonality conditions is thus $m-n+1$ (where m is the number of coordinate functions). In this study, the modified Bubnov-Galerkin method is applied to boundary value problems involving second- and third-order equations.

Materials and Methods. Let the unknown function $u(x) \in C^n[a,b]$, which is continuously differentiable n times, be the solution of a boundary value problem with an ordinary differential equation of order n with variable coefficients $g_i(x), i = \overline{0,n}$

$$\begin{cases} L[u(x)] = f(x),\ x \in (a,b), \\ L[u(x)] \equiv \left(\sum_{i=0}^{n} g_i(x) \dfrac{d^i}{dx^i} \right) u(x). \end{cases} \quad (1)$$

$$\begin{cases} \sum_{i=0}^{n-1} \left(\alpha_\mu^i u^{(i)}(a) \right) = \gamma_\mu,\ \mu = \overline{1,k}, \\ \sum_{i=0}^{n-1} \left(\beta_\mu^i u^{(i)}(b) \right) = \gamma_\mu,\ \mu = \overline{k+1,n}. \end{cases} \quad (2)$$

In the boundary value problem (1)–(2), the functions $g_i(x)(i = \overline{0,n}), f(x) \in C[a,b]$ are given and continuous on the segment [a, b]. The first k equations in the system (2) represent the boundary conditions at point $x = a$, and the last $n–k$ equations represent the boundary conditions at point $x = b$. For the closure of problem (1), it is necessary that the total number of boundary conditions be equal to n. The coefficient matrices $\alpha_\mu^i, \beta_\mu^i, i = \overline{0,n-1}, \mu = \overline{1,n}$, as well as the numbers $\gamma_\mu,\ \mu = \overline{1,n}$ are given.

Boundary conditions of the form (2) are called separated. The relationship between the numbers of boundary conditions $\alpha_\mu^i, \beta_\mu^i$ determines the existence and uniqueness of the solution of the boundary value problem (1)–(2).

Statement 1. Let n linearly independent particular solutions of the homogeneous equation (1) $U_j(x), j = \overline{1,n}$ be given. Then the boundary value problem (1)–(2) has a unique solution if and only if the following condition $\det A_{\mu j} \neq 0, \mu = \overline{1,n}, j = \overline{1,n}$ is satisfied:

$$A_{\mu j} = \begin{cases} \sum_{i=0}^{n-1} \alpha_\mu^i U_j^{(i)}(a), \mu = \overline{1,k} \\ \sum_{i=0}^{n-1} \beta_\mu^i U_j^{(i)}(b), \mu = \overline{k+1,n}. \end{cases}$$

Proof. Let us write the general solution of equation (1) as $u(x) = \sum_{j=1}^{n} U_j(x) D_j + \overline{u(x)}, j = \overline{1,n}$, where D_j are arbitrary integration constants, $\overline{u(x)}$ is a particular solution of the non-homogeneous equation (1), and $U_j(x)$ are linearly independent particular solutions of the homogeneous equation (1).

Substituting this solution $u(x)$ into the boundary conditions (2):

$$\begin{gathered} \sum_{i=0}^{n-1} \left(\alpha_\mu^i u^{(i)}(a) \right) = \sum_{i=0}^{n-1} \alpha_\mu^i \left(\sum_{j=1}^{n} U_j^{(i)}(a) D_j + \overline{u^{(i)}(a)} \right) = \gamma_\mu \Leftrightarrow, \\ \sum_{j=1}^{n} \left(\sum_{i=0}^{n-1} \alpha_\mu^i U_j^{(i)}(a) \right) D_j = \gamma_\mu - \sum_{i=0}^{n-1} \alpha_\mu^i \overline{u^{(i)}(a)}, \mu = \overline{1,k}. \end{gathered} \quad (3)$$

Similarly, for the point $x = b$, we obtain:

$$\sum_{j=1}^{n} \left(\sum_{i=0}^{n-1} \beta_\mu^i U_j^{(i)}(b) \right) D_j = \gamma_\mu - \sum_{i=0}^{n-1} \beta_\mu^i \overline{u^{(i)}(b)}, \mu = \overline{k+1,n}. \quad (4)$$

The resulting non-homogeneous system of n linear algebraic equations (3)–(4) with respect to the n unknowns D_j, j = 1, n as a unique solution if and only if the determinant of the matrix $\det A_{\mu j} \neq 0, \mu = \overline{1,n}, j = \overline{1,n}$, where

$$A_{\mu j} = \begin{cases} \sum_{i=0}^{n-1} \alpha_\mu^i U_j^{(i)}(a), \mu = \overline{1,k} \\ \sum_{i=0}^{n-1} \beta_\mu^i U_j^{(i)}(b), \mu = \overline{k+1,n}. \end{cases} \quad (5)$$

Statement 1 is proven.

Let us now consider a simple case of problem (1) involving a second-order ordinary differential equation (ODE) with Dirichlet boundary conditions:

$$\begin{cases} L[u(x)] = f(x),\ x \in (a,b) \\ L[u(x)] \equiv \left[g_2(x)\dfrac{d^2}{dx^2} + g_1(x)\dfrac{d}{dx} + g_0(x) \right] u(x) \\ u(a) = u_a, u(b) = u_b. \end{cases} \tag{6}$$

Let us generalize the Bubnov-Galerkin method, as proposed in work [6] for solving Fredholm integral equations of the second kind, to the solution of the Dirichlet problem with the second-order ODE (6).

We begin by selecting a system of basis (coordinate) functions $\varphi_i(x)$:

$$\{\varphi_i(x)\}_{i=0}^{m} = \left\{ \left(\frac{2x-a-b}{b-a} \right)^i, x \in [a,b], i = \overline{0,m} \right\}. \tag{7}$$

Statement 2. The coordinate functions of the system (7) $\varphi_i(x) \in C^\infty[a,b]$ are bounded in modulus, differentiable any number of times, and linearly independent.

Proof will be conducted by contradiction. We use a linear mapping $z = \dfrac{2x-a-b}{b-a} \in [-1,1], x \in [a,b]$, which bijectively maps the interval $x \in [a,b]$ onto a symmetric interval $z \in [-1,1]$. Such a straightforward method is employed by the authors of the textbook [5] in the task of constructing integral quadrature formulas. Assume that the system of coordinate functions is linearly dependent, and taking into account the variable z it takes the form $\left\{ \varphi_i(z) = z^i, z \in [-1,1], i = \overline{0,m} \right\}$. If the system of functions is linearly dependent, then there exists a non-trivial solution $(\alpha_0, \alpha_1, \dots \alpha_m)$ to the equation $\alpha_0 + \alpha_1 z + \alpha_2 z^2 + \dots + \alpha_m z^m \equiv 0 \forall z \in [-1,1]$.

The last equation has no more than m real solutions, whereas a solution is required for all points of the interval $z \in [-1,1]$. This contradiction proves the linear independence of the functions in system (7). The functions in (7) are infinitely continuously differentiable with respect to the variable x as they are polynomials of finite degree, and they are also bounded since $\|\varphi_i\|_C = \max\limits_{z\in[-1,1]} \left| z^i \right| = 1$. **Statement 2 is proven.**

We will apply the Bubnov-Galerkin method using the system of linearly independent coordinate functions (7) to solve the Dirichlet boundary value problem (6). The symmetric interval $z \in [-1,1]$ in our problem results in a consistent order of error at the nodes symmetrically located with respect to the midpoint of the interval $c = (a+b)/2$ and generally reduces the norm of the error.

Let us express the solution as a series expansion in terms of the linearly independent system of coordinate functions:

$$u(x) = u(c) + \sum_{j=1}^{m} \varphi_j(x) C_j = u(c) + \sum_{j=1}^{m} \left(\frac{2(x-c)}{b-a} \right)^j C_j. \tag{8}$$

In equation (8), the coefficients C_j are unknown and need to be determined.

From equation (8), we derive the identity $u(c) = u(c)$, which resembles the expansion of an unknown function in a Taylor series centered at some point $x = c = (a+b)/2$, although we do not know either the function itself or its derivatives. Substituting equation (8) into equation (6), we obtain the residual (discrepancy) of equation (6):

$$R(u((x)) = L[u(x)] - f(x) = L\left(u(c) + \sum_{j=1}^{m} \varphi_j(x) C_j \right) - f(x) = L\big(u(c)\big) + \sum_{j=1}^{m} L\varphi_j(x) C_j - f(x).$$

The Bubnov-Galerkin method is orthogonal, so we require the residual to be orthogonal to the maximum number of coordinate functions, $\left\{1, z, z^2, \dots, z^{m-2}\right\}$. Specifically, we impose orthogonality with respect to m–1 functions that contribute the most to the residual of equation (6):

$$\left\langle R\big(u(x)\big), \varphi_i(x) \right\rangle = 0, \overline{i = 0, m-2} \Leftrightarrow \sum_{j=1}^{n} \left\langle L\varphi_j(x), \varphi_i(x) \right\rangle C_j = \left\langle f(x) - L\big(u(c)\big), \varphi_i(x) \right\rangle, i = \overline{0, m-2}. \tag{9}$$

In equation (9), we introduce the notation:

$$\left\langle f, g \right\rangle = \int_a^b f(x) g(x) dx,\ L\big(u(c)\big) = g_0(x) u(c) = g_0(x) u_c.$$

Unlike the method described in [6, p. 140], the last condition, numbered m, for the system of linear algebraic equations (SLAE) with respect to m unknowns $C_j,\ j = \overline{1,m}$, will be derived from the boundary conditions

$$\frac{u_b - u_a}{2} = C_1 + C_3 + \dots + \begin{cases} C_{m-1}, m = 2l \\ C_m, m = 2l+1. \end{cases} \tag{10}$$

Let us demonstrate the validity of equation (10). At the endpoints of the interval, specifically at the points $x = a, x = b$, we can use the expansion given in equation (8) to obtain:

$$u(a) \equiv u_a = u(c) + \sum_{j=1}^{m} \left(\frac{(2a-a-b)}{b-a} \right)^j C_j = u_c + \sum_{j=1}^{m} (-1)^j C_j, u(b) \equiv u_b = u(c) + \sum_{j=1}^{m} \left(\frac{(2b-a-b)}{b-a} \right)^j C_j = u_c + \sum_{j=1}^{m} C_j.$$

By summing the two most recent equations and expressing $u(c) = u_c$, we obtain

$$u_c = \left(\frac{u_a + u_b}{2} \right) - C_2 - C_4 - \ldots - \begin{cases} C_m, m = 2l \\ C_{m-1}, m = 2l+1. \end{cases} \tag{11}$$

Similarly, by subtracting the first equation u_b from the second equation u_a and expressing $\frac{u_b - u_a}{2}$, we obtain equation (10). Next, we substitute the value $u(c)$ obtained from equation (11) into the right-hand side of equation (9). Then, we move all terms involving C_j to the left-hand side of equation (9) to obtain the system of linear algebraic equations (SLAE) for the coefficients C_j:

$$\sum_{j=1}^{m} a_{i,j} C_j = \overline{f_i},\ i = \overline{0, m-1}. \tag{12}$$

The elements of the matrix $a_{i,j}, i = \overline{0, m-1}, j = \overline{1, m}$ and the coefficients on the right-hand side $\overline{f_i}$ in the system of equations (12) are defined as follows:

$$a_{i,j} = \begin{cases} \left\langle L\varphi_j, \varphi_i \right\rangle, \text{если}\, j \equiv 1 (\mathrm{mod}\, 2), i = \overline{0, m=2} \\ \left\langle L(\varphi_j - 1), \varphi_i \right\rangle, \text{если}\, j \equiv 0 (\mathrm{mod}\, 2), i = \overline{0, m-2} \\ 1, \text{если}\ i = m-1,\ j \equiv 1 (\mathrm{mod}\, 2) \\ 0, \text{если}\ i = m-1,\ j \equiv 1 (\mathrm{mod}\, 2) \end{cases},$$

$$\overline{f_i} = \begin{cases} \left\langle f(x) - L\left(\frac{u_a + u_b}{2} \right), \varphi_i(x) \right\rangle, \text{если}\ i = \overline{0, m-2} \\ \frac{u_b - u_a}{2}, \text{если}\ i = m-1 \end{cases},$$

$$L\left(\frac{u_a + u_b}{2} \right) = \left(\frac{u_a + u_b}{2} \right) g_0(x).$$

Remark 1. It is not possible to use both Dirichlet boundary conditions $u(a)$, $u(b)$ directly in the system of linear algebraic equations (12) because these conditions are linearly dependent.

Proof. Let us substitute the value of $u(c) = u_c$ from equation (11) into the expressions for $u(a)$, $u(b)$:

$$u(c) = \left(\frac{u_a + u_b}{2} \right) - C_2 - C_4 - \ldots - \begin{cases} C_m, m = 2l \\ C_{m-1}, m = 2k+1 \end{cases}, u_a = u_c + \sum_{j=1}^{m} (-1)^j C_j = \left(\frac{u_a + u_b}{2} \right) - \left(C_1 + C_3 + \ldots + \begin{cases} C_{m-1}, m = 2l \\ C_m, m = 2l+1 \end{cases} \right).$$

The last expression is equivalent to (10).

$$u_b = u_c + \sum_{j=1}^{m} C_j = \left(\frac{u_a + u_b}{2} \right) + C_1 + C_3 + \ldots + \begin{cases} C_{m-1}, m = 2l \\ C_m, m = 2l+1. \end{cases}$$

The last equation is equivalent to equation (10), which proves the linear dependence of the boundary conditions.

Remark 2. In equations (12), for the matrix coefficients a_{ij} in even columns, the differential operator L acts on the non-positive function $\varphi_j(x)$–1, and in odd columns on the alternating coordinate function $\varphi_j(x)$. If the determinant of the matrix in the SLAE (12) is non-zero, then the numerical solution of (12) is unique. Let us now write the differentiation formulas for the linear operator L as defined in equation (6), applied to the coordinate functions from equation (8):

$$\begin{cases} L\varphi_0 = g_0(x), \text{если}\, j = 0, \\ L\varphi_1 = \frac{2g_1(x)}{(b-a)} + g_0(x)\left(\frac{2x-a-b}{b-a} \right), \text{если}\, j = 1, \\ L\varphi_j = 4j(j-1)g_2(x)\frac{(2x-a-b)^{j-2}}{(b-a)^j} + 2jg_1(x)\frac{(2x-a-b)^{j-1}}{(b-a)^j} + g_0(x)\left(\frac{2x-a-b}{b-a} \right)^j, \text{если}\, j \geq 2. \end{cases} \tag{13}$$

Considering (11), the numerical solution of the Dirichlet problem (6) can be reduced to expression (14) by converting formula (8):

$$u(x)=\left(\frac{u_a+u_b}{2}\right)+\sum_{j=1}^{m}\left[\left(\frac{(2x-a-b}{b-a}\right)^j+\left(\frac{-1+(-1)^{j+1}}{2}\right)\right]C_j. \quad (14)$$

It follows from (12) that the vector C included in formula (14) has the form $C = A^{-1}\overline{f}$.

Let us estimate in absolute value $u(x)$ based on the given formula $C = A^{-1}f$

$$|u(x)|\le\frac{|u_a|+|u_b|}{2}+2\sum_{j=1}^{m}|C_j|\le\frac{|u_a|+|u_b|}{2}+2m\max_{j=\overline{1,m}}C_j=\frac{|u_a|+|u_b|}{2}+2m\|C\|_C\le\frac{|u_a|+|u_b|}{2}+2m\|A^{-1}\|_C\|f\|_C\Rightarrow$$

$$\|u\|_C\le\frac{|u_a|+|u_b|}{2}+2m\|A^{-1}\|_C\|\overline{f}\|_C.$$

It is known that the norm $\|B\|_C$ of an arbitrary square matrix $B(m\times m)$ is determined by the formula $\|B\|_C=\max_{i=\overline{1,m}}\sum_{j=1}^{m}|b_{i,j}|$.

In [9], a composite quadrature integral formula with a uniform step and with the 12th order of error $O(h^{12})$ is obtained, which is used by the program to calculate all matrix elements a_{ij}, as well as the coefficients of the right side: $\overline{f_i}$ of SLAE (12) through the scalar product of two functions:

$$\langle y_1,y_2\rangle=\int_a^b y_1(x)y_2(x)dx=5h\sum_{i=0}^{n_1}y_1(x_i)y_2(x_i)C_i+O(h^{12}),\ n_1=10p,\ h=\frac{b-a}{n_1},\ p\in N, \quad (15)$$

where the weight coefficients of the integral quadrature formula (15) are determined by the value of the remainder modulo 10 of the node number of the uniform grid i:

$$C_i=\begin{cases}\dfrac{16067}{299376},\text{если } i=0 \text{ или } i=n_1,\\ \dfrac{16067}{149688},\text{если } i\equiv 0\ (\mathrm{mod}\,10)\text{ и } (0<i<n_1),\\ \dfrac{26575}{74844},\text{если } i\equiv 1\ (\mathrm{mod}\,10)\text{ или } i\equiv 9\ (\mathrm{mod}\,10),\\ \dfrac{-16175}{99792},\text{если } i\equiv 2\ (\mathrm{mod}\,10)\text{ или } i\equiv 8\ (\mathrm{mod}\,10),\\ \dfrac{5675}{6237},\text{если } i\equiv 3\ (\mathrm{mod}\,10)\text{ или } i\equiv 7\ (\mathrm{mod}\,10),\\ \dfrac{-4825}{5544},\text{если } i\equiv 4\ (\mathrm{mod}\,10)\text{ или } i\equiv 6\ (\mathrm{mod}\,10),\\ \dfrac{17807}{12474},\text{если } i\equiv 5\ (\mathrm{mod}\,10).\end{cases}$$

Here are examples of numerical solution of boundary value problems by the algorithm (12)–(15).

Example 1 [10]. Solve the Dirichlet boundary value problem (16)

$$y''-y=2x,\ y(0)=0,\ y(1)=-1,\ x\in[0,1]. \quad (16)$$

The exact solution $y(x)=sh(x)/sh(1)-2x$.

A program in the Fortran language, where functions and variables are set with double precision according to the algorithm (12)–(15), gives the Chebyshev vector norm of the difference between the exact and approximate solution $\|y-u\|_C=4{,}218847493575595\mathrm{E}-015$, if the number of coordinate functions $m=11$, the number of intervals for calculating the scalar product of functions by formula (15) on a uniform grid is $n_1=50$, $\|y-u\|_C=\max_{i=0,n_1}|y(x_i)-u(x_i)|,\ x_i=a+hi,\ h=\dfrac{b-a}{n_1}$.

The inverse matrix A^{-1} n the system of linear algebraic equations (12) is calculated by the msimsl linear algebra library to find the vector of expansion coefficients $C_j,\ j=\overline{1,m}$.

Example 2 [9]. Solve the Dirichlet problem for the Poisson equation on a rectangle

$$\begin{cases}u_{xx}+u_{yy}=e^y\sin x,\ \ 0<x<\pi, 0<y<\pi\\ u|_{x=0}=u|_{x=\pi}=u|_{y=0}=u|_{y=\pi}=0.\end{cases}$$

We are looking for a solution to the problem in the form $u(x)=\sin(x)f(y)$. This choice of solution automatically fulfills two boundary conditions $u|_{y=0}=u|_{y=\pi}=0$. Substituting the solution $u(x)$ into the Poisson equation $\sin(x)\left(f''(y)-f(y)\right)=e^y\sin(x), \forall x\in(0,\pi)$, we obtain the Dirichlet boundary value problem for $f(y)$:

$$\begin{cases} f''(y)-f(y)=e^y \\ f(0)=f(\pi)=0. \end{cases} \tag{17}$$

The last Dirichlet boundary condition $f(0)=f(\pi)=0$ in (17) fulfills the boundary conditions of the original problem $u|_{y=0}=u|_{y=\pi}=0$.

The general solution of the homogeneous equation (17) $f''(y)-f(y)=0$ can be written as $f_{o,o}(y)=A\operatorname{ch}(y)+B\operatorname{sh}(y)$, and the partial solution of the inhomogeneous equation is sought in the form

$$f_ч(y)=Cye^y, f_ч''(y)=Ce^y\left(y+2\right), f_ч''-f_ч=Ce^y\left(y+2\right)-Cye^y=e^y \Leftrightarrow 2C=1, C=\frac{1}{2}.$$

Let's write down the general solution of the inhomogeneous equation (17) as

$$f_{o,н}(y)=A\operatorname{ch}(y)+B\operatorname{sh}(y)+\frac{ye^y}{2}, f_{o,н}(0)=0\Rightarrow A=0, f_{o,н}(\pi)=0\Rightarrow B=\frac{-\pi e^\pi}{2\operatorname{sh}(\pi)},$$

$f(y)=\dfrac{ye^y\operatorname{sh}(\pi)-\pi e^\pi\operatorname{sh}(y)}{2\operatorname{sh}(\pi)}, u(x,y)=\left(\dfrac{ye^y\operatorname{sh}(\pi)-\pi e^\pi\operatorname{sh}(y)}{2\operatorname{sh}(\pi)}\right)\sin(x)$ the exact solution of the problem from Example 2.

Solving numerically the boundary value problem (17) using the algorithm (12)–(15), we obtain the Chebyshev norm for the difference between the numerical and approximate solutions with the number of coordinate functions $m=11$, the number of intervals for calculating the scalar product of functions on a uniform grid $n_1=100$, $\|f-f_{num}\|_C=8.079448221565144\text{E}-011$.

Let's estimate the uniform rate of computational error in Example 2 using the algorithm (12)–(15) $\|u-u_{num}\|_C\le\|f-f_{num}\|_C\|\sin(x)\|_C=\|f-f_{num}\|_C\approx 8\cdot 10^{-11}$.

In hydrodynamics [3, 4], boundary value problems with a third-order differential equation are encountered. Consider example 3.

Example 3.

$$\begin{cases} u'''(x)+u'(x)=-2\sin(x), x\in(0,\pi), \\ u(0)=0, u'(0)=0, y(\pi)=0. \end{cases} \tag{18}$$

Let 's solve the homogeneous equation $u'''(x)+u'(x)=0$. Its characteristic equation and eigenvalues are equal $\lambda^3+\lambda=0\Leftrightarrow\lambda_1=0,\lambda_{2,3}=\pm i=\pm\sqrt{-1}$, which correspond to 3 partial linearly independent solutions

$$\left\{U_1(x)=1, U_2(x)=\sin(x), U_3(x)=\cos(x)\right\}, \left\{U_1'(x)=0, U_2'(x)=\cos(x), U_3'(x)=-\sin(x)\right\},$$

$$\left\{U_1''(x)=0, U_2''(x)=-\sin(x), U_3''(x)=-\cos(x)\right\}.$$

Let's check the existence and uniqueness of the solution of the boundary value problem (18). Write down the elements of the matrix according to the formula (5):

$$\alpha_1^0=1;\alpha_1^1=0;\alpha_1^2=0;\alpha_2^0=0;\alpha_2^1=1;\alpha_2^2=0;\beta_3^0=1;\beta_3^1=0;\beta_3^2=0,$$

$$A_{\mu j}=\begin{cases} \sum\limits_{i=0}^{n-1}\alpha_\mu^i U_j^{(i)}(a), \mu=\overline{1,k} \\ \sum\limits_{i=0}^{n-1}\beta_\mu^i U_j^{(i)}(b), \mu=\overline{k+1,n},\ k=2, n=3. \end{cases}$$

$$A_{11}=1\cdot1+0\cdot0+0\cdot0=1, A_{21}=0\cdot1+1\cdot0+0\cdot0=0, A_{31}=1\cdot1+0\cdot0+0\cdot0=1,$$

$$A_{12}=1\cdot\sin(0)+0\cdot\cos(0)+0\cdot(-\sin(0))=0, A_{22}=0\cdot\sin(0)+1\cdot\cos(0)+0\cdot(-\sin(0))=1,$$

$$A_{32}=1\cdot\sin(\pi)+0\cdot\cos(\pi)+0\cdot(-\sin(\pi))=0, A_{13}=1\cdot\cos(0)+0\cdot(-\sin(0))+0\cdot(-\cos(0))=1,$$

$$A_{23}=0\cdot\cos(0)+1\cdot(-\sin(0))+0\cdot(-\cos(0))=0, A_{33}=1\cdot\cos(\pi)+0\cdot(-\sin(\pi))+0\cdot(-\cos(\pi))=-1.$$

Since $\begin{vmatrix} 1 & 0 & 1 \\ 0 & 1 & 0 \\ 1 & 0 & -1 \end{vmatrix} = -2 \neq 0$, the boundary value problem (18) has a unique solution.

By direct verification, we will make sure that the exact solution of the boundary value problem (18) is the function

$$u(x) = x\sin(x), u^{'}(x) = \sin(x) + x\cos(x), u^{''}(x) = 2\cos(x) - x\sin(x),$$

$$u^{'''}(x) = -3\sin(x) - x\cos(x), u^{'''}(x) + u^{'}(x) = -3\sin(x) - x\cos(x) + \sin(x) + x\cos(x) = -2\sin(x), u(0) = u(\pi) = u^{'}(0) = 0.$$

Statement 1 for boundary value problem (18) is fulfilled, therefore, the solution of the problem is unique and coincides with $u(x) = x\sin(x)$. There are no other solutions.

Let's calculate the first derivative $u(x)$ by formula (8) and equate it to zero at the point $x = a$.

$$u^{'}(x) = \sum_{j=1}^{m} \varphi^{'}_{j}(x) C_j = \sum_{j=1}^{m} \frac{2j}{(b-a)} \left(\frac{(2x-a-b}{b-a} \right)^{j-1}_{x=a} C_j = 0 \Leftrightarrow C_1 - 2C_2 + 3C_3 + ... + m(-1)^{m-1} C_m = 0. \tag{19}$$

For a boundary value problem with a third-order differential equation (18), we obtain a system of equations

$$\sum_{j=1}^{m} a_{i,j} C_j = \overline{f_i},\ i = \overline{0, m-1}. \tag{20}$$

$$a_{i,j} = \begin{cases} \langle L\varphi_j, \varphi_i \rangle, \text{if } j \equiv 1 (\operatorname{mod} 2), i = \overline{0, m-3} \\ \langle L(\varphi_j - 1), \varphi_i \rangle, \text{if } j \equiv 0 (\operatorname{mod} 2), i = \overline{0, m-3} \\ 1, \text{ if } i = m-2, j \equiv 1 (\operatorname{mod} 2) \\ 0, \text{ if } i = m-2, j \equiv 0 (\operatorname{mod} 2) \\ j(-1)^{j-1}, \text{ if } i = m-1 \end{cases},$$

$$\overline{f_i} = \begin{cases} \left\langle f(x) - L\left(\frac{u_a + u_b}{2} \right), \varphi_i(x) \right\rangle, \text{ if } i = \overline{0, m-3} \\ \frac{u_b - u_a}{2}, \text{ if } i = m-2 \\ 0, \text{ if } i = m-1 \end{cases},$$

$$\begin{cases} L\varphi_0 = g_0(x), \text{if } j = 0, \\ L\varphi_1 = \frac{2g_1(x)}{(b-a)} + g_0(x) \left(\frac{2x-a-b}{b-a} \right), \text{if } j = 1, \\ L\varphi_2 = 8g_2(x) \frac{1}{(b-a)^2} + 4g_1(x) \frac{(2x-a-b)}{(b-a)^2} + g_0(x) \left(\frac{2x-a-b}{b-a} \right)^2, \text{if } j = 2, \\ L\varphi_j = 8j(j-1)(j-2) g_2(x) \frac{(2x-a-b)^{j-3}}{(b-a)^j} + \\ +4j(j-1) g_2(x) \frac{(2x-a-b)^{j-2}}{(b-a)^j} + 2jg_1(x) \frac{(2x-a-b)^{j-1}}{(b-a)^j} + g_0(x) \frac{(2x-a-b)^j}{(b-a)^j}, \text{if } j \geq 3. \end{cases} \tag{21}$$

$$u(x) = \left(\frac{u_a + u_b}{2} \right) + \sum_{j=1}^{m} \left[\left(\frac{(2x-a-b}{b-a} \right)^j + \left(\frac{-1 + (-1)^{j+1}}{2} \right) \right] C_j. \tag{22}$$

The inverse matrix A^{-1} is calculated by the msimsl linear algebra library to find the vector of expansion coefficients $C_j, j = \overline{1, m}$, using the coefficients of the system of linear algebraic equations (20). A program using formulas (14), (20), (21), (22) gives a numerical u_i^{num} and exact $u_i^{exact} = x_i \sin(x_i)$ solution to problem (18) on a uniform grid $x_i = a + h \cdot i, i = \overline{0, n_1}, h = \frac{b-a}{n_1}, n_1 = 50, a = 0, b = \pi$. The number of coordinate functions is $m = 15$. The numerical and exact solution of this problem is presented in Table 1.

Table 1

Problem solution (18)

x_i	u_i^{num}	u_i^{exact}	$u_i^{num} - u_i^{exact}$
0.000000000E+000	0.0000000000E+000	0.00000000000E+000	0.00000000E+000
0.12566370614359	1.5749838632E–002	1.5749838632E–002	3.36702887793E–013
0.25132741228718	6.2502585803E-002	6.2502585803E–002	–7.5051076464E–014
0.37699111843077	0.1387796868382	0.1387796868384	–2.2543078515E–013
0.50265482457436	0.2421558085434	0.2421558085436	–2.5310309403E–013
0.62831853071795	0.3693163660978	0.3693163660980	–2.3742119381E–013
0.75398223686155	0.5161363581649	0.5161363581652	–2.1926904736E–013
0.87964594300514	0.6777788480392	0.6777788480394	–2.0117241206E–013
1.00530964914873	0.8488110105527	0.8488110105529	–1.7474910407E–013
1.13097335529233	1.0233352874866	1.0233352874867	–1.4477308241E–013
1.25663706143592	1.1951328658964	1.1951328658966	–1.3122836151E–013
1.38230076757951	1.3578164206656	1.3578164206658	–1.4432899320E–013
1.50796447372310	1.5049888502957	1.5049888502959	–1.6875389974E–013
1.63362817986669	1.6304045878204	1.6304045878205	–1.7497114868E–013
1.75929188601028	1.72812998993818	1.72812998993833	–1.5254464358E–013
1.88495559215388	1.79269929884481	1.79269929884493	–1.2145839889E–013
2.01061929829747	1.81926273330968	1.81926273330979	–1.1013412404E–013
2.13628300444106	1.80372339742481	1.80372339742493	–1,2212453270E–013
2.26194671058465	1.74285989495849	1.74285989495861	–1.2412293415E–013
2.38761041672824	1.63443180085643	1.63443180085651	–8.038014698286E–014
2.51327412287183	1.47726546439236	1.47726546439237	–5.1070259132E–015
2.63893782901543	1.27131799485423	1.27131799485419	4.50750547997E–014
2.76460153515902	1.01771770348181	1.01771770348179	2.17603712826E–014
2.89026524130261	0.71877973673595	0.71877973673604	–9.7144514654E–014
3.01592894744620	0.37799612718318	0.37799612718362	–4.3676173788E–013
3.07876080051800	0.193316990170226	0.193316990171009	–7.8290152139E–013
3.14159265358979	3.8472143247E-016	–1.0104259667E-015	1.39514739920E–015

The first column of Table 1 shows the value of a node x_i of a uniform grid, the second column contains a numerical solution u_i^{num}, and the third column contains the exact solution u_i^{exact} in nodes x_i. The last column contains their difference $u_i^{num} - u_i^{exact}$.

In Example 3, the program gives the error rate $\left\| u_i^{num} - u_i^{exact} \right\|_C = \max\limits_{i=0,n_1} \left| u_i^{num} - u_i^{exact} \right| \approx 7.829\mathrm{E}-013.$

Results. The authors have developed the following algorithm for the modified Bubnov-Galerkin method:

– in the boundary value problem with an ordinary differential equation of order *n* it is necessary to select a system of *m*+1 coordinate functions $\{1, z, z^2, ..., z^m, m > n\}$;

– from the n boundary conditions, choose a system of linearly independent conditions (in the case of specified function values u_a, u_b there are *n*–1), independent conditions) and include the independent boundary conditions in the system of linear algebraic equations (SLAE);

– require that the first *m*–(*n*–1) = *m*–*n*+1 coordinate functions should be orthogonal to the residual of the differential equation. Then, the non-homogeneous system of linear algebraic equations will have *m*–*n*+1+*n*–1 = *m* rows and m unknowns $C_j, j = \overline{1, m}.$

Discussion and Conclusions. The main results obtained by the authors are as follows:

1. A system of coordinate functions is proposed that is infinitely differentiable, bounded, and linearly independent on the interval [−1,1], designed for solving boundary value problems with a linear differential equation of order *n*.

2. For the first time, a modified Bubnov-Galerkin method is introduced, in which the system of linear algebraic equations (12), (20) includes *n*–1 boundary conditions of the problem.

3. A criterion (5) for the existence and uniqueness of the solution to the boundary value problem with separated boundary conditions is obtained for the case where n linearly independent solutions of the linear homogeneous differential equation are known (Statement 1).

4. The modified Bubnov-Galerkin algorithm is proposed for boundary value problems with second- and third-order equations (12)–(15) and (20)–(22).

5. Three examples have been numerically solved using the modified algorithm, achieving a uniform error norm of no more than 10^{-11}.

References

1. Morozova E.A. Solvability of a boundary value problem for a system of ordinary differential equations. *Bulletin of Perm University. Mathematics. Mechanics. Computer science*. 2010;3(3):46–50. (in Russ.).

2. Abdullaev A.R., Skachkova E.A. On one multipoint boundary value problem for a second-order differential equation. *Bulletin of Perm University. Mathematics. Mechanics. Informatics*. 2014;2(25):5–9. (in Russ.).

3. Ershova T.Ya. Boundary value problem for a third-order differential equation with a strong boundary layer. *Bulletin of Moscow University. Episode 15: Computational mathematics and cybernetics*. 2020;1:30–39. (in Russ.).

4. Ershova T.Ya. On the convergence of a grid solution to the problem for a third-order equation in the case of a strong boundary layer. *Lomonosov readings: scientific conference*. 2020:77–78. (in Russ.).

5. Bakhvalov N.S., Zhidkov N.P., Kobelkov G.M. *Numerical methods: a textbook for students of physics and mathematics specialties of higher educational institutions*. Moscow: Binom. lab. Knowledge; 2011. 636 p. (in Russ.).

6. Bakhvalov N.S., Lapin A.V., Chizhonkov E.V. *Numerical methods in problems and exercises*. Moscow: BINOM. Knowledge laboratory; 2010. 240 p. (in Russ.).

7. Alekseev V.M., Galeev E.M., Tikhomirov V.M. *Collection of optimization problems: Theory. Examples. Problems*. Moscow: FIZMATLIT; 2008. 256 p. (in Russ.).

8. Pastukhov D.F., Pastukhov Yu.F., Volosova N.K. *Numerical methods. Lectures. Numerical workshop*. Novopolotsk; 2021. 237 p. (in Russ.).

9. Pikulin V.P., Pohozhaev S.I. *Practical course on the equations of mathematical physics*. Moscow: MTsNMO; 2004. 208 p. (in Russ.).

10. Filippov A.F. *Collection of problems on differential equations*. URSS, 2009. 176 p. (in Russ.).

About the Authors:

Natalya K. Volosova, Post-graduate Student of Bauman Moscow State Technical University (5–1, 2nd Baumanskaya St., Moscow, Russian Federation, 105005), ORCID, navalosova@yandex.ru

Konstantin A. Volosov, Doctor of Physical and Mathematical Sciences, Professor of the Department of Applied Mathematics of the Russian University of Transport (9–9, Obraztsova St., Moscow, GSP-4, Russian Federation, 127994), ORCID, konstantinvolosov@yandex.ru

Aleksandra K. Volosova, Candidate of Physical and Mathematical Sciences, Chief Analytical Department "Tramplin" LLC, Russian University of Transport (9–9, Obraztsova St., Moscow, GSP-4, Russian Federation, 127994), ORCID, alya01@yandex.ru

Dmitriy F. Pastukhov, Candidate of Physical and Mathematical Sciences, Associate Professor of Polotsk State University (29, Blokhin St., Novopolotsk, 211440, Republic of Belarus), ORCID, dmitrij.pastuhov@mail.ru

Yuriy F. Pastukhov, Candidate of Physical and Mathematical Sciences, Associate Professor of Polotsk State University (29, Blokhin St., Novopolotsk, 211440, Republic of Belarus), ORCID, pulsar1900@mail.ru

Contributions of the authors: **all authors have made an equivalent contribution to the preparation of the publication.**

Conflict of Interest Statement: the authors declare no conflict of interest.

All authors have read and approved the final manuscript.

Об авторах:

Наталья Константиновна Волосова, аспирант МГТУ им. Н.Э. Баумана (105005, Российская Федерация, г. Москва, ул. 2-я Бауманская, 5, стр. 1), ORCID, navalosova@yandex.ru

Константин Александрович Волосов, доктор физико-математических наук, профессор кафедры прикладной математики Российского университета транспорта (127994, Российская Федерация, ГСП-4, г. Москва, ул. Образцова, 9, стр. 9), ORCID, konstantinvolosov@yandex.ru

Александра Константиновна Волосова, кандидат физико-математических наук, начальник аналитического отдела ООО «Трамплин» Российского университета транспорта (127994, Российская Федерация, ГСП-4, г. Москва, ул. Образцова, 9, стр. 9), ORCID, alya01@yandex.ru

Дмитрий Феликсович Пастухов, кандидат физико-математических наук, доцент кафедры технологий программирования Полоцкого государственного университета (211440, Республика Беларусь, г. Новополоцк, ул. Блохина, 29), ORCID, dmitrij.pastuhov@mail.ru

Юрий Феликсович Пастухов, кандидат физико-математических наук, доцент кафедры технологий программирования Полоцкого государственного университета (211440, Республика Беларусь, г. Новополоцк, ул. Блохина, 29), ORCID, pulsar1900@mail.ru

Заявленный вклад авторов: **все авторы сделали эквивалентный вклад в подготовку публикации.**

Конфликт интересов: **авторы заявляют об отсутствии конфликта интересов.**

Все авторы прочитали и одобрили окончательный вариант рукописи.

Received / Поступила в редакцию 30.07.2024
Revised / Поступила после рецензирования 19.08.2024
Accepted / Принята к публикации 26.08.2024

MATHEMATICAL MODELLING
МАТЕМАТИЧЕСКОЕ МОДЕЛИРОВАНИЕ

UDC 532.517.2:536.24
https://doi.org/10.23947/2587-8999-2024-8-3-34-42

Check for updates

Original Theoretical Research

Mathematical Modelling of the Impact of IR Laser Radiation on an Oncoming Flow of Nanoparticles with Methane

Elizaveta E. Peskova[1] ✉, **Valeriy N. Snytnikov**[2]

[1] National Research Mordovia State University, Saransk, Russian Federation
[2] Boreskov Institute of Catalysis SB RAS, Novosibirsk, Russian Federation
✉ e.e.peskova@math.mrsu.ru

Abstract

Introduction. The study is devoted to the numerical investigation of laser radiation's effect on an oncoming two-phase flow of nanoparticles and multicomponent hydrocarbon gases. Under such exposure, the hydrogen content in the products increases, and methane is bound into more complex hydrocarbons on the surface of catalytic nanoparticles and in the gas phase. The hot walls of the tube serve as the primary source of heat for the reactive two-phase medium containing catalytic nanoparticles.

Materials and Methods. The main method used is mathematical modelling, which includes the numerical solution of a system of equations for a viscous gas-dust two-phase medium, taking into account chemical reactions and laser radiation. The model accounts for the two-phase gas-dust medium's multicomponent and multi-temperature nature, ordinary differential equations (ODEs) for the temperature of catalytic nanoparticles, ODEs of chemical kinetics, endothermic effects of radical chain reactions, diffusion of light methyl radicals CH_3 and hydrogen atoms H, which initiate methane conversion, as well as absorption of laser radiation by ethylene and particles.

Results. The distributions of parameters characterizing laminar subsonic flows of the gas-dust medium in an axisymmetric tube with chemical reactions have been obtained. It is shown that the absorption of laser radiation by ethylene in the oncoming flow leads to a sharp increase in methane conversion and a predominance of aromatic compounds in the product output.

Discussion and Conclusion. Numerical modelling of the dynamics of reactive two-phase media is of interest for the development of theoretical foundations for the processing of methane into valuable products. The results obtained confirm the need for joint use of mathematical modelling and laboratory experiments in the development of new resource-saving and economically viable technologies for natural gas processing.

Keywords: mathematical modelling, subsonic flows, two-phase medium, laser radiation, chemical reactions

Funding information. The work was supported by the Ministry of Science and Higher Education of the Russian Federation as part of the state assignment for the Boreskov Institute of Catalysis SB RAS (project FWUR–2024–0033).

For citation. Peskova E.E., Snytnikov V.N. Mathematical modelling of the IR laser radiation's effect on the oncoming flow of nanoparticles with methane. *Computational Mathematics and Information Technologies*. 2024;8(3):34–42. https://doi.org/10.23947/2587-8999-2024-8-3-34-42

Оригинальное теоретическое исследование

Математическое моделирование воздействия ИК-лазерного излучения на встречный поток наночастиц с метаном

Е.Е. Пескова[1] ✉, **В.Н. Снытников**[2]

[1]Мордовский государственный университет им. Н.П. Огарёва, г. Саранск, Российская Федерация

[2]Институт катализа Сибирского отделения Российской академии наук, г. Новосибирск, Российская Федерация

✉e.e.peskova@math.mrsu.ru

Аннотация

Введение. Работа посвящена численному исследованию воздействия лазерного излучения на встречный двухфазный поток наночастиц с многокомпонентным газом из углеводородов. При таком воздействии увеличивается содержание водорода в продуктах и происходит связывание метана в углеводороды более сложного строения на поверхности каталитических наночастиц и в газовой фазе. Горячие стенки трубы являются источником основного прогрева реакционной двухфазной среды с каталитическими наночастицами.

Материалы и методы. В качестве основного метода используется математическое моделирование, включающее численное решение системы уравнений вязкой газопылевой двухфазной среды с учетом химических реакций и лазерного излучения. Модель позволяет одновременно учитывать двухфазную газопылевую среду, многокомпонентность и многотемпературность среды, обыкновенные дифференциальные уравнения (ОДУ) для температуры каталитических наночастиц, ОДУ химической кинетики, эндотермические эффекты радикально-цепных реакций, диффузию легких метильных радикалов CH_3 и атомов водорода H, которые инициируют конверсию метана, поглощение лазерного излучения этиленом и частицами.

Результаты исследования. Получены распределения параметров, характеризующих ламинарные дозвуковые течения газопылевой среды в осесимметричной трубе с химическими реакциями. Показано, что поглощение лазерного излучения этиленом во встречном потоке приводит к резкому увеличению конверсии метана и преимущественному выходу ароматических соединений.

Обсуждение и заключение. Численное моделирование динамики реакционных двухфазных сред представляет интерес для разработки теоретических основ переработки метана в ценные продукты. Полученные результаты естественным образом подтверждают вывод о необходимости совместного использования средств математического моделирования и лабораторных экспериментов для разработки новых ресурсосберегающих и экономически обоснованных технологий переработки природного газа.

Ключевые слова: математическое моделирование, дозвуковые потоки, двухфазная среда, лазерное излучение, химические реакции

Финансирование. Работа выполнена при финансовой поддержке Министерства науки и высшего образования РФ в рамках государственного задания Института катализа СО РАН (проект FWUR–2024–0033).

Для цитирования. Пескова Е.Е., Снытников В.Н. Математическое моделирование воздействия ИК-лазерного излучения на встречный поток наночастиц с метаном. *Computational Mathematics and Information Technologies*. 2024;8(3):34–42. https://doi.org/10.23947/2587-8999-2024-8-3-34-42

Introduction. In laser thermochemistry, the impact of laser radiation on an oncoming two-phase flow of methane and catalytic nanoparticles is considered [1, 2]. In such a flow, at temperatures above 1000 K, methane is converted into ethylene, acetylene, hydrogen, and aromatic compounds [3, 4]. The chemical reactions involved in the conversion of hydrocarbons in the gas phase and on the surface of catalytic nanoparticles are chain reactions involving radicals, which require a description that includes a large number of components and stages, including the convective and diffusive dynamics of active radicals [5]. These chemical reactions generally define an endothermic process, which shifts toward higher product yields with additional energy absorption. Such absorption can be provided by infrared (IR) radiation from a CO_2 laser directed along the flow into the initial zone of chemical transformations [2]. At the same time, the case when laser radiation is directed at the oncoming flow into the region of high methane conversion is of particular interest. The consideration of this case is the purpose of this publication.

The complexity of multicomponent chemical processes, along with heat and mass transfer, requires mathematical modelling of subsonic flows of reactive two-phase media, consisting of gas and solid ultrafine particles. The authors have developed their own CFD code for calculating the dynamics of such media [2]. This code comprehensively considers subsonic multicomponent gas dynamics with volume changes due to chemical reactions, multicomponent dust dynamics, heterogeneous-homogeneous kinetics of radical chain reactions for hydrocarbons, radiation transfer, and absorption. As a simplification of the model, the flow is considered in an axisymmetric cylindrical 2D space.

Materials and Methods

Mathematical Model. IR laser radiation excites vibrational degrees of freedom in ethylene molecules, which appear as products of gas-phase chemical reactions and on the surface of catalytically active nanoparticles. Thermal relaxation of ethylene, which absorbed laser radiation, leads to heating of all components of the gas. The heat exchange between the gas and nanoparticles, occurring in the free molecular regime (for nanoparticles with diameters in the tens of nanometers), tends to bring the temperatures of the particles and gas to thermal equilibrium. The heated walls of the tube provide the bulk of the energy necessary for the highly endothermic conversion of methane.

To study the effect of laser radiation on the oncoming flow of methane and nanoparticles, a mathematical model was developed based on a system of equations for a viscous gas-dust two-phase medium, taking into account chemical reactions and laser radiation [1, 2]. This system of equations is based on the Navier-Stokes equations, using the approximation of small Mach numbers [6, 7]. The system describes significantly subsonic flows (M << 1) with volume changes, small pressure variations, and simultaneous significant increases in velocity due to chemical reactions, laser radiation, heat exchange between the gas and particles, and dissipative processes.

The mathematical model consists of a system of time-parabolic and space-elliptic equations, owing to the solution of the equation for the dynamic pressure component. The model accounts for: a two-phase gas-dust medium; multicomponent and multi-temperature aspects; ODEs for the temperature of catalytic nanoparticles; ODEs for chemical kinetics; endothermic effects of radical chain reactions; diffusion of light methyl radicals (CH_3) and hydrogen atoms (H), which initiate methane conversion; and the absorption of laser radiation by ethylene and particles.

The mass transfer equation for the gas mixture components is given as:

$$\frac{\partial \rho_g Y_m}{\partial t} + \nabla \cdot \left(\rho_g Y_m \vec{v}\right) = -\nabla \cdot \overrightarrow{J_m} + R_m, \quad m = \overline{1, M}. \tag{1}$$

The equations for the mass transfer of nanoparticles are:

$$\frac{\partial \rho_i}{\partial t} + \nabla \cdot \left(\rho_i \vec{v}\right) = 0, \quad i = \overline{1, N}. \tag{2}$$

The momentum transfer equation is:

$$\frac{\partial \rho \vec{v}}{\partial t} + \nabla \cdot \left(\rho \vec{v} \vec{v}\right) + \nabla \pi = \nabla \cdot \overline{\overline{\tau}}. \tag{3}$$

The equations for gas and particle enthalpy are:

$$\frac{\partial}{\partial t}\left(\rho_g h_g + \sum\nolimits_i \rho_i h_i\right) + \nabla \cdot \left(\left(\rho_g h_g + \sum\nolimits_i \rho_i h_i\right)\vec{v}\right) = -\nabla \cdot \vec{q} - \sum\nolimits_i 4\pi s_i^2 n_i \sigma \left(T_i^4 - T_g^4\right) \tag{4}$$

$$+\left(n_g \alpha + \sum\nolimits_{i=1}^{N} n_i \alpha_i\right) F.$$

Condition for the divergence of the velocity vector is:

$$S \equiv \nabla \cdot \vec{v} = \frac{1}{\rho_g C_p T_g}\left(-\sum\nolimits_{i=1}^{N} \rho_i \frac{C_p\left(T_g - T_i\right)}{\zeta_i}\right) + \frac{1}{\rho_g C_p T_g}\left(\nabla \cdot \lambda \nabla T_g + \sum\nolimits_m \rho_g D_{m,mix} \nabla Y_m \nabla h_m\right) \tag{5}$$

$$+\frac{1}{\rho_g}\sum\nolimits_m \frac{M_w}{M_{wm}}\left(\nabla \cdot \rho_g D_{m,mix} \nabla Y_m\right).$$

Equation for the intensity of radiation is:

$$\frac{dF}{dl} + \left(n_g \alpha + \sum\nolimits_{i=1}^{N} n_i \alpha_i\right) F = 0. \tag{6}$$

Equations for the temperature of nanoparticles are:

$$\frac{dT_i}{dt} = \frac{1}{m_i C_{DV}}\left(\alpha_i F - 4\pi s_i^2 \sigma \left(T_i^4 - T_g^4\right) - a\pi \frac{s_i^2}{2} p_g c_t \frac{\gamma + 1}{\gamma - 1}\left(\frac{T_i}{T_g} - 1\right) - Q \cdot R\right). \tag{7}$$

Equations of chemical kinetics are:

$$\frac{\partial \rho_g Y_m}{\partial t} = R_m, \quad m = \overline{1, M}. \tag{8}$$

Here ρ_g is the density of the gas mixture; Y_m is the mass fraction of the m-th gas component; M is the number of components in the gas mixture; $\overrightarrow{J_m}$ is the diffusion flux vector; R_m is the rate of formation or consumption of the m-th component of the mixture; $\vec{v}$ is the velocity of the gas and particle flow; ρ_i is the density of the i-th particle; N is the number of particle fractions; $\rho = \rho_g + \sum_{i=1}^{N} \rho_i$ is the total density of the gas and particles; $\pi = \rho_g - \rho_0$ is the dynamic pressure component; where ρ_g is the pressure and ρ_0 is the constant pressure in the region; $\overline{\overline{\tau}}$ is the viscous stress tensor; h_g is the enthalpy of the gas, h_i is the enthalpy of each particle fraction, $\vec{q}$ is the heat flux vector, n_g is the average concentration of absorbing gas molecules per unit volume; n_i is the concentration of particles in the dust fraction; F is the radiation intensity; α, α_i are the absorption coefficients; T_g is the gas temperature; T_i is the temperature of the particles in the dust fraction; s_i is the particle radius; σ is the Stefan-Boltzmann constant; C_p is the heat capacity of the mixture at constant pressure; $\zeta_i = \frac{2m_i C_{DV}(\gamma - 1)T_g}{a\pi s_i^2 p_g c_t(\gamma + 1)}$ is the thermal relaxation time of the particle in the medium; m_i is the mass of the particle; C_{DV} is the heat capacity of the particle material at constant volume; γ is the adiabatic index of the gas mixture; a is the accommodation coefficient; c_t is the average thermal velocity of gas molecules; M_w is the average molecular weight of the mixture; M_{wm} is the molecular weight of the m-th component of the mixture; l is the laser radiation propagation coordinate; c_t is the average thermal velocity of gas molecules; Q is the heat effect of the reaction; R is the number of transformations per unit time.

Information on the expressions for determining the diffusion flux vector, the rate of formation or consumption of gas components, the viscous stress tensor, the enthalpy of each particle fraction, the heat flux vector, absorption coefficients, thermal relaxation time, the average thermal velocity of gas molecules, and the heat effect of the reaction is provided in [1].

Chemical processes in the heated medium are calculated based on a kinetic scheme of interconnected heterogeneous and homogeneous radical-chain reactions, which includes 40 elementary stages and 15 components of the gas mixture. The scheme was designed for a temperature range from 900 K to 1400 K [8]. The laser beam diameter, power, and duration are parameters that are defined in the initial and boundary conditions. Further, the use of continuous CO_2 laser radiation is assumed, although single-pulse and pulse-periodic radiation modes for the CO_2 laser may also be studied.

The presented system of equations is complemented by initial and boundary conditions. The initial conditions include the concentrations of gas components Y_m^0, particle concentrations n_i^0, gas temperature T_g^0, particle temperature T_i^0, pressure p^0, and flow velocity $\overrightarrow{v^0}$. The boundary conditions consider the inflow conditions ($Y_m^{in}, n_i^{in}, T_g^{in}, T_i^{in}, p^{in}, \overrightarrow{v^{in}}$), outflow conditions p^{out}, and adhesion conditions ($T_g^{bound}, \vec{v} = 0$).

During one time integration step, the equations of chemical kinetics (8) are solved sequentially to account for the contribution of chemical reactions to the component composition, the equations for particle temperature (7) and laser radiation (6) are solved, and the system of equations (1)–(4) is integrated without considering the dynamic pressure component. The values of the gas component and nanoparticle densities, the total enthalpy of the gas and particles, and the preliminary velocity vector are obtained. From the computed values, the gas mixture temperature, gas component concentrations, and nanoparticle concentrations are derived. At the final stage, Poisson's equation is solved using the condition for the divergence of the velocity vector (5) to find the dynamic pressure component π\piπ, and the velocity vector is corrected.

The described computational algorithm was implemented in C++ using MPI parallel computing technology. The most labor-intensive step is the calculation of the chemical kinetics equations [9], as it involves solving a stiff system of equations that includes dozens of gas mixture components. Another labor-intensive step is solving Poisson's equation for the dynamic pressure component, where it is necessary to solve a system of linear algebraic equations (SLAE), the size of which depends on the computational grid. The computational algorithm for individual equations was tested on known solutions. The algorithm was previously tested in limiting cases on analytical solutions for model problems of Poiseuille flow, Couette flow, and heat conduction with a chemical reaction (in the flat variant), as well as experimental data on ethane pyrolysis. The convergence of the numerical method was verified and confirmed on a sequence of refined grids.

Results

Inlet and Outlet Flows in the Computational Domain. The cylindrical shape of the computational domain is determined by the typical design of reactors in chemical technologies and the well-studied nature of flows in straight pipes with circular cross-sections. The cross-section of the laser radiation beam, in the geometric optics approximation, is often also circular, with the radius adjustable by optical elements. The coaxial propagation of the laser beam through a circular tube is easily achievable in laboratory experiments. For computational experiments aimed at determining the influence of laser radiation on the counterflow of reagents, such a configuration of the computational domain, along with the radiation, is of particular interest. This setup eliminates the need to calculate flow distributions over the azimuthal angle in the cylindrical coordinate system, reducing the problem to a two-dimensional formulation, which greatly simplifies the development of the computational algorithm. The main expected result of introducing laser radiation into the reaction medium is the creation of a high-temperature region, which serves as a source of additional radicals outside this region. This significantly enhances the reactive capacity of the system at the outlet and allows for higher methane conversion rates under otherwise equal conditions.

The computational domain (Fig. 1) represents a cylindrical tube with a total length of 600 mm and a diameter of 20 mm. The domain consists of four zones from **A** to **D**. Zone **A** has reduced wall temperatures and is intended for the calculation of radiation input. It is isolated from the main reaction zone **C** by an annular inlet **1** for relatively cold methane. In zone **B**, the walls heat the methane to a certain temperature. Reaction zone **C** is 330 mm long and is bounded by an annular inlet **3** for the gas-dust mixture and an annular outlet **2** for the reaction products. In zone **D**, a flow of methane with nanoparticles is formed, moving towards the laser radiation. Such an arrangement of the reaction zone is necessary to organize the impact of laser radiation on the reacting mixture in the product outlet area and to prevent overheating of the tube's end walls.

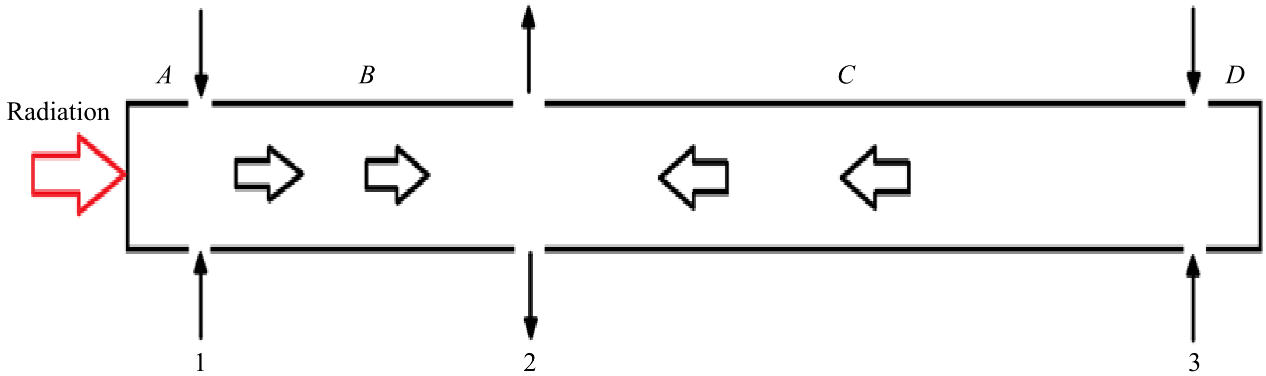

Fig. 1. Scheme of the calculation area with inlet and outlet flows

Initial and boundary conditions. At the initial moment, the area is filled with methane at a temperature of 973 K and a pressure of 101.325 Pa. Inlets **1** and **3** define conditions for the inflow of a flow with a specified constant flow rate of 10 L/h (10 % from inlet 1, 90 % from inlet 3) and the composition of the mixture. A gas-particle mixture (methane and catalytic nanoparticles with a radius of $5 \cdot 10^{-9}$ m, and a concentration of $1.2 \cdot 10^{18}$ m^{-3}) is supplied through inlet **3**, preheated to 1173 K. Energy is introduced into the reaction zone through walls **B** and **C**, which are at a temperature of 1173 K. As it moves through the reaction zone, the gas and particles are heated from the walls to the center. A relatively cold methane with a temperature of 573 K is supplied through inlet **1**. At the wall temperature of 1173 K, it remains inert and flows counter to the gas-particle mixture. The mixing of flows and the output of reaction products occur at outlet **2**. The wall temperature in zones **A** and **D** is 573 K. To the left along the axis, radiation from a 30 W CO_2 laser with a beam diameter of 12 mm is introduced. The width of the annular inlets 1 and 3 is 5 mm, and the outlet 2 is 8 mm.

The described problem is solved in a cylindrical coordinate system for the case of axisymmetric flow. The calculations are based on a 2D grid of rectangles, with 6000 cells, a spatial step of h=10^{-3}, and a time step of $\Delta t = 10^{-5}$.

For the chosen size and initial concentration of nanoparticles, particle aggregation into fractal agglomerates may occur, but the time for this process significantly exceeds the residence time of the nanoparticles in zone **C**. Furthermore, the total surface area of fractal agglomerates changes little, maintaining a total catalytic surface sufficient for methane conversion. For the given parameters, the ratio of the thermal conductivity length of the gas to the radius of the pipe and the ratio of the diffusion length of a hydrogen atom to the radius is greater than 1. This defines the heating of the medium in the pipe. The filling of the entire mixture with hydrogen atoms radially ensures the occurrence of radical chain reactions with methane and secondary hydrocarbons. The mixing of the relatively cold counterflow of methane in the annular output zone 2 and the absorption of laser radiation provides the cooling of the gas-particle mixture at the outlet.

Flow without Laser Radiation Input. Let's consider the flow of a two-phase gas-particle mixture with chemical reactions in the axisymmetric pipe presented in Fig. 1, without the introduction of laser radiation. The conversion of methane is an endothermic process, and the energy required to initiate the reactions is supplied to the system through the continuous heating of the walls of the area.

Counterflows of the supplied gas-particle mixture through the annular inlet **3** on the side surface of the pipe mix effectively, reverse, and form a laminar flow along the axis (from right to left). At a distance of one diameter of the pipe from inlet **3**, under the influence of wall heating, the velocity reaches its maximum value of 11 cm/s (Fig. 2). In this area, the conversion of methane begins, accompanied by a redistribution of reaction products. The presence of hydrogen in the products leads to a significant change in the volume of the medium, causing flow deceleration that starts at a distance of two diameters from inlet **3**. The decrease in velocity corresponds to an increase in particle concentration in the second part of the reaction zone (closer to outlet 2). The presence of inlet **1** also affects the formation of gas flows, resulting in the methane supplied to this area limiting the reaction zone. The gas-particle flow and the methane flow mix, creating a deceleration zone at the outlet **2** (Fig. 2).

The maximum concentration of particles, which is twice that of the concentration at inlet **3**, is observed at outlet **2** (Fig. 3). The temperature of the mixture in the reaction zone is close to the wall temperature (Fig. 4), illustrating the condition in which the energy supplied from the walls of the pipe is sufficient to heat the entire area and facilitate the endothermic chemical reactions. The special design of the pipe also plays a role here — lower temperatures at the end walls due to gas insulation in these areas protect the windows (for potential laser radiation input) from heating.

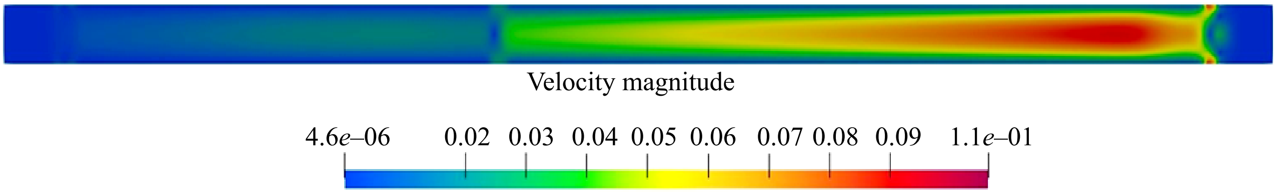

Fig. 2. Velocity distribution, m/s

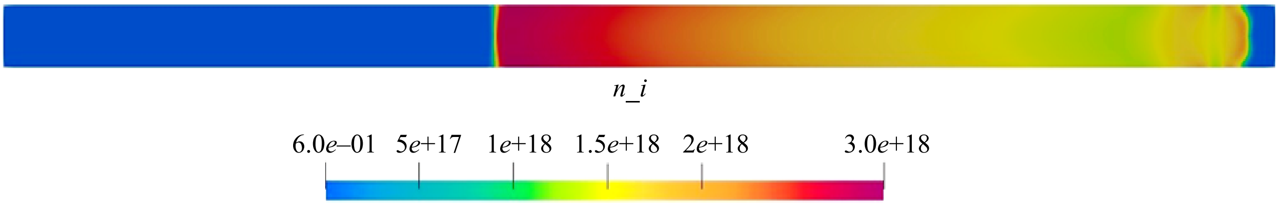

Fig. 3. Nanoparticle distribution, m^{-3}

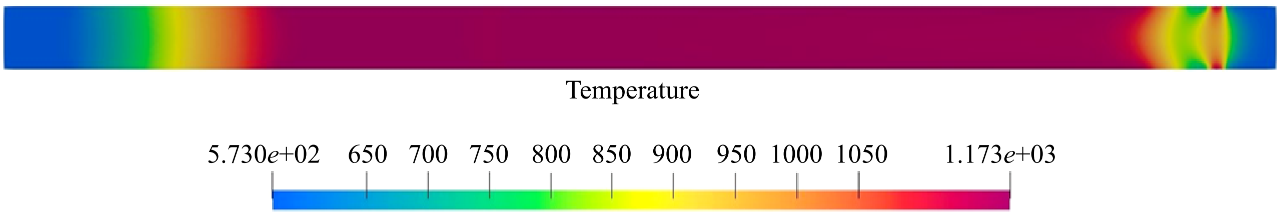

Fig. 4. Temperature distribution, K

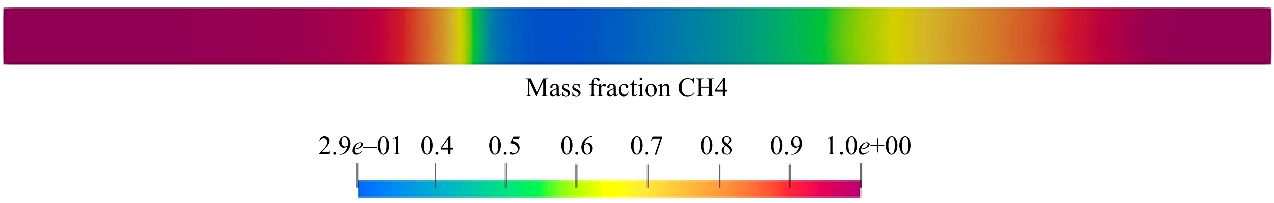

Fig. 5. Methane mass fraction distribution

Chemical reactions are initiated at a distance of one pipe diameter from inlet **3** due to wall heating and proceed throughout most of the reaction zone **C**, with more active methane conversion (71 %) near outlet **2**. The maximum methane conversion is observed in this area due to the accumulation of nanoparticles (Figs. 3, 5), which act as active centers for chemical reactions, and the mixture's temperature, which is approximately equal to the wall temperature. As the gas-particle flow moves, reaction products are formed and accumulate, with their maximum concentrations occurring near outlet **2**. The main products are aromatic compounds — 31.5 %, ethylene — 16.2 %, and hydrogen — 10.0 %. At outlet **2**, the methane conversion is 65.0 %, as the reaction mixture mixes with the counterflow of methane (10.0 % comes from inlet 1, 90 % from inlet **3**).

Effect of Laser Radiation. Let's consider the results of the calculation for a chemically active two-phase flow in the presence of laser radiation. A laser beam with a power of 30 W and a diameter of 12 mm is introduced along the axis of the pipe through the left end.

The laser radiation, entering the pipe from the left, passes through the buffer zone filled with optically transparent methane and is absorbed in the outflow area by nanoparticles and ethylene (Fig. 6).

The energy input leads to the formation of a high-temperature region, with values reaching 1364 K (Fig. 7). The shift of the elevated temperature into the buffer zone is explained by the diffusion of ethylene and hydrogen, which absorb the radiation, with hydrogen having thermal conductivity several times higher than other components of the mixture. Despite the temperature increase in this area by almost 200 K compared to the calculation without radiation, the flow velocity and, consequently, the particle concentration do not change throughout the pipe volume (Figs. 8, 9). The energy from the laser radiation, along with the temperature increase, is consumed by endothermic chemical reactions.

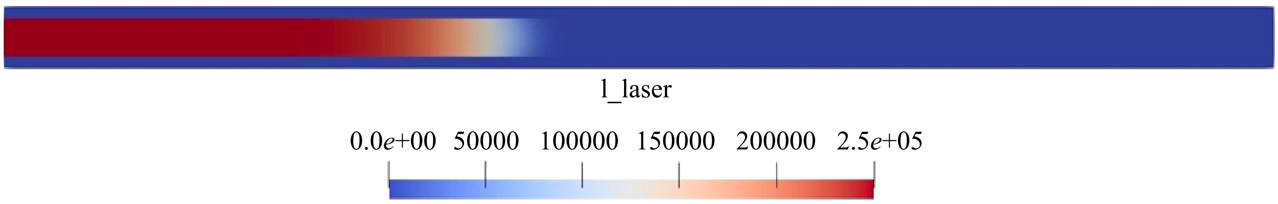

Fig. 6. Radiation intensity distribution, W/m^2

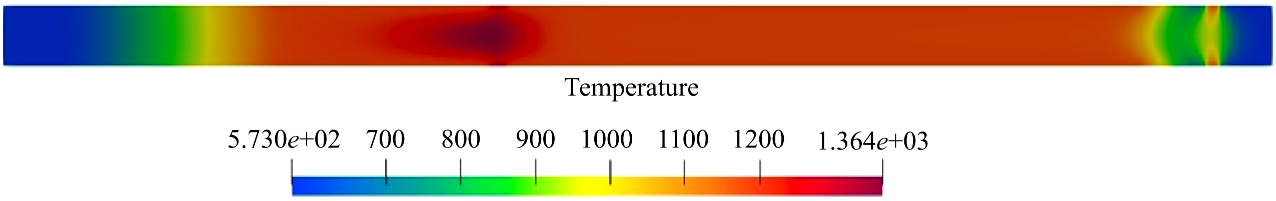

Fig. 7. Temperature distribution, K

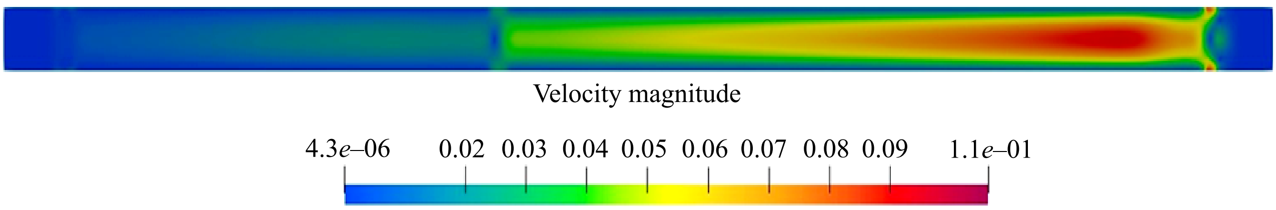

Fig. 8. Velocity distribution, m/s

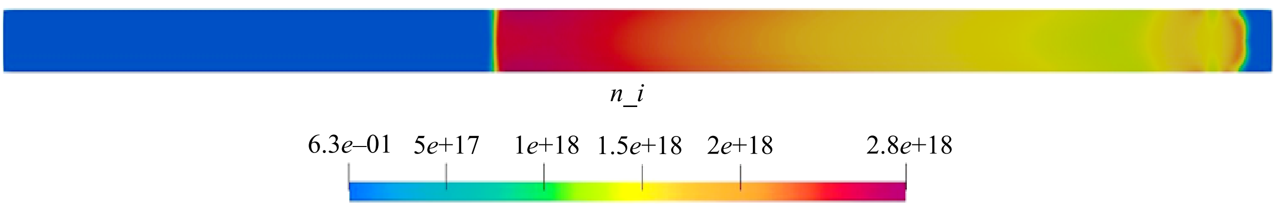

Fig. 9. Nanoparticle distribution, m^{-3}

Figures 10–12 show the distribution of the main components of the gas mixture along the pipe. From the graphs, it is evident, as in the case without radiation, that there is a gradual increase in reaction products toward outlet **2**, with methane conversion reaching 73 %. However, with the introduction of laser radiation, a significant redistribution of the component composition occurs along the pipe. The highest mass fractions of hydrogen (Fig. 11) and aromatic compounds (Fig. 12) are observed near outlet **2**, as these products form at temperatures above 1300 K, provided by the laser radiation input. The mass fraction of ethane in this area rapidly decreases, as it undergoes pyrolysis at such high temperatures. The maximum ethylene fraction of 19 % is observed in the central part of the reactor, decreasing to 6 % toward the outlet. The appearance of about 5 % hydrogen in the left "protected" area of the pipe is explained by its diffusion.

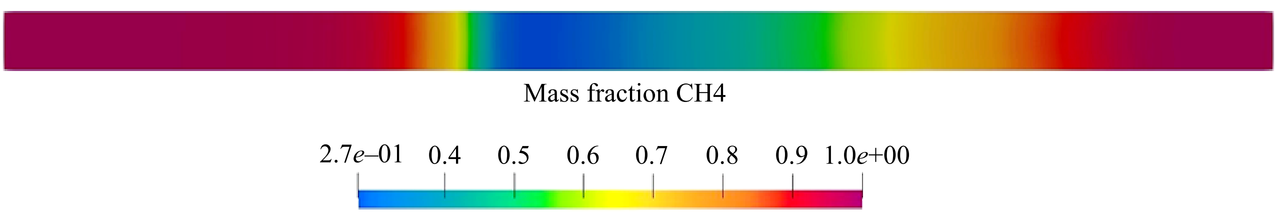

Fig. 10. Methane mass fraction distribution

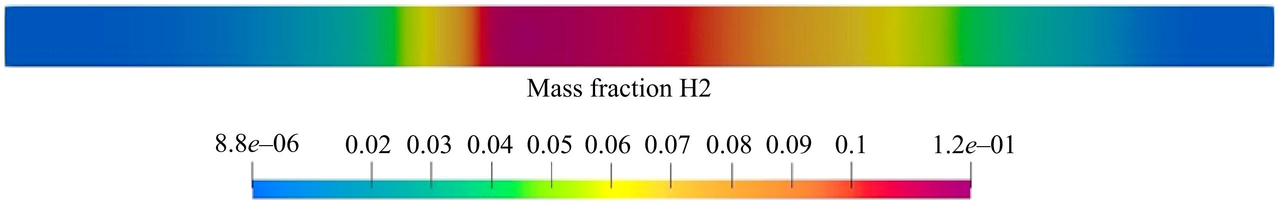

Fig. 11. Hydrogen mass fraction distribution

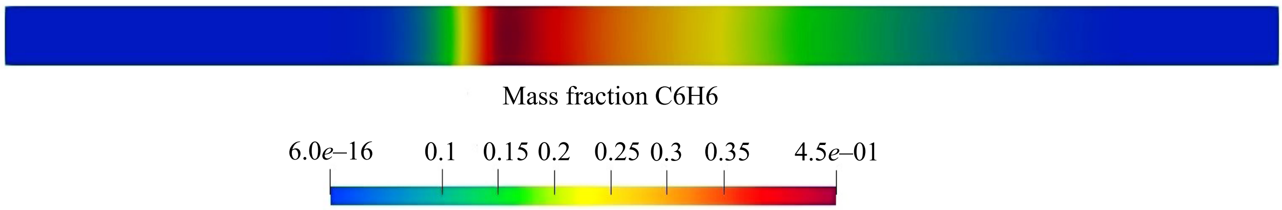

Fig. 12. Aromatic compounds mass fraction distribution

Since the counterflows of methane mix at the pipe outlet, the observed methane conversion decreases to 69.0 %, with the following mass fraction distribution of target reaction products: aromatic compounds — 44.0 %, ethylene — 6.0 %, and hydrogen — 11.6 %.

To study the influence of parameters in the computational experiment, calculations were performed for other values of wall temperatures in reaction zone **C**, ranging from 1073 K to 1173 K, with all other initial and boundary conditions unchanged. In the presence of laser radiation, the dependence of methane conversion on wall temperature is linear: with a 25 K increase in the mixture temperature, the additional methane conversion is around 10 %, primarily forming aromatic compounds. This is due to the fact that, upon reaching a certain temperature, the kinetics of the chemical reactions shift toward the formation of these compounds.

Discussion and Conclusion. Mathematical modelling of chemically active two-phase gas-particle flows was carried out using a self-developed program. The program is designed for calculations in cylindrical coordinates for axisymmetric subsonic flows with small pressure variations. The numerical algorithm imposes no restrictions on changes in flow velocity within the computational domain or on significant volume changes due to chemical reactions. The developed program was adapted to study methane conversion in a pipe with counterflows of reacting gas and IR laser radiation. In a series of computational experiments without radiation and with 30 W radiation, the effect of laser radiation on the dynamics of the chemically active counterflow of the gas-particle mixture was investigated.

It was found that relatively low-power and low-intensity IR laser radiation, around 30 W/cm^2, absorbed directly in the gas, has a strong impact on the counterflow of the two-phase nanoparticle and hydrocarbon gas mixture. This influence results in the creation of a higher temperature zone at the outlet of the reaction medium. Elevated temperatures and the heat power input in the presence of radiation lead to a shift in methane conversion products toward increased yields of aromatic hydrocarbons. The increase in aromatic output is achieved by introducing laser energy at the final stage of the chemical process. The quenching of the resulting products occurs as the reaction mixture exits the laser radiation zone. Numerical modelling of the dynamics of reactive two-phase media is of interest for developing the theoretical foundations for methane conversion into valuable products. The results naturally confirm the conclusion that mathematical modelling, combined with laboratory experiments, is essential for developing new resource-efficient and economically viable technologies for natural gas processing.

References

1. Snytnikov V.N., Peskova E.E., Stoyanovskaya O.P. Mathematical Model of a Two-Temperature Medium of Gas–Solid Nanoparticles with Laser Methane Pyrolysis. *Mathematical Models and Computer Simulations*. 2023;15:877–893. https://doi.org/10.1134/S2070048223050095

2. Peskova E.E. Mathematical Modeling of Nonstationary Problems Related to Laser Thermochemistry of Methane in the Presence of Catalytic Nanoparticles. *Doklady Mathematics*. 2024;109(3):256–261. https://doi.org/10.1134/S1064562424702107

3. Pinaeva L.G., Noskov A.S., Parmon V.N. Potentialities of the Direct Catalytic Processing of Methane into in-Demand Chemicals. Review. *Kataliz v promyshlennosti*. 2017;17(3):184–200. (In Russ.) https://doi.org/10.18412/1816-0387-2017-3-184-200

4. Guo X., Fang G., Li G. et al. Direct, Nonoxidative Conversion of Methane to Ethylene, Aromatics, and Hydrogen. *Science*. 2014;344(6184):616–619. https://doi.org/10.1126/science.1253150

5. Frank-Kamenetskii D.A. Diffusion and Heat Transfer in Chemical Kinetics. Plenum Press, New York; 1969. (In Russ.)

6. Day M.S., Bell J.B. Numerical simulation of laminar reacting flows with complex chemistry. *Combustion Theory and Modelling*. 2000;4(4):535–556.

7. Borisov V.E., Yakush S.E., Sysoeva E.Y. Numerical Simulation of Cellular Flame Propagation in Narrow Gaps. *Mathematical Models and Computer Simulations*. 2022;14:755–770. https://doi.org/10.1134/S2070048222050039

8. Lashina E.A., Peskova E.E., Snytnikov V.N. Mathematical modeling of the homogeneous-heterogeneous non-oxidative CH4 conversion: the role of gas-phase H or CH3. *Reaction Kinetics, Mechanisms and Catalysis*. 2023;136:1775-1789. https://doi.org/10.1007/s11144-023-02442-8

9. Hairer E., Wanner G. *Solving Ordinary Differential Equations II. Stiff and Differential-Algebraic Problems*. Springer-Verlag, Berlin; 1996.

About the Authors:

Elizaveta E. Peskova, Associate professor, Department of Applied Mathematics, Differential Equations and Theoretical Mechanics, National Research Mordovia State University (68/1, Bolshevistskaya St., Saransk, Russian Federation, 430005), ORCID, MathNet, e.e.peskova@math.mrsu.ru

Valeriy N. Snytnikov, Leading Researcher, Boreskov Institute of Catalysis SB RAS (5, Lavrentiev Av., Novosibirsk, Russian Federation, 630090), ORCID, MathNet, snyt@catalysis.ru

Claimed Contributorship:

E.E. Peskova: development of research methods, numerical calculations, visualization and analysis of results.

V.N. Snytnikov: problem statement, development of research methods, analysis of results.

Conflict of Interest Statement: **the authors declare no conflict of interest.**

All authors have read and approved the final manuscript.

Об авторах:

Елизавета Евгеньевна Пескова, кандидат физико-математических наук, доцент кафедры прикладной математики, дифференциальных уравнений и теоретической механики Национального исследовательского Мордовского государственного университета им. Н.П. Огарёва (430005, Российская Федерация, г. Саранск, ул. Большевистская, 68), ORCID, MathNet, e.e.peskova@math.mrsu.ru

Валерий Николаевич Снытников, кандидат физико-математических наук, ведущий научный сотрудник, Институт катализа им. Г.К. Борескова СО РАН (630090, Российская Федерация, г. Новосибирск, пр. Лаврентьева, 5), ORCID, MathNet, snyt@catalysis.ru

Заявленный вклад авторов:

Е.Е. Пескова: разработка методов исследования, проведение численных расчетов, визуализация и анализ результатов.

В.Н. Снытников: постановка задачи, разработка методов исследования, анализ результатов.

Конфликт интересов: **авторы заявляют об отсутствии конфликта интересов.**

Все авторы прочитали и одобрили окончательный вариант рукописи.

Received / Поступила в редакцию 05.08.2024
Reviewed / Поступила после рецензирования 19.08.2024
Accepted / Принята к публикации 26.08.2024

COMPUTATIONAL MATHEMATICS
ВЫЧИСЛИТЕЛЬНАЯ МАТЕМАТИКА

UDC 519.6

https://doi.org/10.23947/2587-8999-2024-8-3-43-59

Original Theoretical Research

Construction of Second-Order Finite Difference Schemes for Diffusion-Convection Problems of Multifractional Suspensions in Coastal Marine Systems

Valentina V. Sidoryakina[1,2]

[1] Don State Technical University, 1, Gagarin Sq., Rostov-on-Don, Russian Federation

[2] Taganrog Institute named after A.P. Chekhov (branch) of RSUE, Taganrog, Russian Federation

✉cvv9@mail.ru

Abstract

Introduction. This paper addresses an initial-boundary value problem for the transport of multifractional suspensions applied to coastal marine systems. This problem describes the processes of transport, deposition of suspension particles, and the transitions between its various fractions. To obtain monotonic finite difference schemes for diffusion-convection problems of suspensions, it is advisable to use schemes that satisfy the maximum principle. When constructing a finite difference scheme that adheres to the maximum principle, it is desirable to achieve second-order spatial accuracy for both interior and boundary points of the domain under study.

Materials and Methods. This problem presents certain difficulties when considering the boundaries of the geometric domain, where boundary conditions of the second and third kinds are applied. In these cases, to maintain second-order approximation accuracy, an "extended" grid is introduced (a grid supplemented with fictitious nodes). The guideline is the approximation of the given boundary conditions using the central difference formula, with the exclusion of the concentration function at the fictitious node from the resulting expressions.

Results. Second-order accurate finite difference schemes for the diffusion-convection problem of multifractional suspensions in coastal marine systems are constructed.

Discussion and Conclusion. The proposed schemes are not absolutely stable, and a detailed analysis of stability and convergence, particularly concerning the grid step ratio, remains an important problem that the author plans to address in the future.

Keywords: coastal marine systems, multifractional suspension, diffusion-convection problem, difference scheme, approximation error

Funding information. The study was supported by the Russian Science Foundation grant no. 23–21–00509, https://rscf.ru/project/23-21-00509

For citation. Sidoryakina V.V. Construction of Second-Order Finite Difference Schemes for Diffusion-Convection Problems of Multifract Suspensions in Coastal Marine Systems. *Computational Mathematics and Information Technologies*. 2024;8(3):43–59. https://doi.org/10.23947/2587-8999-2024-8-3-43-59

Оригинальное теоретическое исследование

Построение разностных схем второго порядка точности для задач диффузии-конвекции мультифракционных взвесей в прибрежных морских системах

В.В. Сидорякина[1,2]

[1] Донской государственный технический университет, г. Ростов-на-Дону, Российская Федерация

[2] Таганрогский институт имени А.П. Чехова (филиал) РГЭУ (РИНХ), г. Таганрог, Российская Федерация

✉cvv9@mail.ru

Аннотация

Введение. Рассматривается начально-краевая задача транспорта мультифракционных взвесей применительно к прибрежным морским системам. Данная задача описывает процессы переноса и осаждения частиц взвеси, а также взаимный переход между её различными фракциями. С целью получения монотонных разностных схем для задач диффу-

зии-конвекции взвесей целесообразно использовать разностные схемы, удовлетворяющие принципу максимума. При построении разностной схемы, для которой будет выполнен принцип максимума, желательно получить второй порядок аппроксимации по пространственной переменной как для внутренних, так и для граничных точек исследуемой области.
Материалы и методы. Данная задача вызывает определенные трудности при рассмотрении границ геометрической области, для которых выполнены граничные условия второго и третьего рода. В этих случаях, чтобы сохранить второй порядок погрешности аппроксимации, вводится «расширенная» сетка (сетка, дополненная фиктивными узлами). Ориентиром служит аппроксимация указанных граничных условий по формуле центральных разностей и исключение из полученных выражений функций концентрации взвеси в фиктивном узле.
Результаты исследования. Построены разностные схемы второго порядка точности для задачи диффузии-конвекции мультифракционных взвесей в прибрежных морских системах.
Обсуждение и заключение. Предложенные схемы не являются абсолютно стабильными и подробный анализ устойчивости и сходимости, связанный с отношением шагов сетки, является важной проблемой, которую автор планирует решать в будущем.

Ключевые слова: прибрежные морские системы, мультифракционная взвесь, задача диффузии-конвекции, разностная схема, погрешность аппроксимации

Финансирование. Исследование выполнено за счет гранта Российского научного фонда № 23–21–00509, https://rscf.ru/project/23-21-00509

Для цитирования. Сидорякина В.В. Построение разностных схем второго порядка точности для задач диффузии-конвекции мультифракционных взвесей в прибрежных морских системах. *Computational Mathematics and Information Technologies.* 2024;8(3):43–59. https://doi.org/10.23947/2587-8999-2024-8-3-43-59

Introduction. Suspended matter (suspension) is a natural component of marine systems. Changes in the quantitative and qualitative composition of the suspension can shape the landscape, negatively affect ecological communities, and shorten the lifespan of infrastructure. To address these issues, a clear understanding of the transport processes of suspended matter, accounting for spatial and temporal variations, is necessary. Typically, mathematical and numerical modelling methods are employed for these purposes [1–4].

In this article, we present a mathematical model of suspension transport based on a three-dimensional diffusion-convection equation. The model considers the multifractional composition of the suspension, water flow velocity, hydraulic particle size, complex bottom geometry, wind stress, bed friction, and other factors [5–8]. Special attention is paid to the approximation of the proposed model at both internal and boundary points of the computational domain. The proposed methods enable the construction of a finite difference scheme that approximates the model with second-order accuracy in relation to the spatial grid steps, taking into account boundary conditions of the second and third kinds.

Materials and Methods

1. Formulation of the Diffusion-Convection Problem for Multifractional Suspensions. In a rectangular Cartesian coordinate system, we consider the three-dimensional diffusion-convection equation using a skew-symmetric form of the convective transport operator [5–7]:

$$\frac{\partial c_r}{\partial t}+C_0c_r=Dc_r+F_r,\ r=1,2,3,\ (x,y,z)\in\overline{G},\ \overline{G}=\{0\le x\le L_x, 0\le y\le L_y, 0\le z\le L_z\};$$

$$C_0c_r\equiv\frac{1}{2}\left[u\frac{\partial c_r}{\partial x}+v\frac{\partial c_r}{\partial y}+\frac{\partial c_r}{\partial z}+w_r'\frac{\partial(uc_r)}{\partial x}+\frac{\partial(vc_r)}{\partial y}+\frac{\partial(w_r'c_r)}{\partial z}\right],$$

$$Dc_r=\frac{\partial}{\partial x}\left(\mu_{h,r}\frac{\partial c_r}{\partial x}\right)+\frac{\partial}{\partial y}\left(\mu_{h,r}\frac{\partial c_r}{\partial y}\right)+\frac{\partial}{\partial z}\left(\mu_{v,r}\frac{\partial c_r}{\partial z}\right),\tag{1}$$

$$F_1=(\alpha_2c_2(x,y,z,t)-\beta_1c_1)+\gamma_1c_1,$$

$$F_2=(\beta_1c_1(x,y,z,t)-\alpha_2c_2)+(\alpha_3c_3(x,y,z,t)-\beta_2c_2)+\gamma_2c_2,$$

$$F_3=(\beta_2c_2(x,y,z,t)-\alpha_3c_3)+\gamma_3c_3,$$

where c_r, $c_r=c_r(x,y,z,t)$ is the concentration of particles at time t, $t\in[0;T]$; u, v, w are the components of the velocity vector of the water medium $\vec{U}$; w_r', $w_r'=w+w_{g,r}$ are the hydraulic sizes of the particles; $\mu_{h,r},\mu_{v,r}$ are the horizontal and vertical diffusion coefficients of the particles, respectively; F_r is the source term; $\alpha_r\beta_r$ are the coefficients describing the intensity of conversion of particles from one fraction to another, and $\alpha_r\ge0$, $\beta_r\ge0$; γ_r is the external source power of particles. Here, the subscript r indicates that the particle belongs to fraction number r.

The equation (1) is supplemented by the initial conditions:

$$c_r(x,y,z,0)=c_{r,0}(x,y,z),\ (x,y,z)\in\bar{G};\tag{2}$$

and the boundary conditions:

− on the lateral faces of the parallelepiped G:

$$c_r=c_r',\ \text{if } u_{\vec{n}}<0;\tag{3}$$

$$\frac{\partial c_r}{\partial \vec{n}}=0,\ \text{if } u_{\vec{n}}\geq 0;\tag{4}$$

($u_{\vec{n}}$ is the projection of the velocity vector onto the outward normal $\vec{n}$ at the boundary, and c_r' represents known concentration values);

− on the upper surface of the parallelepiped G:

$$\frac{\partial c_r}{\partial z}=0;\tag{5}$$

− on the lower surface of the parallelepiped G:

$$\frac{\partial c_r}{\partial z}=-\varepsilon_r c_r.\tag{6}$$

Using the methods described in [9], a transformation with a "time lag" on the time grid $\bar{\omega}_\tau=\{t_n=n\tau, n=0,1,\ldots,N_t,\ N_t\tau=T\}$ was performed, along with a transition to a new coordinate system $Oxy\theta$, $\theta\in[0;1]$ according to the formulas:

$$\theta=\frac{z-\eta}{h},\ x_\theta=x,\ y_\theta=y,\tag{7}$$

where h is the depth and η is the height of the free surface relative to the mean free surface [10].

Equation (1) is then transformed as follows:

$$\begin{gathered}\frac{\partial c_r^n}{\partial t}+C_0c_r^n=Dc_r^n+F_r^n,\ r=1,2,3,\ t_{n-1}<t\leq t_n,\ n=1,2,\ldots,N_t,\\ C_0c_r^n\equiv\frac{1}{2}\left[u\frac{\partial c_r^n}{\partial x}+v\frac{\partial c_r^n}{\partial y}+w_r'\frac{1}{H}\frac{\partial c_r^n}{\partial\theta}+\frac{\partial\left(uc_r^n\right)}{\partial x}+\frac{\partial\left(vc_r^n\right)}{\partial y}+\frac{1}{H}\frac{\partial\left(w_r'c_r^n\right)}{\partial\theta}\right],\\ Dc_r^n=\frac{\partial}{\partial x}\left(\mu_{h,r}\frac{\partial c_r^n}{\partial x}\right)+\frac{\partial}{\partial y}\left(\mu_{h,r}\frac{\partial c_r^n}{\partial y}\right)+\frac{1}{H^2}\frac{\partial}{\partial\theta}\left(\mu_{v,r}\frac{\partial c_r^n}{\partial\theta}\right),\\ F_1^n=\left(\alpha_2c_2^{n-1}(x,y,\theta,t_{n-1})-\beta_1c_1^n\right)+\gamma_1^nc_1^n,\\ F_2^n=\left(\beta_1c_1^{n-1}(x,y,\theta,t_{n-1})-\alpha_2c_2^n\right)+\left(\alpha_3c_3^{n-1}(x,y,\theta,t_{n-1})-\beta_2c_2^n\right)+\gamma_2^n\tilde{c}_2^n,\\ F_3^n=\left(\beta_2c_2^{n-1}(x,y,\theta,t_{n-1})-\alpha_3c_3^n\right)+\gamma_3^nc_3^n.\end{gathered}\tag{8}$$

The initial and boundary conditions (2)–(6) will be transformed as follows:

$$\begin{gathered}c_r^1(x,y,\theta,0)=c_{r,0},\ (x,y,\theta)\in\bar{G},\\ c_r^n(x,y,\theta,t_{n-1})=c_r^{n-1}(x,y,\theta,t_{n-1}),\ n=2,\ldots,N_t,\ (x,y,\theta)\in G;\end{gathered}\tag{9}$$

$$c_r^n=c_r',\ \text{if } u_{\vec{n}}<0;\tag{10}$$

$$\frac{\partial c_r^n}{\partial\vec{n}}=0,\ \text{if } u_{\vec{n}}\geq 0,\tag{11}$$

$$\frac{\partial c_r^n}{\partial\theta}=0;\tag{12}$$

$$\frac{\partial c_r^n}{\partial\theta}=-\varepsilon_rc_r^n.\tag{13}$$

2. Second-Order Finite Difference Scheme for the Diffusion-Convection Problem of Multifractional Suspensions at Internal Nodes. Let us assume the existence of continuous (bounded) fourth-order partial derivatives with respect to the spatial variables (x, y, θ) for the functions c_r^n, $r=1,2,3$, and continuous second-order partial derivatives with respect to the time variable t. In other words, the derivatives $\frac{\partial^4 c_r^n}{\partial x^4}, \frac{\partial^4 c_r^n}{\partial y^4}, \frac{\partial^4 c_r^n}{\partial \theta^4}, \frac{\partial^2 c_r^n}{\partial t^2}$ are continuous and thus bounded for all $(x,y,\theta)\in\overline{G}$, $t_{n-1}\le t\le t_n$, $n=1,...,N_t$. and we also assume the continuity of second-order partial derivatives: $\frac{\partial^2 \mu_{h,r}}{\partial x^2}, \frac{\partial^2 \mu_{h,r}}{\partial y^2}, \frac{\partial^2 \mu_{v,r}}{\partial \theta^2}, \frac{\partial^2 u}{\partial x^2}, \frac{\partial^2 v}{\partial y^2}, \frac{\partial^2 w_r'}{\partial \theta^2}$.

For the approximation of the problem (8)–(13), we will use the following grids:

$$\omega=\omega_x\times\omega_y\times\omega_\theta,\ \overline{\omega}=\overline{\omega}_x\times\overline{\omega}_y\times\overline{\omega}_\theta,$$

$$\omega_x=\{x: x=ih_x;\ i=1,...,N_x-1;\ (N_x-1)h_x\equiv L_x-h_x\},$$

$$\omega_y=\{y: y=jh_y;\ j=1,...,N_y-1;\ (N_y-1)h_y\equiv L_y-h_y\},$$

$$\omega_\theta=\{\theta: \theta=kh_\theta;\ k=1,...,N_\theta-1;\ (N_\theta-1)h_\theta\equiv 1-h_\theta\},$$

$$\overline{\omega}_x=\{x: x=ih_x;\ i=0,1,...,N_x;\ N_xh_x\equiv L_x\},$$

$$\overline{\omega}_y=\{y: y=jh_y;\ j=0,1,...,N_y;\ N_yh_y\equiv L_y\},$$

$$\overline{\omega}_\theta=\{\theta: \theta=kh_\theta;\ k=0,1,...,N_\theta;\ N_\theta h_\theta\equiv 1\}.$$

Next, in the notation of the grid functions for c_r^n and F_r^n we will use a bar over them. Based on the assumptions introduced, we arrive at the approximation of equation (8):

$$\frac{\overline{c}_r^n(x_i,y_j,\theta_k)-\overline{c}_r^{n-1}(x_i,y_j,\theta_k)}{\tau}+C_0\overline{c}_r^n=D\overline{c}_r^n+\overline{F}_r^n,\ r=1,2,3,\ (x_i,y_j,\theta_k)\in\omega,\ t_n\in\overline{\omega}_\tau,$$

$$C_0\overline{c}_r^n=\frac{1}{2h_x}\left(u^n(x_i+0.5h_x,y_j,\theta_k)\overline{c}_r^n(x_i+h_x,y_j,\theta_k)-u^n(x_i-0.5h_x,y_j,\theta_k)\overline{c}_r^n(x_i-h_x,y_j,\theta_k)\right)+$$

$$+\frac{1}{2h_y}\left(v^n(x_i,y_j+0.5h_y,\theta_k)\overline{c}_r^n(x_i,y_j+h_y,\theta_k)-v^n(x_i,y_j-0.5h_y,\theta_k)\overline{c}_r^n(x_i,y_j-h_y,\theta_k)\right)+$$

$$+\frac{1}{2H(x,y)h_\theta}\left(w_r'^n(x_i,y_j,\theta_k+0.5h_\theta)\overline{c}_r^n(x_i,y_j,\theta_k+h_\theta)-w_r'^n(x_i,y_j,\theta_k-0.5h_\theta)\overline{c}_r^n(x_i,y_j,\theta_k-h_\theta)\right),$$

$$D\overline{c}_r^n=\frac{1}{h_x^2}\Big(\mu_{h,r}(x_i+0.5h_x,y_j,\theta_k)\left(\overline{c}_r^n(x_i+h_x,y_j,\theta_k)-\overline{c}_r^n(x_i,y_j,\theta_k)\right)-\mu_{h,r}(x_i-0.5h_x,y_j,\theta_k)\cdot \tag{14}$$

$$\cdot\left(\overline{c}_r^n(x_i,y_j,\theta_k)-\overline{c}_r^n(x_i-h_x,y_j,\theta_k)\right)\Big)+\frac{1}{h_y^2}\Big(\mu_{h,r}(x_i,y_j+0.5h_y,\theta_k)\left(\overline{c}_r^n(x_i,y_j+h_y,\theta_k)-\overline{c}_r^n(x_i,y_j,\theta_k)\right)-$$

$$-\mu_{h,r}(x_i,y_j-0.5h_y,\theta_k)\left(\overline{c}_r^n(x_i,y_j,\theta_k)-\overline{c}_r^n(x_i,y_j-h_y,\theta_k)\right)\Big)+\frac{1}{H^2(x_i,y_j)h_\theta^2}\Big(\mu_{v,r}(x_i,y_j,\theta_k+0.5h_\theta)\cdot$$

$$\cdot\left(\overline{c}_r^n(x_i,y_j,\theta_k+h_\theta)-\overline{c}_r^n(x_i,y_j,\theta_k)\right)-\mu_{v,r}(x_i,y_j,\theta_k-0.5h_\theta)\left(\overline{c}_r^n(x_i,y_j,\theta_k)-\overline{c}_r^n(x_i,y_j,\theta_k-h_\theta)\right)\Big),$$

$$\overline{F}_1^n=\left(\alpha_2\overline{c}_2^{n-1}(x,y,\theta,t_{n-1})-\beta_1\overline{c}_1^n\right)+\gamma_1^n\overline{c}_1^n,$$

$$\overline{F}_2^n=\left(\beta_1\overline{c}_1^{n-1}(x,y,\theta,t_{n-1})-\alpha_2\overline{c}_2^n\right)+\left(\alpha_3\overline{c}_3^{n-1}(x,y,\theta,t_{n-1})-\beta_2\overline{c}_2^n\right)+\gamma_2^n\overline{c}_2^n,$$

$$\overline{F}_3^n=\left(\beta_2\overline{c}_2^{n-1}(x,y,\theta,t_{n-1})-\alpha_3\overline{c}_3^n\right)+\gamma_3^n\overline{c}_3^n.$$

We will verify that the finite difference scheme (14) has second-order accuracy. To this end, we will substitute the exact solution $c_r^n(x_i,y_j,\theta_k)\equiv c_r(x_i,y_j,\theta_k,t_n)$, $(x_i,y_j,\theta_k)\in G$, $t_n\in\omega_\tau$, $n=0,1,...,N_t$ of the problem (3)–(8) into equation (14) and demonstrate that for the approximation error

$$\psi^n(x_i,y_j,\theta_k)=-\frac{c_r^n(x_i,y_j,\theta_k)-c_r^{n-1}(x_i,y_j,\theta_k)}{\tau}-C_0c_r^n(x_i,y_j,\theta_k)+Dc_r^n(x_i,y_j,\theta_k)+F_r^n(x_i,y_j,\theta_k) \tag{15}$$

the following relationship holds:

$$\psi^n(x_i,y_j,\theta_k)=O(\tau+h^2),\ n=0,1,\ldots,N_t, \tag{16}$$

where $h^2=h_x^2+h_y^2+h_\theta^2$.

We express the function c_r^{n-1} in a Taylor series expansion around the node (x_i,y_j,θ_k,t_n):

$$c_r^{n-1}(x_i,y_j,\theta_k,t_{n-1})=c_r^n(x_i,y_j,\theta_k,t_n)-\frac{\partial c_r^n(x_i,y_j,\theta_k,t_n)}{\partial t}\tau+\frac{\partial^2 c_r^n(x_i,y_j,\theta_k,t_n)}{\partial t^2}\frac{\tau^2}{2}+O(\tau^3). \tag{17}$$

Using relation (17) for the first term from the left-hand side of equation (15), we find:

$$\frac{c_r^n(x_i,y_j,\theta_k,t_n)-c_r^{n-1}(x_i,y_j,\theta_k,t_{n-1})}{\tau}=\frac{1}{\tau}\left[c_r^n(x_i,y_j,\theta_k,t_n)-\left(c_r^n(x_i,y_j,\theta_k,t_n)-\frac{\partial c_r^n(x_i,y_j,\theta_k,t^n)}{\partial t}\tau+\right.\right.$$
$$\left.\left.+\frac{\partial^2 c_r^n(x_i,y_j,\theta_k,t_n)}{\partial t^2}\frac{\tau^2}{2}+O(\tau^3)\right)\right]=\frac{\partial c_r^n(x_i,y_j,\theta_k,t_n)}{\partial t}+O(\tau). \tag{18}$$

To estimate the approximation error of the convective transport operator from equation (15) we utilize the Taylor series expansions $c_r^n, u^n, v^n, w_r'^n$ around the node (x_i,y_j,θ_k,t_n):

$$c_r^n(x_i\pm h_x,y_j,\theta_k)=c_r^n(x_i,y_j,\theta_k)\pm\frac{\partial c_r^n(x_i,y_j,\theta_k)}{\partial x}h_x+\frac{\partial^2 c_r^n(x_i,y_j,\theta_k)}{\partial x^2}\frac{h_x^2}{2}+O(h_x^3), \tag{19}$$

$$c_r^n(x_i,y_j\pm h_y,\theta_k)=c_r^n(x_i,y_j,\theta_k)\pm\frac{\partial c_r^n(x_i,y_j,\theta_k)}{\partial y}h_x+\frac{\partial^2 c_r^n(x_i,y_j,\theta_k)}{\partial y^2}\frac{h_y^2}{2}+O(h_y^3), \tag{20}$$

$$c_r^n(x_i,y_j,\theta_k\pm h_\theta)=c_r^n(x_i,y_j,\theta_k)\pm\frac{\partial c_r^n(x_i,y_j,\theta_k)}{\partial \theta}h_\theta+\frac{\partial^2 c_r^n(x_i,y_j,\theta_k)}{\partial \theta^2}\frac{h_\theta^2}{2}+O(h_\theta^3), \tag{21}$$

$$u^n(x_i+0.5h_x,y_j,\theta_k)+u^n(x_i-0.5h_x,y_j,\theta_k)=2u^n(x_i,y_j,\theta_k)+O(h_x^2), \tag{22}$$

$$u^n(x_i+0.5h_x,y_j,\theta_k)-u^n(x_i-0.5h_x,y_j,\theta_k)=\frac{\partial u^n(x_i,y_j,\theta_k)}{\partial x}h_x+O(h_x^3), \tag{23}$$

$$v^n(x_i,y_j+0.5h_y,\theta_k)+v^n(x_i,y_j-0.5h_y,\theta_k)=2v^n(x_i,y_j,\theta_k)+O(h_y^2), \tag{24}$$

$$v^n(x_i,y_j+0.5h_y,\theta_k)-v^n(x_i,y_j-0.5h_y,\theta_k)=\frac{\partial v^n(x_i,y_j,\theta_k)}{\partial y}h_y+O(h_y^3), \tag{25}$$

$$w_r'^n(x_i,y_j,\theta_k+0.5h_\theta)+w_r'^n(x_i,y_j,\theta_k-0.5h_\theta)=2w_r'^n(x_i,y_j,\theta_k)+O(h_\theta^2), \tag{26}$$

$$w_r'^n(x_i,y_j,\theta_k+0{,}5h_\theta)+w_r'^n(x_i,y_j,\theta_k-0{,}5h_\theta)=2w_r'^n(x_i,y_j,\theta_k)+O(h_\theta^2), \tag{27}$$

By substituting the corresponding expressions (19)–(27) into expression (15) for $C_0c_r^n$ we obtain:

$$C_0c_r^n=\frac{1}{2}\frac{\partial u^n(x_i,y_j,\theta_k)}{\partial x}c_r^n(x_i,y_j,\theta_k)+u^n\frac{\partial c_r^n(x_i,y_j,\theta_k)}{\partial x}+\frac{1}{2}\frac{\partial v^n(x_i,y_j,\theta_k)}{\partial y}c_r^n(x_i,y_j,\theta_k)+v^n(x_i,y_j,\theta_k)\cdot$$
$$\cdot\frac{\partial c_r^n(x_i,y_j,\theta_k)}{\partial y}+\frac{1}{2H(x_i,y_j)}\frac{\partial w_r'^n(x_i,y_j,\theta_k)}{\partial \theta}c_r^n(x_i,y_j,\theta_k)+\frac{1}{H(x_i,y_j)}w_r'^n(x_i,y_j,\theta_k)\frac{\partial c_r^n(x_i,y_j,\theta_k)}{\partial \theta}+$$
$$+O(h_x^2+h_y^2+h_\theta^2). \tag{28}$$

To estimate the approximation error of the diffusion transport operator from equation (15), we utilize c_r^n, $\mu_{h,r}$, $\mu_{v,r}$ in the Taylor series expansions around the point (x_i,y_j,θ_k):

$$c_r^n(x_i\pm h_x,y_j,\theta_k)=c_r^n(x_i,y_j,\theta_k)\pm\frac{\partial c_r^n(x_i,y_j,\theta_k)}{\partial x}h_x+\frac{\partial^2 c_r^n(x_i,y_j,\theta_k)}{\partial x^2}\frac{h_x^2}{2}\pm\frac{\partial^3 c_r^n(x_i,y_j,\theta_k)}{\partial x^3}\frac{h_x^3}{6}+O(h_x^4), \tag{29}$$

$$c_r^n(x_i,y_j\pm h_y,\theta_k)=c_r^n(x_i,y_j,\theta_k)\pm\frac{\partial c_r^n(x_i,y_j,\theta_k)}{\partial y}h_y+\frac{\partial^2 c_r^n(x_i,y_j,\theta_k)}{\partial y^2}\frac{h_y^2}{2}\pm\frac{\partial^3 c_r^n(x_i,y_j,\theta_k)}{\partial y^3}\frac{h_y^3}{6}+O(h_y^4), \tag{30}$$

$$c_r^n\left(x_i,y_j,\theta_k \pm h_\theta\right)=c_r^n\left(x_i,y_j,\theta_k\right)\pm\frac{\partial c_r^n\left(x_i,y_j,\theta_k\right)}{\partial\theta}h_\theta+\frac{\partial^2 c_r^n\left(x_i,y_j,\theta_k\right)}{\partial\theta^2}\frac{h_\theta^2}{2}\pm\frac{\partial^3 c_r^n\left(x_i,y_j,\theta_k\right)}{\partial\theta^3}\frac{h_\theta^3}{6}+O\left(h_\theta^4\right), \tag{31}$$

$$\mu_{h,r}\left(x_i+0.5h_x,y_j,\theta_k\right)+\mu_{h,r}\left(x_i-0.5h_x,y_j,\theta_k\right)=2\mu_{h,r}\left(x_i,y_j,\theta_k\right)+O\left(h_x^2\right), \tag{32}$$

$$\mu_{h,r}\left(x_i+0.5h_x,y_j,\theta_k\right)-\mu_{h,r}\left(x_i-0.5h_x,y_j,\theta_k\right)=\frac{\partial\mu_{h,r}\left(x_i,y_j,\theta_k\right)}{\partial x}h_x+O\left(h_x^3\right), \tag{33}$$

$$\mu_{h,r}\left(x_i,y_j+0.5h_y,\theta_k\right)+\mu_{h,r}\left(x_i,y_j-0.5h_y,\theta_k\right)=2\mu_{h,r}\left(x_i,y_j,\theta_k\right)+O\left(h_y^2\right), \tag{34}$$

$$\mu_{h,r}\left(x_i,y_j+0.5h_y,\theta_k\right)-\mu_{h,r}\left(x_i,y_j-0.5h_y,\theta_k\right)=\frac{\partial\mu_{h,r}\left(x_i,y_j,\theta_k\right)}{\partial y}h_y+O\left(h_y^3\right), \tag{35}$$

$$\mu_{v,r}\left(x_i,y_j,\theta_k+0.5h_\theta\right)+\mu_{v,r}\left(x_i,y_j,\theta_k-0.5h_\theta\right)=2\mu_{v,r}\left(x_i,y_j,\theta_k\right)+O\left(h_\theta^2\right), \tag{36}$$

$$\mu_{v,r}\left(x_i,y_j,\theta_k+0.5h_\theta\right)-\mu_{v,r}\left(x_i,y_j,\theta_k-0.5h_\theta\right)=\frac{\partial\mu_{v,r}\left(x_i,y_j,\theta_k\right)}{\partial\theta}h_\theta+O\left(h_\theta^3\right). \tag{37}$$

By substituting the corresponding expressions from equations (29)–(37) into the expression for Dc_r^n we obtain:

$$Dc_r^n=\frac{\partial\mu_{h,r}\left(x_i,y_j,\theta_k\right)}{\partial x}\frac{\partial c_r^n\left(x_i,y_j,\theta_k\right)}{\partial x}+\mu_{h,r}\left(x_i,y_j,\theta_k\right)\frac{\partial^2 c_r^n\left(x_i,y_j,\theta_k\right)}{\partial x^2}+\frac{\partial\mu_{h,r}\left(x_i,y_j,\theta_k\right)}{\partial y}\frac{\partial c_r^n\left(x_i,y_j,\theta_k\right)}{\partial y}+$$
$$+\mu_{h,r}\left(x_i,y_j,\theta_k\right)\frac{\partial^2 c_r^n\left(x_i,y_j,\theta_k\right)}{\partial y^2}+\frac{1}{H^2\left(x_i,y_j\right)}\left(\frac{\partial\mu_{h,r}\left(x_i,y_j,\theta_k\right)}{\partial\theta}\frac{\partial c_r^n\left(x_i,y_j,\theta_k\right)}{\partial\theta}+\mu_{h,r}\left(x_i,y_j,\theta_k\right)\cdot\right. \tag{38}$$
$$\left.\cdot\frac{\partial^2 c_r^n\left(x_i,y_j,\theta_k\right)}{\partial\theta^2}\right)+O\left(h_x^2+h_y^2+h_\theta^2\right).$$

From the equalities (18), (28), and (38), it follows that the overall order of the approximation error of the finite difference scheme (14) at the grid nodes $\overline{\omega}_\tau\times\omega$ is equal to $O\left(\tau+h^2\right)$, $h^2=h_x^2+h_y^2+h_\theta^2$.

It is important to note that the initial condition (9) is set exactly on the grid $\overline{\omega}_\tau\times\omega$.

3. Second-Order Finite Difference Scheme for the Diffusion-Convection Problem of Multifractional Suspensions at Boundary Nodes. We will assume the existence and continuity of the derivatives $\frac{\partial^4 c_r^n}{\partial x^4},\frac{\partial^4 c_r^n}{\partial y^4},\frac{\partial^4 c_r^n}{\partial\theta^4},\frac{\partial^2 c_r^n}{\partial t^2}$, r = 1,2,3 as well as the continuity of the second-order partial derivatives: $\frac{\partial^2 u}{\partial x^2},\frac{\partial^2 v}{\partial y^2},\frac{\partial^2 w_r'}{\partial\theta^2}$, $\frac{\partial^2\mu_{h,r}}{\partial x^2},\frac{\partial^2\mu_{h,r}}{\partial y^2},\frac{\partial^2\mu_{v,r}}{\partial\theta^2}$ Additionally, we assume the existence and continuity of mixed partial derivatives. We will consider that the following conditions are satisfied:

$$\frac{\partial^2 c_r^n}{\partial x\partial t},\frac{\partial^2 c_r^n}{\partial y\partial t},\frac{\partial^2 c_r^n}{\partial\theta\partial t},\frac{\partial^4 c_r^n}{\partial t\partial x^3},\frac{\partial^4 c_r^n}{\partial t\partial y^3},\frac{\partial^4 c_r^n}{\partial t\partial\theta^3},\frac{\partial^4 c_r^n}{\partial y\partial x^3},\frac{\partial^4 c_r^n}{\partial\theta\partial x^3},\frac{\partial^4 c_r^n}{\partial x\partial y^3},\frac{\partial^4 c_r^n}{\partial\theta\partial y^3},\frac{\partial^4 c_r^n}{\partial x\partial\theta^3},\frac{\partial^4 c_r^n}{\partial y\partial\theta^3},$$

$$\frac{\partial^5 c_r^n}{\partial y^2\partial x^3},\frac{\partial^5 c_r^n}{\partial\theta^2\partial x^3},\frac{\partial^5 c_r^n}{\partial x^2\partial y^3},\frac{\partial^5 c_r^n}{\partial\theta^2\partial y^3},\frac{\partial^5 c_r^n}{\partial x^2\partial\theta^3},\frac{\partial^5 c_r^n}{\partial y^2\partial\theta^3},$$

$$\frac{\partial^2\mu_{h,r}}{\partial x\partial y},\frac{\partial^2\mu_{h,r}}{\partial x\partial\theta},\frac{\partial^2\mu_{h,r}}{\partial y\partial x},\frac{\partial^2\mu_{h,r}}{\partial\theta\partial x},\frac{\partial^2\mu_{v,r}}{\partial y\partial\theta},\frac{\partial^2 v^n}{\partial x\partial y},\frac{\partial^2 v^n}{\partial\theta\partial y},\frac{\partial^2 v^n}{\partial y\partial x},\frac{\partial^2 v^n}{\partial y\partial\theta},\frac{\partial^2 w_r'^n}{\partial x\partial\theta},\frac{\partial^2 w_r'^n}{\partial y\partial\theta},\frac{\partial^2 w_r'^n}{\partial\theta\partial x},\frac{\partial^2 w_r'^n}{\partial\theta\partial y}.$$

We will assume that the following conditions are satisfied:

$$k_{11}\le\frac{h_x}{h_y}\le k_{12},\ k_{21}\le\frac{h_\theta}{h_x}\le k_{22},\ k_{31}\le\frac{h_\theta}{h_y}\le k_{32}, \tag{39}$$

$k_{11}, k_{12}, k_{21}, k_{22}, k_{31}, k_{32}$ represents some positive constants.

To approximate the boundary conditions, we introduce an extended grid:

$$\overline{\omega}^+=\left\{\left(x_i,y_j,\theta_k\right), i=-1,0,\ldots,N_x+1, j=-1,0,\ldots,N_y+1, k=-1,0,\ldots,N_\theta+1,\right.$$
$$\left.x_i=ih_x; y_j=jh_y; \theta_k=kh_\theta; N_xh_x=L_x; N_yh_y=L_y; N_\theta h_\theta=1\right\}.$$

For the nodes of the $\overline{\omega}^{+}\backslash\overline{\omega}$ we assume the values of the components of the velocity vector are equal to zero:

$$\overline{c}_r^{\,n}\left(x_i,y_j,\theta_k\right)=0,\ \text{if}\ \left(x_i,y_j,\theta_k\right)\in\overline{\omega}^{+}\backslash\overline{\omega} \tag{40}$$

furthermore, we consider the values of the components of the velocity vector of the water medium and the hydraulic diameter of the particles in the suspension at the grid nodes $\overline{\omega}^{+}\backslash\overline{\omega}$ with fractional indices to be known: $u^n\left(-0.5h_x,y_j,\theta_k\right)$, $u^n\left(L_x+0.5h_x,y_j,\theta_k\right)$, $v^n\left(x_i,-0.5h_y,\theta_k\right)$, $v^n\left(x_i,L_y+0.5h_y,\theta_k\right)$, $w_r'^{\,n}\left(x_i,y_j,-0.5h_\theta\right)$, $w_r'^{\,n}\left(x_i,y_j,1+0.5h_\theta\right)$.

The boundary conditions (10) are approximated as follows:

$$\begin{cases}\overline{c}_r^{\,n}\left(0,y_j,\theta_k\right)=c_r',\ \text{if}\ u^n\left(0.5h_x,y_j,\theta_k\right)+u^n\left(-0.5h_x,y_j,\theta_k\right)>0,\\ \overline{c}_r^{\,n}\left(L_x,y_j,\theta_k\right)=c_r',\ \text{if}\ u^n\left(L_x-0.5h_x,y_j,\theta_k\right)+u^n\left(L_x+0.5h_x,y_j,\theta_k\right)<0,\ \left(x_i,y_j,\theta_k\right)\in\overline{\omega}^{+};\end{cases}$$
$$\begin{cases}\overline{c}_r^{\,n}\left(x_i,0,\theta_k\right)=c_r',\ \text{if}\ v^n\left(x_i,0.5h_y,\theta_k\right)+v^n\left(x_i,-0.5h_y,\theta_k\right)>0,\\ \overline{c}_r^{\,n}\left(x_i,L_y,\theta_k\right)=c_r',\ \text{if}\ v^n\left(x_i,L_y-0.5h_y,\theta_k\right)+v^n\left(x_i,L_y+0.5h_y,\theta_k\right)<0,\ \left(x_i,y_j,\theta_k\right)\in\overline{\omega}^{+}.\end{cases} \tag{41}$$

In the case of flows on the lateral surfaces of the domain G, that coincide in direction with the external normals to the surfaces, i. e., when the conditions are met:

$$\begin{gathered}u^n\left(0.5h_x,y_j,\theta_k\right)+u^n\left(-0.5h_x,y_j,\theta_k\right)<0,\\ u^n\left(L_x-0.5h_x,y_j,\theta_k\right)+u^n\left(L_x+0.5h_x,y_j,\theta_k\right)>0,\ \left(x_i,y_j,\theta_k\right)\in\overline{\omega}^{+};\\ v^n\left(x_i,0.5h_y,\theta_k\right)+v^n\left(x_i,-0.5h_y,\theta_k\right)<0,\\ v^n\left(x_i,L_y-0.5h_y,\theta_k\right)+v^n\left(x_i,L_y+0.5h_y,\theta_k\right)>0,\ \left(x_i,y_j,\theta_k\right)\in\overline{\omega}^{+}\end{gathered} \tag{42}$$

Neumann boundary conditions are applicable.

Let us proceed to the construction of the difference scheme for the case when condition (11) is satisfied.

The condition (11) is equivalent to the following in case of $x_i = 0$:

$$\frac{\partial\overline{c}_r^{\,n}\left(0,y_j,\theta_k\right)}{\partial x}=0. \tag{43}$$

On the grid $\overline{\omega}^{+}$ the node   is internal (Fig. 1).

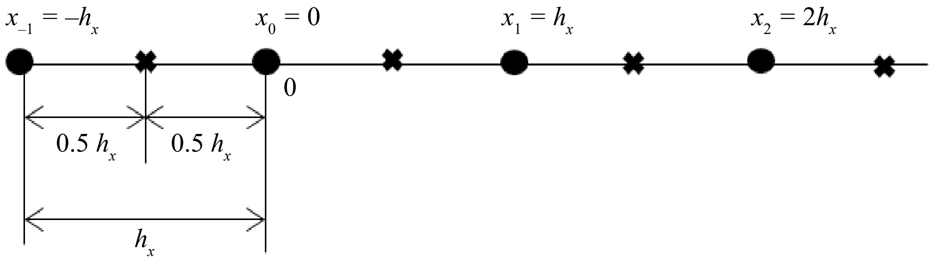

Fig. 1. Construction of the extended grid at the left end of the segment $0 \le x_i \le L_x$

The difference scheme at the nodes $\left(0,y_j,\theta_k\right)$ will be written as follows:

$$\begin{gathered}\frac{\overline{c}_r^{\,n}\left(0,y_j,\theta_k\right)-\overline{c}_r^{\,n-1}\left(0,y_j,\theta_k\right)}{\tau}+\frac{1}{2h_x}\left(u^n\left(0.5h_x,y_j,\theta_k\right)\overline{c}_r^{\,n}\left(h_x,y_j,\theta_k\right)-u^n\left(-0.5h_x,y_j,\theta_k\right)\overline{c}_r^{\,n}\left(-h_x,y_j,\theta_k\right)\right)+\\ +\frac{1}{2h_y}\left(v^n\left(0,y_j+0.5h_y,\theta_k\right)\overline{c}_r^{\,n}\left(0,y_j+h_y,\theta_k\right)-v^n\left(0,y_j-0.5h_y,\theta_k\right)\left(\overline{c}_r^{\,n}\left(0,y_j-h_y,\theta_k\right)\right)+\frac{1}{2H\left(0,y_j\right)h_\theta}\cdot\\ \cdot\left(w_r'^{\,n}\left(0,y_j,\theta_k+0.5h_\theta\right)\overline{c}_r^{\,n}\left(0,y_j,\theta_k+h_\theta\right)-w_r'^{\,n}\left(0,y_j,\theta_k-0.5h_\theta\right)\overline{c}_r^{\,n}\left(0,y_j,\theta_k-h_\theta\right)\right)=\frac{1}{h_x^2}\left(\mu_{h,r}\left(0.5h_x,y_j,\theta_k\right)\cdot\right.\\ \left.\cdot\left(\overline{c}_r^{\,n}\left(h_x,y_j,\theta_k\right)-\overline{c}_r^{\,n}\left(0,y_j,\theta_k\right)\right)-\mu_{h,r}\left(-0.5h_x,y_j,\theta_k\right)\left(\overline{c}_r^{\,n}\left(0,y_j,\theta_k\right)-\overline{c}_r^{\,n}\left(-h_x,y_j,\theta_k\right)\right)\right)+\frac{1}{h_y^2}\cdot\end{gathered} \tag{44}$$

$$\cdot\left(\mu_{h,r}\left(0,y_j+0.5h_y,\theta_k\right)\left(\overline{c}_r^n\left(0,y_j+h_y,\theta_k\right)-\overline{c}_r^n\left(0,y_j,\theta_k\right)\right)-\mu_{h,r}\left(0,y_j-0.5h_y,\theta_k\right)\left(\overline{c}_r^n\left(0,y_j,\theta_k\right)-\right.\right.$$

$$\left.\left.-\overline{c}_r^n\left(0,y_j-h_y,\theta_k\right)\right)\right)+\frac{1}{H^2\left(0,y_j\right)h_\theta^2}\left(\mu_{v,r}\left(0,y_j,\theta_k+0.5h_\theta\right)\left(\overline{c}_r^n\left(0,y_j,\theta_k+h_\theta\right)-\overline{c}_r^n\left(0,y_j,\theta_k\right)\right)-\right.$$

$$\left.-\mu_{v,r}\left(0,y_j,\theta_k-0.5h_\theta\right)\left(\overline{c}_r^n\left(0,y_j,\theta_k\right)-\overline{c}_r^n\left(0,y_j,\theta_k-h_\theta\right)\right)\right)+\overline{F}_r^n,$$

$$\left(0,y_j,\theta_k\right)\in\overline{\omega}^+,\ r=1,2,3,\ n=1,\ldots,N_t.$$

In our reasoning, we focus on the approximation of the given boundary condition using the central difference formula and the exclusion of values at the fictitious node $\left(-h_x,y_j,\theta_k\right)$ from the resulting expression and equation (44). The functions $\overline{c}_r^n\left(-h_x,y_j,\theta_k\right)$ will be included in the expressions

$$\frac{1}{2h_x}\left(u^n\left(0.5h_x,y_j,\theta_k\right)\overline{c}_r^n\left(h_x,y_j,\theta_k\right)-u^n\left(-0.5h_x,y_j,\theta_k\right)\overline{c}_r^n\left(-h_x,y_j,\theta_k\right)\right)$$

$$\frac{1}{h_x^2}\left(\mu_{h,r}\left(0.5h_x,y_j,\theta_k\right)\left(\overline{c}_r^n\left(h_x,y_j,\theta_k\right)-\overline{c}_r^n\left(0,y_j,\theta_k\right)\right)-\mu_{h,r}\left(-0.5h_x,y_j,\theta_k\right)\left(\overline{c}_r^n\left(0,y_j,\theta_k\right)-\overline{c}_r^n\left(-h_x,y_j,\theta_k\right)\right)\right),$$

which we will denote as $C_0\overline{c}_r^n\big|_{x_i=0}$ and $D\overline{c}_r^n\big|_{x_i=0}$.

We will write condition (43) as follows:

$$\frac{\overline{c}_r^n\left(h_x,y_j,\theta_k\right)-\overline{c}_r^n\left(-h_x,y_j,\theta_k\right)}{2h_x}=0 \tag{45}$$

and from this, we obtain:

$$\overline{c}_r^n\left(-h_x,y_j,\theta_k\right)=\overline{c}_r^n\left(h_x,y_j,\theta_k\right). \tag{46}$$

Substituting the value $\overline{c}_r^n\left(-h_x,y_j,\theta_k\right)$ obtained from formula (46) into the expression for $C_0\overline{c}_r^n\big|_{x_i=0}$, we find:

$$C_0\overline{c}_r^n\big|_{x_i=0}\cong\frac{1}{2h_x}\left(u^n\left(0.5h_x,y_j,\theta_k\right)-u^n\left(-0.5h_x,y_j,\theta_k\right)\right)\overline{c}_r^n\left(h_x,y_j,\theta_k\right). \tag{47}$$

Preliminary calculations showed that when using equality (45), the approximation error of the expression for $C_0\overline{c}_r^n\big|_{x_i=0}$ will be $O(h^2)$, while the expression for $D\overline{c}_r^n\big|_{x_i=0}$ will be $O(h_x)$. To determine the overall order of the approximation error $O(h^2)$ of the difference scheme, a different approach will be proposed for the operator $D\overline{c}_r^n\big|_{x_i=0}$.

By expanding the functions $c_r^n\left(\pm h_x,y_j,\theta_k\right)$ in a Taylor series around the point $\left(0,y_j,\theta_k\right)$ we obtain:

$$c_r^n\left(\pm h_x,y_j,\theta_k\right)=c_r^n\left(0,y_j,\theta_k\right)\pm\frac{\partial c_r^n\left(0,y_j,\theta_k\right)}{\partial x}h_x+\frac{\partial^2 c_r^n\left(0,y_j,\theta_k\right)}{\partial x^2}\frac{h_x^2}{2}\pm\frac{\partial^3 c_r^n\left(0,y_j,\theta_k\right)}{\partial x^3}\frac{h_x^3}{6}+ \tag{48}$$

$$+\frac{\partial^4 c_r^n\left(0,y_j,\theta_k\right)}{\partial x^4}\frac{h_x^4}{24}+O\left(h_x^5\right).$$

Using relation (48), we will explicitly write the leading term of the residual:

$$\frac{\overline{c}_r^n\left(h_x,y_j,\theta_k\right)-\overline{c}_r^n\left(-h_x,y_j,\theta_k\right)}{2h_x}=\frac{\partial c_r^n\left(0,y_j,\theta_k\right)}{\partial x}+\frac{\partial^3 c_r^n\left(0,y_j,\theta_k\right)}{\partial x^3}\frac{h_x^2}{6}+O\left(h_x^4\right).$$

The last expression, taking into account the condition $\dfrac{\partial c_r^n\left(0,y_j,\theta_k\right)}{\partial x}=0$ can be written as:

$$\frac{\overline{c}_r^n\left(h_x,y_j,\theta_k\right)-\overline{c}_r^n\left(-h_x,y_j,\theta_k\right)}{2h_x}=\frac{h_x^2}{6}\frac{\partial^3 c\left(0,y_j,\theta_k\right)}{\partial x^3}+O\left(h_x^4\right). \tag{49}$$

Using equality (49), we will find the value of the function c_r^{n-1} at the fictitious node $(-h_x,y,\theta)$ from the expression:

$$\overline{c}_r^n\left(-h_x,y_j,\theta_k\right)=\overline{c}_r^n\left(h_x,y_j,\theta_k\right)-\frac{h_x^3}{3}\frac{\partial^3 c\left(0,y_j,\theta_k\right)}{\partial x^3}+O\left(h_x^5\right). \tag{50}$$

Further reasoning will focus on the approximation of the derivative $\dfrac{\partial^3 c_r^n\left(0,y_j,\theta_k\right)}{\partial x^3}$.

We will differentiate both sides of equation (8) with respect to the variable and express the derivative $\dfrac{\partial^3 \tilde{c}_r^n}{\partial x^3}$ from the resulting equality. Next, we will take the limit as $x \to 0$ and considering that $\dfrac{\partial c_r^n\left(0,y_j,\theta_k\right)}{\partial x}=0$, we find:

$$\frac{\partial^3 c_r^n\left(0,y_j,\theta_k\right)}{\partial x^3}=\frac{1}{\mu_{h,r}\left(0,y_j,\theta_k\right)}\left[\frac{\partial^2 c_r^n\left(0,y_j,\theta_k\right)}{\partial x\partial t}+u^n\left(0,y_j,\theta_k\right)\frac{\partial^2 c_r^n\left(0,y_j,\theta_k\right)}{\partial x^2}+\frac{\partial v^n\left(0,y_j,\theta_k\right)}{\partial x}\frac{\partial c_r^n\left(0,y_j,\theta_k\right)}{\partial y}+\right.$$
$$+v^n\left(0,y_j,\theta_k\right)\frac{\partial^2 c_r^n\left(0,y_j,\theta_k\right)}{\partial x\partial y}+\frac{1}{H\left(0,y_j\right)}\frac{\partial w_r'^n\left(0,y_j,\theta_k\right)}{\partial x}\frac{\partial c_r^n\left(0,y_j,\theta_k\right)}{\partial \theta}+\frac{1}{H\left(0,y_j\right)}w_r'^n\left(0,y_j,\theta_k\right)\frac{\partial^2 c_r^n\left(0,y_j,\theta_k\right)}{\partial x\partial\theta}+$$
$$+\frac{1}{2}\frac{\partial^2 u^n\left(0,y_j,\theta_k\right)}{\partial x^2}c_r^n\left(0,y_j,\theta_k\right)+\frac{1}{2}\frac{\partial^2 v^n\left(0,y_j,\theta_k\right)}{\partial x\partial y}c_r^n\left(0,y_j,\theta_k\right)+\frac{1}{2H\left(0,y_j,\right)}\frac{\partial^2 w_r'^n\left(0,y_j,\theta_k\right)}{\partial x\partial\theta}c_r^n\left(0,y_j,\theta_k\right)-$$
$$-\frac{\partial \mu_{h,r}\left(0,y_j,\theta_k\right)}{\partial x}\frac{\partial^2 c_r^n\left(0,y_j,\theta_k\right)}{\partial x^2}-\frac{\partial \mu_{h,r}\left(0,y_j,\theta_k\right)}{\partial x}\frac{\partial^2 \tilde{c}_r^n\left(0,y_j,\theta_k\right)}{\partial y^2}-\mu_{h,r}\left(0,y_j,\theta_k\right)\frac{\partial^3 \tilde{c}_r^n}{\partial x\partial y^2}-\frac{1}{H^2\left(0,y_j\right)}\cdot \tag{51}$$
$$\cdot\left(\frac{\partial^2 \mu_{v,r}\left(0,y_j,\theta_k\right)}{\partial x\partial\theta}\frac{\partial c_r^n\left(0,y_j,\theta_k\right)}{\partial\theta}+\frac{\partial \mu_{v,r}\left(0,y_j,\theta_k\right)}{\partial\theta}\frac{\partial^2 c_r^n\left(0,y_j,\theta_k\right)}{\partial x\partial\theta}+\frac{\partial \mu_{v,r}\left(0,y_j,\theta_k\right)}{\partial x}\frac{\partial^2 c_r^n\left(0,y_j,\theta_k\right)}{\partial\theta^2}+\right.$$
$$\left.\left.+\mu_{v,r}\left(0,y_j,\theta_k\right)\frac{\partial^3 c_r^n\left(0,y_j,\theta_k\right)}{\partial x\partial\theta^2}\right)\right],\ r=1,2,3,\left(0,y_j,\theta_k\right)\in\bar{G}.$$

It is evident that the equality holds:

$$\frac{\partial F_1^n\left(0,y_j,\theta_k\right)}{\partial x}=\frac{\partial F_2^n\left(0,y_j,\theta_k\right)}{\partial x}=\frac{\partial F_3^n\left(0,y_j,\theta_k\right)}{\partial x}=0.$$

For the reader's convenience, we will approximate the expression in parentheses from the right side of expression (51) for each term separately. Initially, we note that for the coefficient $\dfrac{1}{\mu_{h,r}\left(0,y_j,\theta_k\right)}$, which stands before this parentheses, we will use the expression:

$$\frac{1}{\mu_{h,r}\left(0,y_j,\theta_k\right)}=\frac{2}{\mu_{h,r}\left(0.5h_x,y_j,\theta_k\right)+\mu_{h,r}\left(-0.5h_x,y_j,\theta_k\right)}.$$

Let us consider the derivative $\dfrac{\partial^2 c_r^n\left(0,y_j,\theta_k\right)}{\partial x\partial t}$. For it, we have:

$$\frac{\partial^2 c_r^n\left(0,y_j,\theta_k\right)}{\partial x\partial t}=\frac{1}{2h_x}\left(\frac{\partial \bar{c}_r^n\left(h_x,y_j,\theta_k,t_n\right)}{\partial t}-\frac{\partial \bar{c}_r^n\left(-h_x,y_j,\theta_k,t_n\right)}{\partial t}\right)+O\left(h_x^2\right)=\frac{1}{2h_x}\cdot$$
$$\cdot\left(\frac{\bar{c}_r^n\left(h_x,y_j,\theta_k,t_n+\tau\right)-\bar{c}_r^n\left(h_x,y_j,\theta_k,t^n-\tau\right)}{2\tau}-\frac{\bar{c}_r^n\left(-h_x,y_j,\theta_k,t^n+\tau\right)-\bar{c}_r^n\left(-h_x,y_j,\theta_k,t^n-\tau\right)}{2\tau}+O\left(\tau^2\right)\right)+$$
$$+O\left(h_x^2\right)=\frac{1}{2h_x}\left(\frac{\bar{c}_r^n\left(h_x,y_j,\theta_k,t^n+\tau\right)-\bar{c}_r^n\left(-h_x,y_j,\theta_k,t^n+\tau\right)}{2h_x}-\frac{\bar{c}_r^n\left(h_x,y_j,\theta_k,t^n-\tau\right)-\bar{c}_r^n\left(-h_x,y_j,\theta_k,t^n-\tau\right)}{2h_x}\right)+ \tag{53}$$
$$+\frac{1}{2h_x}O\left(\tau^2\right)+O\left(h_x^2\right).$$

Using equality (50), the relationships can be written as:

$$\frac{\bar{c}_r^n\left(h_x,y_j,\theta_k,t_n\pm\tau\right)-\bar{c}_r^n\left(-h_x,y_j,\theta_k,t_n\pm\tau\right)}{2h_x}=\frac{h_x^2}{6}\frac{\partial^3 c_r^n\left(0,y_j,\theta_k,t_n\pm\tau\right)}{\partial x^3}+O\left(h_x^4\right). \tag{54}$$

With the help of equality (54), we will transform equality (53):

$$\frac{\partial^2 c_r^n}{\partial x \partial t} = \frac{1}{2\tau} \frac{h_x^2}{6} \left(\frac{\partial^3 c_r^n (0, y_j, \theta_k, t_n + \tau)}{\partial x^3} - \frac{\partial^3 c_r^n (0, y_j, \theta_k, t_n - \tau)}{\partial x^3} \right) + \frac{1}{2h_x} O(\tau^2) + O(h_x^2).$$

Introducing the notation $\varphi(0, y_j, \theta_k, t_n \pm \tau) = \dfrac{\partial^3 c_r^n (0, y_j, \theta_k, t_n \pm \tau)}{\partial x^3}$, we will write the last equality as:

$$\frac{\partial^2 c_r^n}{\partial x \partial t} = \frac{h_x^2}{6} \left(\frac{\varphi(0, y_j, \theta_k, t_n + \tau) - \varphi(0, y_j, \theta_k, t_n - \tau)}{2\tau} \right) + \frac{1}{2h_x} O(\tau^2) + O(h_x^2). \quad (55)$$

From which it follows:

$$\frac{\partial^2 c_r^n}{\partial x \partial t} = \frac{h_x^2}{6} \left(\frac{\partial \varphi(0, y_j, \theta_k, t_n)}{\partial t} + O(\tau^2) \right) + \frac{1}{2h_x} O(\tau^2) + O(h_x^2).$$

In accordance with the Courant condition [11], the quantity   is bounded, and we can assume that the equality holds: $\dfrac{1}{2h_x} O(\tau^2) = O(h_x)$. Taking this into account, we have:

$$\frac{\partial^2 c_r^n}{\partial x \partial t} = \frac{h_x^2}{6} \frac{\partial \varphi(0, y_j, \theta_k, t_n)}{\partial t} + O(h_x). \quad (56)$$

Considering relation (56) and the boundedness of the derivative $\dfrac{\partial \varphi(0, y_j, \theta_k, t_n \pm \tau)}{\partial t} = \dfrac{\partial^4 c_r^n (0, y_j, \theta_k, t_n \pm \tau)}{\partial t \partial x^3}$ the expression $\dfrac{\partial^2 c_r^n (0, y_j, \theta_k)}{\partial x \partial t}$ is equal to zero up to $O(h_x)$.

Next, we will show that the derivative $\dfrac{\partial^3 c_r^n (0, y_j, \theta_k)}{\partial x \partial y^2}$ when approximated with an error of $O(h_x)$ also tends to zero.

Taking into account the inequality $k_{11} \le \dfrac{h_x}{h_y} \le k_{12}$ from (39), we have:

$$\frac{\partial^3 c_r^n (0, y_j, \theta_k)}{\partial x \partial y^2} = \frac{1}{2h_x} \left(\frac{\partial^2 \overline{c}_r^n (h_x, y_j, \theta_k)}{\partial y^2} - \frac{\partial^2 \overline{c}_r^n (-h_x, y_j, \theta_k)}{\partial y^2} \right) + O(h_x^2) =$$

$$= \frac{1}{2h_x} \left(\frac{\overline{c}_r^n (h_x, y_j + h_y, \theta_k) - 2\overline{c}_r^n (h_x, y_j, \theta_k) + \overline{c}_r^n (h_x, y_j - h_y, \theta_k)}{h_y^2} - \right.$$

$$\left. - \frac{\overline{c}_r^n (-h_x, y_j + h_y, \theta_k) - 2\overline{c}_r^n (-h_x, y_j, \theta_k) + \overline{c}_r^n (-h_x, y_j - h_y, \theta_k)}{h_y^2} + O(h_y^2) \right) + O(h_x^2) =$$

$$= \frac{1}{h_y^2} \left(\frac{\overline{c}_r^n (h_x, y_j + h_y, \theta_k) - \overline{c}_r^n (-h_x, y_j + h_y, \theta_k)}{2h_x} - 2 \frac{\overline{c}_r^n (h_x, y_j, \theta_k) - \overline{c}_r^n (-h_x, y_j, \theta_k)}{2h_x} + \right. \quad (57)$$

$$\left. + \frac{\overline{c}_r^n (h_x, y_j - h_y, \theta_k) - \overline{c}_r^n (-h_x, y_j - h_y, \theta_k)}{2h_x} \right) + \frac{1}{2h_x} O(h_y^2) + O(h_x^2) =$$

$$= \frac{1}{h_y^2} \left(\frac{\overline{c}_r^n (h_x, y_j + h_y, \theta_k) - \overline{c}_r^n (-h_x, y_j + h_y, \theta_k)}{2h_x} - 2 \frac{\overline{c}_r^n (h_x, y_j, \theta_k) - \overline{c}_r^n (-h_x, y_j, \theta_k)}{2h_x} + \right.$$

$$\left. + \frac{\overline{c}_r^n (h_x, y_j - h_y, \theta_k) - \overline{c}_r^n (-h_x, y_j - h_y, \theta_k)}{2h_x} \right) + O(h_x^2 + h_y).$$

Based on equality (57), the relationship can be written as:

$$\frac{\overline{c}_r^n (h_x, y_j \pm h_y, \theta_k) - \overline{c}_r^n (-h_x, y_j \pm h_y, \theta_k)}{2h_x} = \frac{h_x^2}{6} \frac{\partial^3 c_r^n (0, y_j \pm h_y, \theta_k)}{\partial x^3} + O(h_x^4). \quad (58)$$

Using equalities (58), we will transform relationship (57):

$$\frac{\partial^3 c_r^n (0, y_j, \theta_k)}{\partial x \partial y^2} = \frac{1}{h_y^2} \frac{h_x^2}{6} \left(\frac{\partial^3 c_r^n (0, y_j + h_y, \theta_k)}{\partial x^3} - 2 \frac{\partial^3 c_r^n (0, y_j, \theta_k)}{\partial x^3} + \frac{\partial^3 c_r^n (0, y_j - h_y, \theta_k)}{\partial x^3} \right) + O(h_x^2 + h_y).$$

Let $\varphi\left(0,y_j \pm h_y,\theta_k\right)=\dfrac{\partial^3 c_r^n\left(0,y_j \pm h_y,\theta_k\right)}{\partial x^3}$, $\varphi\left(0,y_j,\theta_k\right)=\dfrac{\partial^3 c_r^n\left(0,y_j,\theta_k\right)}{\partial x^3}$. Then the last equality can be written as:

$$\frac{\partial^3 c_r^n\left(0,y_j,\theta_k\right)}{\partial x \partial y^2}=\frac{h_x^2}{6}\left(\frac{\varphi\left(0,y_j+h_y,\theta_k\right)-2\varphi\left(0,y_j,\theta_k\right)+\varphi\left(0,y_j-h_y,\theta_k\right)}{h_y^2}\right)+O\left(h_x^2+h_y\right). \tag{59}$$

From equality (59), it follows that:

$$\frac{\partial^3 c_r^n\left(0,y_j,\theta_k\right)}{\partial x \partial y^2}=\frac{h_x^2}{6}\left(\frac{\partial^2 \varphi\left(0,y_j,\theta_k\right)}{\partial y^2}+O\left(h_y^2\right)\right)+O\left(h_x^2+h_y\right).$$

The last equality can be transformed into the form:

$$\frac{\partial^3 c_r^n\left(0,y_j,\theta_k\right)}{\partial x \partial y^2}=\frac{h_x^2}{6}\frac{\partial^2 \varphi\left(0,y_j,\theta_k\right)}{\partial y^2}+O\left(h_x\right). \tag{60}$$

Considering relation (60) and the boundedness of the derivative $\dfrac{\partial^2 \varphi\left(0,y_j,\theta_k\right)}{\partial y^2}=\dfrac{\partial^5 c_r^n\left(0,y_j,\theta_k\right)}{\partial y^2 \partial x^3}$ with respect to $O(h_x)$ the expression $\dfrac{\partial^3 c_r^n\left(0,y_j,\theta_k\right)}{\partial x \partial y^2}$ is equal to zero.

By applying similar reasoning for the derivatives $\dfrac{\partial^3 c_r^n\left(0,y_j,\theta_k\right)}{\partial x \partial \theta^2}$, $\dfrac{\partial^2 c_r^n\left(0,y_j,\theta_k\right)}{\partial x \partial y}$, $\dfrac{\partial^2 c_r^n\left(0,y_j,\theta_k\right)}{\partial x \partial \theta}$ it can be easily verified that when the inequalities from (40) are satisfied, these derivatives are equal to zero up to $O(h_x)$.

Let us consider the derivative $\dfrac{\partial^2 c_r^n\left(0,y_j,\theta_k\right)}{\partial x^2}$. We have:

$$\frac{\partial^2 c_r^n\left(0,y_j,\theta_k\right)}{\partial x^2}=\frac{\overline{c}_r^n\left(h_x,y_j,\theta_k\right)-2\overline{c}_r^n\left(0,y_j,\theta_k\right)+\overline{c}_r^n\left(-h_x,y_j,\theta_k\right)}{h_x^2}+O\left(h_x^2\right). \tag{61}$$

In the last equality, the value of the function $\overline{c}_r^n$ at the fictitious node $\left(-h_x,y_j,\theta_k\right)$ will be replaced using expression (50). We obtain

$$\frac{\partial^2 c_r^n\left(0,y_j,\theta_k\right)}{\partial x^2}=\frac{1}{h_x^2}\left(\overline{c}_r^n\left(h_x,y_j,\theta_k\right)-2\overline{c}_r^n\left(0,y_j,\theta_k\right)+\left(\overline{c}_r^n\left(h_x,y_j,\theta_k\right)-\frac{h_x^3}{3}\frac{\partial^3 c_r^n\left(0,y_j,\theta_k\right)}{\partial x^3}+O\left(h_x^5\right)\right)\right)+$$

$$+O\left(h_x^2\right)=\frac{1}{h_x^2}\left(2\left(\overline{c}_r^n\left(h_x,y_j,\theta_k\right)-\overline{c}_r^n\left(0,y_j,\theta_k\right)\right)-\frac{h_x^3}{3}\frac{\partial^3 c_r^n\left(0,y_j,\theta_k\right)}{\partial x^3}\right)+O\left(h_x^2\right)$$

or

$$\frac{\partial^2 c_r^n\left(0,y_j,\theta_k\right)}{\partial x^2}\cong\frac{2}{h_x^2}\left(\overline{c}_r^n\left(h_x,y_j,\theta_k\right)-\overline{c}_r^n\left(0,y_j,\theta_k\right)\right)-\frac{h_x}{3}\frac{\partial^3 c_r^n\left(0,y_j,\theta_k\right)}{\partial x^3}. \tag{62}$$

The terms $u^n\left(0,y_j,\theta_k\right)\dfrac{\partial^2 c_r^n\left(0,y_j,\theta_k\right)}{\partial x^2}$ and $\dfrac{\partial \mu_{h,r}\left(0,y_j,\theta_k\right)}{\partial x}\dfrac{\partial^2 c_r^n\left(0,y_j,\theta_k\right)}{\partial x^2}$ from equality (51), which include the factor $\dfrac{\partial^2 c_r^n\left(0,y_j,\theta_k\right)}{\partial x^2}$, are approximated by the expressions using relation (62):

$$u^n\left(0,y_j,\theta_k\right)\frac{\partial^2 c_r^n\left(0,y_j,\theta_k\right)}{\partial x^2}\cong\frac{1}{2}\left(u^n\left(0.5h_x,y_j,\theta_k\right)+u^n\left(-0.5h_x,y_j,\theta_k\right)\right)\left(\frac{2}{h_x^2}\left(\overline{c}_r^n\left(h_x,y_j,\theta_k\right)-\overline{c}_r^n\left(0,y_j,\theta_k\right)\right)-\right.$$
$$\left.-\frac{h_x}{3}\frac{\partial^3 c_r^n\left(0,y_j,\theta_k\right)}{\partial x^3}\right); \tag{63}$$

$$\frac{\partial \mu_{h,r}\left(0,y_j,\theta_k\right)}{\partial x}\frac{\partial^2 c_r^n\left(0,y_j,\theta_k\right)}{\partial x^2}\cong\frac{1}{h_x}\left(\mu_{h,r}\left(0.5h_x,y_j,\theta_k\right)-\mu_{h,r}\left(-0.5h_x,y_j,\theta_k\right)\right)\left(\frac{2}{h_x^2}\left(\overline{c}_r^n\left(h_x,y_j,\theta_k\right)-\right.\right.$$
$$\left.\left.-\overline{c}_r^n\left(0,y_j,\theta_k\right)\right)-\frac{h_x}{3}\frac{\partial^3 c_r^n\left(0,y_j,\theta_k\right)}{\partial x^3}\right). \tag{64}$$

When approximating the derivative $\frac{\partial^2 c_r^n\left(0,y_j,\theta_k\right)}{\partial y^2}$, we obtain:

$$\frac{\partial^2 c_r^n\left(0,y_j,\theta_k\right)}{\partial y^2}=\frac{\overline{c}_r^n\left(0,y_j+h_y,\theta_k\right)-2\overline{c}_r^n\left(0,y_j,\theta_k\right)+\overline{c}_r^n\left(0,y_j-h_y,\theta_k\right)}{h_y^2}+O\left(h_y^2\right). \tag{65}$$

Approximating the term $\frac{\partial \mu_{h,r}\left(0,y_j,\theta_k\right)}{\partial x}\frac{\partial^2 c_r^n\left(0,y_j,\theta_k\right)}{\partial y^2}$ from equality (51), which includes the factor $\frac{\partial^2 c_r^n\left(0,y_j,\theta_k\right)}{\partial y^2}$, using relation (65), we get:

$$\begin{gathered}\frac{\partial \mu_{h,r}\left(0,y_j,\theta_k\right)}{\partial x}\frac{\partial^2 c_r^n\left(0,y_j,\theta_k\right)}{\partial y^2}\cong\frac{1}{h_x h_y^2}\left(\mu_{h,r}\left(0.5h_x,y_j,\theta_k\right)-\mu_{v,r}\left(-0.5h_x,y_j,\theta_k\right)\right)\left(\overline{c}_r^n\left(0,y_j+h_y,\theta_k\right)-\right.\\ \left.-2\overline{c}_r^n\left(0,y_j,\theta_k\right)+\overline{c}_r^n\left(0,y_j-h_y,\theta_k\right)\right).\end{gathered} \tag{66}$$

The approximation of the form (66) is carried out with an accuracy of $O(h_x)$. Indeed, it is not difficult to verify:

$$\overline{c}_r^n\left(0,y_j+h_y,\theta_k\right)-2\overline{c}_r^n\left(0,y_j,\theta_k\right)+\overline{c}_r^n\left(0,y_j-h_y,\theta_k\right)=\frac{\partial^2 c_r^n\left(0,y_j,\theta_k\right)}{\partial y^2}h_y^2+O\left(h_y^3\right), \tag{67}$$

$$\mu_{h,r}\left(0.5h_x,y_j,\theta_k\right)-\mu_{h,r}\left(-0.5h_x,y_j,\theta_k\right)=\frac{\partial \mu_{h,r}\left(0,y_j,\theta_k\right)}{\partial x}h_x+O\left(h_x^3\right). \tag{68}$$

Taking into account equalities (67) and (68) for relation (66), we obtain:

$$\begin{gathered}\frac{\partial \mu_{h,r}\left(0,y_j,\theta_k\right)}{\partial x}\frac{\partial^2 c_r^n\left(0,y_j,\theta_k\right)}{\partial y^2}=\frac{1}{h_x h_y^2}\left(\frac{\partial \mu_{h,r}\left(0,y_j,\theta_k\right)}{\partial x}h_x+O\left(h_x^3\right)\right)\left(\frac{\partial^2 \overline{c}_r^n\left(0,y_j,\theta_k\right)}{\partial y^2}h_y^2+O\left(h_y^3\right)\right)=\\ =\frac{\partial \mu_{h,r}\left(0,y_j,\theta_k\right)}{\partial x}\frac{\partial^2 \overline{c}_r^n\left(0,y_j,\theta_k\right)}{\partial y^2}+O\left(h_x\right).\end{gathered} \tag{69}$$

When approximating the derivative $\frac{\partial^2 c_r^n\left(0,y_j,\theta_k\right)}{\partial \theta^2}$, we obtain:

$$\frac{\partial^2 c_r^n\left(0,y_j,\theta_k\right)}{\partial \theta^2}=\frac{\overline{c}_r^n\left(0,y_j,\theta_k+h_\theta\right)-2\overline{c}_r^n\left(0,y_j,\theta_k\right)+\overline{c}_r^n\left(0,y_j,\theta_k-h_\theta\right)}{h_\theta^2}+O\left(h_\theta^2\right). \tag{70}$$

Then for the term $\frac{1}{H^2\left(0,y_j\right)}\frac{\partial \mu_{v,r}\left(0,y_j,\theta_k\right)}{\partial x}\frac{\partial^2 c_r^n\left(0,y_j,\theta_k\right)}{\partial \theta^2}$ from equality (51), which includes the factor $\frac{\partial^2 c_r^n\left(0,y_j,\theta_k\right)}{\partial \theta^2}$, we find:

$$\begin{gathered}\frac{1}{H^2\left(0,y_j\right)}\frac{\partial \mu_{v,r}\left(0,y_j,\theta_k\right)}{\partial x}\frac{\partial^2 c_r^n\left(0,y_j,\theta_k\right)}{\partial \theta^2}\cong\frac{1}{h_x h_\theta^2 H^2\left(0,y_j\right)}\left(\mu_{v,r}\left(0.5h_x,y_j,\theta_k\right)-\mu_{v,r}\left(-0.5h_x,y_j,\theta_k\right)\right)\cdot\\ \cdot\left(\overline{c}_r^n\left(0,y_j,\theta_k+h_\theta\right)-2\overline{c}_r^n\left(0,y_j,\theta_k\right)+\overline{c}_r^n\left(0,y_j,\theta_k-h_\theta\right)\right).\end{gathered} \tag{71}$$

The error of the approximation of the expression $\frac{1}{H^2\left(0,y_j\right)}\frac{\partial \mu_{v,r}\left(0,y_j,\theta_k\right)}{\partial x}\frac{\partial^2 c_r^n\left(0,y_j,\theta_k\right)}{\partial \theta^2}$ using relation (71) is $O(h_x)$. Indeed, taking into account the equality

$$\overline{c}_r^n\left(0,y_j,\theta_k+h_\theta\right)-2\overline{c}_r^n\left(0,y_j,\theta_k\right)+\overline{c}_r^n\left(0,y_j,\theta_k-h_\theta\right)=2\frac{\partial^2 c_r^n\left(0,y_j,\theta_k\right)}{\partial \theta^2}\frac{h_\theta^2}{2}+O\left(h_\theta^3\right), \tag{72}$$

we obtain:

$$\begin{gathered}\frac{1}{H^2\left(0,y_j\right)}\frac{\partial \mu_{v,r}\left(0,y_j,\theta_k\right)}{\partial x}\frac{\partial^2 c_r^n\left(0,y_j,\theta_k\right)}{\partial \theta^2}=\frac{1}{h_x h_\theta^2 H^2\left(0,y_j\right)}\left(\frac{\partial \mu_{h,r}\left(0,y_j,\theta_k\right)}{\partial x}h_x+O\left(h_x^3\right)\right)\left(\frac{\partial^2 \overline{c}_r^n\left(0,y_j,\theta_k\right)}{\partial \theta^2}h_\theta^2+\right.\\ \left.+O\left(h_\theta^3\right)\right)=\frac{\partial \mu_{h,r}\left(0,y_j,\theta_k\right)}{\partial x}\frac{\partial^2 \overline{c}_r^n\left(0,y_j,\theta_k\right)}{\partial \theta^2}+O\left(h_x\right).\end{gathered} \tag{73}$$

Next, let us consider the derivative $\frac{\partial c_r^n(0,y_j,\theta_k)}{\partial y}$. When approximating it with central differences, we get:

$$\frac{\partial c_r^n(0,y_j,\theta_k)}{\partial y}=\frac{\bar{c}_r^n(0,y_j+h_y,\theta_k)-\bar{c}_r^n(0,y_j-h_y,\theta_k)}{2h_y}+O(h_y^2). \tag{74}$$

Then for the term $\frac{\partial v^n(0,y_j,\theta_k)}{\partial x}\frac{\partial c_r^n(0,y_j,\theta_k)}{\partial y}$ from equality (51), which includes the factor $\frac{\partial c_r^n(0,y_j,\theta_k)}{\partial y}$, we find:

$$\frac{\partial v^n(0,y_j,\theta_k)}{\partial x}\frac{\partial c_r^n(0,y_j,\theta_k)}{\partial y}\cong\frac{1}{2h_xh_y}\left(v^n(0.5h_x,y_j,\theta_k)-v^n(-0.5h_x,y_j,\theta_k)\right)\left(\bar{c}_r^n(0,y_j+h_y,\theta_k)-\right.$$
$$\left.-\bar{c}_r^n(0,y_j-h_y,\theta_k)\right). \tag{75}$$

Here

$$\frac{\partial v^n(0,y_j,\theta_k)}{\partial x}=\frac{v^n(0.5h_x,y_j,\theta_k)-v^n(-0.5h_x,y_j,\theta_k)}{h_x}+O(h_x^2). \tag{76}$$

It is not difficult to verify that the approximation error for expression $\frac{\partial v^n(0,y_j,\theta_k)}{\partial x}\frac{\partial c_r^n(0,y_j,\theta_k)}{\partial y}$, carried out using relation (75), is $O(h_x^2)$ and the equality holds:

$$\frac{\partial v^n(0,y_j,\theta_k)}{\partial x}\frac{\partial c_r^n(0,y_j,\theta_k)}{\partial y}=\frac{1}{2h_xh_y}\left(\frac{\partial v^n(0,y_j,\theta_k)}{\partial x}h_x+O(h_x^3)\right)\left(2\frac{\partial \bar{c}_r^n(0,y_j,\theta_k)}{\partial y}h_y+O(h_y^3)\right)=$$
$$=2\frac{\partial v^n(0,y_j,\theta_k)}{\partial x}\frac{\partial \bar{c}_r^n(0,y_j,\theta_k)}{\partial y}+O(h_x^2). \tag{77}$$

When approximating the derivative $\frac{\partial c_r^n(0,y_j,\theta_k)}{\partial \theta}$, we obtain:

$$\frac{\partial c_r^n(0,y_j,\theta_k)}{\partial \theta}=\frac{\bar{c}_r^n(0,y_j,\theta_k+h_\theta)-\bar{c}_r^n(0,y_j,\theta_k-h_\theta)}{2h_\theta}+O(h_\theta^2). \tag{78}$$

Then for the terms $\frac{1}{H(0,y_j)}\frac{\partial w_r'^n(0,y_j,\theta_k)}{\partial x}\frac{\partial c_r^n(0,y_j,\theta_k)}{\partial \theta}$ and $\frac{1}{H^2(0,y_j)}\frac{\partial^2 \mu_{v,r}(0,y_j,\theta_k)}{\partial x\partial \theta}\frac{\partial c_r^n(0,y_j,\theta_k)}{\partial \theta}$ from equality (51), which include the factor $\frac{\partial c_r^n(0,y_j,\theta_k)}{\partial \theta}$, we find:

$$\frac{1}{H(0,y_j)}\frac{\partial w_r'^n(0,y_j,\theta_k)}{\partial x}\frac{\partial c_r^n(0,y_j,\theta_k)}{\partial \theta}\cong\frac{1}{2h_xh_\theta H(0,y_j)}\left(w_r'^n(0.5h_x,y_j,\theta_k)-w_r'^n(-0.5h_x,y_j,\theta_k)\right)\cdot$$
$$\cdot\left(\bar{c}_r^n(0,y_j,\theta_k+h_\theta)-\bar{c}_r^n(0,y_j,\theta_k-h_\theta)\right); \tag{79}$$

$$\frac{1}{H^2(0,y_j)}\frac{\partial^2 \mu_{v,r}(0,y_j,\theta_k)}{\partial x\partial \theta}\frac{\partial c_r^n(0,y_j,\theta_k)}{\partial \theta}\cong\frac{1}{2h_xh_\theta^2H^2(0,y_j)}\left[\left(\mu_{v,r}(0.5h_x,y_j,\theta_k+0.5h_\theta)-\right.\right.$$
$$\left.-\mu_{v,r}(-0.5h_x,y_j,\theta_k+0.5h_\theta)\right)-\left.\left(\mu_{v,r}(0.5h_x,y_j,\theta_k-0.5h_\theta)-\mu_{v,r}(-0.5h_x,y_j,\theta_k-0.5h_\theta)\right)\right]\cdot$$
$$\cdot\left(\bar{c}_r^n(0,y_j,\theta_k+h_\theta)-\bar{c}_r^n(0,y_j,\theta_k-h_\theta)\right). \tag{80}$$

Here, the equalities used in writing relations (79) and (80) are:

$$\frac{\partial w_r'^n(0,y_j,\theta_k)}{\partial x}=\frac{w_r'^n(0.5h_x,y_j,\theta_k)-w_r'^n(-0.5h_x,y_j,\theta_k)}{h_x}+O(h_x^2) \tag{81}$$

$$\frac{\partial^2\mu_{v,r}(0,y_j,\theta_k)}{\partial x\partial\theta}=\frac{1}{h_\theta}\left(\frac{\mu_{v,r}(0.5h_x,y_j,\theta_k+0.5h_\theta)-\mu_{v,r}(-0.5h_x,y_j,\theta_k+0.5h_\theta)}{h_x}-\right.$$
$$\left.-\frac{\mu_{v,r}(0.5h_x,y_j,\theta_k-0.5h_\theta)-\mu_{v,r}(-0.5h_x,y_j,\theta_k-0.5h_\theta)}{h_x}\right)+\frac{1}{h_x}O(h_\theta^2)+O(h_x^2). \tag{82}$$

Taking into account the inequality $k_{21}\leq\frac{h_\theta}{h_x}\leq k_{22}$ from (39), we can assert that the approximation of the form (80) is carried out with an error of $O(h_x)$.

When approximating $c_r^n(0,y_j,\theta_k)$, we replace it with its grid analog $\overline{c}_r^n(0,y_j,\theta_k)$.

Then for the terms $\frac{1}{2}\frac{\partial^2u^n(0,y_j,\theta_k)}{\partial x^2}c_r^n(0,y_j,\theta_k)$, $\frac{1}{2}\frac{\partial^2v^n(0,y_j,\theta_k)}{\partial x\partial y}c_r^n(0,y_j,\theta_k)$ and $\frac{1}{2H(0,y_j)}\frac{\partial^2w_r'^n(0,y_j,\theta_k)}{\partial x\partial\theta}c_r^n(0,y_j,\theta_k)$, which include the factor $\overline{c}_r^n(0,y_j,\theta_k)$, we find:

$$\frac{1}{2}\frac{\partial^2u^n(0,y_j,\theta_k)}{\partial x^2}c_r^n(0,y_j,\theta_k)\cong\frac{1}{0.5h_x^2H(0,y_j)}\left(u^n(0.5h_x,y_j,\theta_k)-2u^n(0,y_j,\theta_k)+u^n(-0.5h_x,y_j,\theta_k)\right)\cdot$$
$$\cdot\overline{c}_r^n(0,y_j,\theta_k); \tag{83}$$

$$\frac{1}{2}\frac{\partial^2v^n(0,y_j,\theta_k)}{\partial x\partial y}c_r^n(0,y_j,\theta_k)\cong\frac{1}{2h_xh_y}\left[\left(v^n(0.5h_x,y_j+0.5h_y,\theta_k)-v^n(-0.5h_x,y_j+0.5h_y,\theta_k)\right)-\right.$$
$$\left.-\left(v^n(0.5h_x,y_j-0.5h_y,\theta_k)-v^n(-0.5h_x,y_j-0.5h_y,\theta_k)\right)\right]\overline{c}_r^n(0,y_j,\theta_k). \tag{84}$$

$$\frac{1}{2H(0,y_j)}\frac{\partial^2w_r'^n(0,y_j,\theta_k)}{\partial x\partial\theta}c_r^n(0,y_j,\theta_k)\cong\frac{1}{2h_xh_\theta H(0,y_j)}\left[\left(w_r'^n(0.5h_x,y,\theta_k+0.5h_\theta)-\right.\right.$$
$$\left.-\left(w_r'^n(-0.5h_x,y_j,\theta_k+0.5h_\theta)\right)\left(w_r'^n(0.5h_x,y_j,\theta_k-0.5h_\theta)-w_r'^n(-0.5h_x,y_j,\theta_k-0.5h_\theta)\right)\right]\overline{c}_r^n(0,y_j,\theta_k). \tag{85}$$

It is evident that expression (83) is obtained with an accuracy of $O(h^2_x)$.

In writing relations (84) and (85), the equalities used are:

$$\frac{\partial^2v^n(0,y_j,\theta_k)}{\partial x\partial y}=\frac{1}{h_y}\left(\frac{v^n(0.5h_x,y_j+0.5h_y,\theta_k)-v^n(-0.5h_x,y_j+0.5h_y,\theta_k)}{h_x}-\right.$$
$$\left.-\frac{v^n(0.5h_x,y_j-0.5h_y,\theta_k)-v^n(-0.5h_x,y_j-0.5h_y,\theta_k)}{h_x}\right)+\frac{1}{h_x}O(h_y^2)+O(h_x^2), \tag{86}$$

$$\frac{\partial^2w_r'^n(0,y_j,\theta_k)}{\partial x\partial\theta}=\frac{1}{h_\theta}\left(\frac{w_r'^n(0.5h_x,y_j,\theta_k+0.5h_\theta)-w_r'^n(-0.5h_x,y_j,\theta_k+0.5h_\theta)}{h_x}-\right.$$
$$\left.-\frac{w_r'^n(0.5h_x,y_j-0.5h_y,\theta_k)-w_r'^n(-0.5h_x,y_j-0.5h_y,\theta_k)}{h_x}\right)+\frac{1}{h_x}O(h_\theta^2)+O(h_x^2). \tag{87}$$

Considering equalities (86) and (87), we obtain that the error of the approximations (84) and (85) is $O(h_x)$.

Thus, we have obtained the approximations for all terms located in the parentheses on the right side of equality (51). As a result of substituting into equality (51) the approximations carried out by expressions (63), (64), (66), (71), (75), (79), (80), (83)–(85) with an error of $O(h_x)$ ((or higher), we obtain:

$$\frac{\partial^3\overline{c}_r^n(0,y_j,\theta_k)}{\partial x^3}=\vartheta_1+O(h_x), \tag{88}$$

where

$$\vartheta_1=\vartheta_{10}\left(\vartheta_{11}\overline{c}(h_x,y_j,\theta_k)+\vartheta_{12}\overline{c}(0,y_j+h_y,\theta_k)+\vartheta_{13}\overline{c}(0,y_j-h_y,\theta_k)+\vartheta_{14}\overline{c}(0,y_j,\theta_k+h_\theta)+\vartheta_{15}\overline{c}(0,y_j,\theta_k-h_\theta)+\right.$$
$$\left.+\vartheta_{16}\overline{c}(0,y_j,\theta_k)\right),$$

$$\vartheta_{10}=\frac{3\left(\mu_{h,r}\left(0.5h_x,y_j,\theta_k\right)+\mu_{h,r}\left(-0.5h_x,y_j,\theta_k\right)\right)}{4\mu_{h,r}\left(0.5h_x,y_j,\theta_k\right)+2\mu_{h,r}\left(-0.5h_x,y_j,\theta_k\right)-\left(u^n\left(0.5h_x,y_j,\theta_k\right)+u^n\left(-0.5h_x,y_j,\theta_k\right)\right)h_x};$$

$$\vartheta_{11}=\frac{1}{h_x^2}\left(u^n\left(0.5h_x,y_j,\theta_k\right)+u^n\left(-0.5h_x,y_j,\theta_k\right)\right)-\frac{2}{h_x^3}\left(\mu_{h,r}\left(0.5h_x,y_j,\theta_k\right)-\mu_{h,r}\left(-0.5h_x,y_j,\theta_k\right)\right);$$

$$\vartheta_{12}=\frac{1}{2h_xh_y}\left(v^n\left(0.5h_x,y_j,\theta_k\right)-v^n\left(-0.5h_x,y_j,\theta_k\right)\right)-\frac{1}{h_xh_y^2}\left(\mu_{h,r}\left(0.5h_x,y_j,\theta_k\right)-\mu_{v,r}\left(-0.5h_x,y_j,\theta_k\right)\right);$$

$$\vartheta_{12}=\frac{1}{2h_xh_y}\left(v^n\left(0.5h_x,y_j,\theta_k\right)-v^n\left(-0.5h_x,y_j,\theta_k\right)\right)-\frac{1}{h_xh_y^2}\left(\mu_{h,r}\left(0.5h_x,y_j,\theta_k\right)-\mu_{v,r}\left(-0.5h_x,y_j,\theta_k\right)\right);$$

$$\vartheta_{13}=-\frac{1}{2h_xh_y}\left(v^n\left(0.5h_x,y_j,\theta_k\right)-v^n\left(-0.5h_x,y_j,\theta_k\right)\right)-\frac{1}{h_xh_y^2}\left(\mu_{h,r}\left(0.5h_x,y_j,\theta_k\right)-\mu_{v,r}\left(-0.5h_x,y_j,\theta_k\right)\right);$$

$$\vartheta_{14}=\frac{1}{2h_xh_\theta H\left(0,y_j\right)}\left(w_r'^n\left(0.5h_x,y_j,\theta_k\right)-w_r'^n\left(-0.5h_x,y_j,\theta_k\right)\right)-\frac{1}{h_xh_\theta^2H^2\left(0,y_j\right)}\left(\mu_{v,r}\left(0.5h_x,y_j,\theta_k\right)-\right.$$

$$\left.-\mu_{v,r}\left(-0.5h_x,y_j,\theta_k\right)\right)-\frac{1}{2h_xh_\theta^2H^2\left(0,y_j\right)}\left(\mu_{v,r}\left(0.5h_x,y_j,\theta_k+0.5h_\theta\right)-\mu_{v,r}\left(-0.5h_x,y_j,\theta_k+0.5h_\theta\right)-\right.$$

$$\left.-\mu_{v,r}\left(0.5h_x,y_j,\theta_k-0.5h_\theta\right)+\mu_{v,r}\left(-0.5h_x,y_j,\theta_k-0.5h_\theta\right)\right);$$

$$\vartheta_{15}=-\frac{1}{2h_xh_\theta H\left(0,y_j\right)}\left(w_r'^n\left(0.5h_x,y_j,\theta_k\right)-w_r'^n\left(-0.5h_x,y_j,\theta_k\right)\right)-\frac{1}{h_xh_\theta^2H^2\left(0,y_j\right)}\left(\mu_{v,r}\left(0.5h_x,y_j,\theta_k\right)-\right.$$

$$\left.-\mu_{v,r}\left(-0.5h_x,y_j,\theta_k\right)\right)+\frac{1}{2h_xh_\theta^2H^2\left(0,y_j\right)}\left(\mu_{v,r}\left(0.5h_x,y_j,\theta_k+0.5h_\theta\right)-\mu_{v,r}\left(-0.5h_x,y_j,\theta_k+0.5h_\theta\right)-\right.$$

$$\left.-\mu_{v,r}\left(0.5h_x,y_j,\theta_k-0.5h_\theta\right)+\mu_{v,r}\left(-0.5h_x,y_j,\theta_k-0.5h_\theta\right)\right);$$

$$\vartheta_{16}=-\frac{1}{h_x^2}\left(u^n\left(0.5h_x,y_j,\theta_k\right)+u^n\left(-0.5h_x,y_j,\theta_k\right)\right)+\frac{2}{h_x^2H\left(0,y_j\right)}\left(u^n\left(0.5h_x,y_j,\theta_k\right)-\right.$$

$$\left.-2u^n\left(0,y_j,\theta_k\right)+u^n\left(-0.5h_x,y_j,\theta_k\right)\right)+\frac{1}{2h_xh_y}\left(v^n\left(0.5h_x,y_j+0.5h_y,\theta_k\right)-v^n\left(-0.5h_x,y_j+0.5h_y,\theta_k\right)-\right.$$

$$\left.-v^n\left(0.5h_x,y_j-0.5h_y,\theta_k\right)+v^n\left(-0.5h_x,y_j-0.5h_y,\theta_k\right)\right)+\frac{1}{2h_xh_\theta H\left(0,y_j\right)}\left(w_r'^n\left(0.5h_x,y_j,\theta_k+0.5h_\theta\right)-\right.$$

$$\left.-w_r'^n\left(-0.5h_x,y_j,\theta_k+0.5h_\theta\right)-w_r'^n\left(0.5h_x,y_j,\theta_k-0.5h_\theta\right)+w_r'^n\left(-0.5h_x,y_j,\theta_k-0.5h_\theta\right)\right)+$$

$$+2\left(\frac{1}{h_x^3}+\frac{1}{h_xh_y^2}+\frac{1}{h_xh_\theta^2H^2\left(0,y_j\right)}\right)\left(\mu_{h,r}\left(0.5h_x,y,\theta\right)-\mu_{h,r}\left(-0.5h_x,y_j,\theta_k\right)\right)\cdot$$

Using equality (88) for $D\overline{c}_r^n\big|_{x_i=0}$, we can construct the expression:

$$D\overline{c}_r^n\big|_{x_i=0}\cong\frac{1}{h_x^2}\left(\mu_{h,r}\left(0.5h_x,y_j,\theta_k\right)+\mu_{h,r}\left(-0.5h_x,y_j,\theta_k\right)\right)\left(\overline{c}_r^n\left(h_x,y_j,\theta_k\right)-\overline{c}_r^n\left(0,y_j,\theta_k\right)\right)-$$
$$-\mu_{h,r}\left(-0.5h_x,y_j,\theta_k\right)\frac{h_x}{3}\vartheta_1. \tag{89}$$

Ultimately, the difference scheme (44), taking into account relations (47) and (89), will take the form:

$$\frac{\overline{c}_r^n-\overline{c}_r^{n-1}}{\tau}+\frac{1}{2h_x}\left(u^n\left(0.5h_x,y_j,\theta_k\right)-u^n\left(-0.5h_x,y_j,\theta_k\right)\right)\overline{c}_r^n\left(h_x,y_j,\theta_k\right)+$$

$$+\frac{1}{2h_y}\left(v^n\left(0,y_j+0.5h_y,\theta_k\right)\overline{c}_r^n\left(0,y_j+h_y,\theta_k\right)-v^n\left(0,y_j-0.5h_y,\theta_k\right)\overline{c}_r^n\left(0,y_j-h_y,\theta_k\right)\right)+\frac{1}{2H\left(0,y_j\right)h_\theta}\cdot$$

$$\cdot\left(w_r'^n\left(0,y_j,\theta_k+0.5h_\theta\right)\overline{c}_r^n\left(0,y_j,\theta_k+h_\theta\right)-w_r'^n\left(0,y_j,\theta_k-0.5h_\theta\right)\overline{c}_r^n\left(0,y_j,\theta_k-h_\theta\right)\right)=\frac{1}{h_x^2}\left(\mu_{h,r}\left(0.5h_x,y_j,\theta_k\right)+\right.$$

$$+\mu_{h,r}\left(-0.5h_x,y_j,\theta_k\right)\left(\bar{c}_r^n\left(h_x,y_j,\theta_k\right)-\bar{c}_r^n\left(0,y_j,\theta_k\right)\right)-\mu_{h,r}\left(-0.5h_x,y_j,\theta_k\right)\frac{h_x}{3}\vartheta_1+\frac{1}{h_y^2}\left(\mu_{h,r}\left(0,y_j+0.5h_y,\theta_k\right)\cdot\right. \tag{90}$$

$$\cdot\left(\bar{c}_r^n\left(0,y_j+h_y,\theta_k\right)-\bar{c}_r^n\left(0,y_j,\theta_k\right)\right)-\mu_{h,r}\left(0,y_j-0.5h_y,\theta_k\right)\left(\bar{c}_r^n\left(0,y,\theta\right)-\bar{c}_r^n\left(0,y_j-h_y,\theta_k\right)\right)\Big)+$$

$$+\frac{1}{H^2\left(0,y_j\right)h_\theta^2}\left(\mu_{v,r}\left(0,y_j,\theta_k+0.5h_\theta\right)\left(\bar{c}_r^n\left(0,y_j,\theta_k+h_\theta\right)-\bar{c}_r^n\left(0,y_j,\theta_k\right)\right)-\mu_{v,r}\left(0,y_j,\theta_k-0.5h_\theta\right)\cdot\right.$$

$$\left.\cdot\left(\bar{c}_r^n\left(0,y_j,\theta_k\right)-\bar{c}_r^n\left(0,y_j,\theta_k-h_\theta\right)\right)\right)+\bar{F}_r^n,\ \left(0,y_j,\theta_k\right)\in\bar{\omega}^+,\ r=1,2,3,\ n=1,\ldots,N_T.$$

The error of the approximation of scheme (90) at the boundary nodes of the grid $\bar{\omega}^+$ in case of $x_i = 0$ is equal to $O\left(\tau+h_x^2\right)$.

For the case when the boundary condition (11) is satisfied and $x_i = L_i$, as well as for the cases of boundary conditions (12) and (13), the methods for constructing the difference scheme for the problem (8)–(13) are analogous to those described above, starting from relation (43). Due to the complexity of their description within this article, they are not provided.

Discussion and Conclusion. A second-order difference scheme for approximation on a uniform grid is proposed, which approximates the initial-boundary value problem for the three-dimensional diffusion-convection equation of multifractional suspensions at all nodes of the uniform grid, including boundary nodes. Special attention is given to the description of the approximation methods at the boundary nodes of the grid using an extended grid. The proposed scheme has an approximation error in the norm of the grid space C: second order with respect to the spatial grid steps and first order accuracy with respect to the time step. Further research is focused on proving the stability and convergence of the constructed difference scheme based on the grid maximum principle under mild constraints on the grid Peclet number, the satisfaction of the Courant condition, the aforementioned smoothness conditions, and other restrictions that are naturally satisfied for discrete models of hydro-physical coastal systems.

References

1. Sukhinov A.I., Chistyakov A.E., Bondarenko Yu.S. Error estimation of the solution to the equation based on weighted schemes. *Izvestiya YUFU. Technical Sciences*. 2011;8(121):6–13. (in Russ.)

2. Sukhinov A.I., Chistyakov A.E., Protsenko E.A. Construction of a discrete two-dimensional mathematical model of sediment transport. *Izvestiya YUFU. Technical Sciences.* 2011; 8(121):32–44. (in Russ.)

3. Sukhinov A.I., Chistyakov A.E., Protsenko E.A., Sidorakina V.V., Protsenko S.V. Parallel algorithms for solving the problem of dynamics of bottom relief changes in coastal systems. *Computational Methods and Programming*. 2020; 21(3):196–206. (in Russ.) https://doi.org/10.26089/NumMet.v21r318

4. Sukhinov A.I., Chistyakov A.E., Protsenko E.A., Sidorakina V.V., Protsenko S.V. A complex of combined models for sediment and suspension transport considering three-dimensional hydrodynamic processes in the coastal zone. Mathematical Modelling. 2020; 32(2):3–23. (in Russ.) https://doi.org/10.20948/mm-2020-02-01

5. Sukhinov A.I., Chistyakov A.E., Protsenko S.V., Sidoryakina V.V. Coupled 3D wave and 2D bottom deposit transportation models for the prediction of harmful phenomena in coastal zone. В сборнике: *Trends in the Analysis and Design of Marine Structures — Proceedings of the 7th International Conference on Marine Structures, MARSTRUCT* 2019. 2019. P. 597–603. https://doi.org/10.1201/9780429298875-68

6. Sukhinov A.I., Sidoryakina V.V. Development and analysis of the correctness of a mathematical model for the transport and sedimentation of suspensions, taking into account changes in bottom relief. *Computational Mathematics and Information Technologies*. 2018;2(2):76–90. https://doi.org/10.23947/2587-8999-2018-2-76-90

7. Sukhinov A.I., Sukhinov A.A., Sidoryakina V.V. Uniqueness of solving the problem of transport and sedimentation of multicomponent suspensions in coastal systems. В сборнике: *Journal of Physics: Conference Series. Applied Mathematics, Computational Science and Mechanics: Current Problems*. Bristol, 2020; 1479:012081. https://doi.org/10.1088/1742-6596/1479/1/012081

8. Sukhinov A.I., Sidoryakina V.V. Development and correctness analysis of the mathematical model of transport and suspension sedimentation depending on bottom relief variation. *Vestnik of Don State Technical University.* 2018;18(4): 350–361. https://doi.org/10.23947/1992-5980-2018-18-4-350-361

9. Sukhinov A.I., Chistyakov A.E., Sidoryakina V.V., Protsenko S.V., Atayan A.M. Locally two-dimensional splitting schemes for parallel solving of the three-dimensional problem of suspended substance transport. *Mathematical Physics and Computer Simulation.* 2021;24(2):38–53. (in Russ.) https://doi.org/10.15688/mpcm.jvolsu.2021.2.4

10. Sidoryakina V.V., Sukhinov A.I. Construction and analysis of the proximity of solutions in L2 for two boundary problems in the model of multicomponent suspension transport in coastal systems. *Journal of Computational Mathematics and Mathematical Physics*. 2023;63(10):1721–1732. (in Russ.) https://doi.org/10.1134/S0965542523100111

11. Courant R. *Partial Differential Equations*. Moscow: MIR; 1964. 832 p. (in Russ.)

About the Author:

Valentina V. Sidoryakina, Associate Professor of the Department of Mathematics and Computer Science, Don State Technical University (1, Gagarin Sq., Rostov-on-Don, Russian Federation, 344003), Candidate of Physical and Mathematical Sciences, MathSciNet, Spin-code, ORCID, ResearcherID, ScopusID, cvv9@mail.ru

Conflict of Interest Statement: **the author declares no conflict of interest.**

The author has read and approved the final version of manuscript.

Об авторе:

Валентина Владимировна Сидорякина, доцент кафедры математики и информатики, Донской государственный технический университет (344003, Российская Федерация, г. Ростов-на-Дону, пл. Гагарина, 1), кандидат физико-математических наук, MathSciNet, Spin-код, ORCID, ResearcherID, ScopusID, cvv9@mail.ru

Конфликт интересов: **автор заявляет об отсутствии конфликта интересов.**

Автор прочитал и одобрил окончательный вариант рукописи.

Received / Поступила в редакцию 19.08.2024
Reviewed / Поступила после рецензирования 02.09.2024
Accepted / Принята к публикации 02.09.2024